COMBRINCK, M

INTEGRATED APPROACH TO GROUNDWATER EXPLORATION ON THE LEBOWA GRANITE SUITE

MSc UP 1999

Integrated approach to groundwater exploration on the Lebowa Granite Suite.

by

Magdalena Combrinck

Submitted in partial fulfilment of the requirements
for the degree of

MAGISTER SCIENTIAE

in the Faculty of Science of the
University of Pretoria.

PRETORIA
February 1999

Integrated approach to groundwater exploration on the Lebowa Granite Suite.

by

Magdalena Combrinck

Supervisor: *Prof. W. J. Botha*

Department: *Geology*

Degree: *Magister Scientiae in Exploration Geophysics*

ABSTRACT

The main objective of this project was to improve the success rate in the siting of groundwater boreholes on a typical hard rock terrain. The study was done on a 10X10 km area, underlain by the Lebowa Granite Suite, covering villages in the Ga-Masemola district in the Northern Province. This specific site has been declared as unsuitable for groundwater development due to the fact that there wasn't enough water in the existing boreholes to supply the villages even with their minimum requirements. In order to improve the previously applied exploration approach of siting boreholes within a specific radius of a village in need of water, a more regional, exploration approach was investigated as an alternative. This included the use of high resolution airborne geophysical data, structural mapping and ground geophysics to follow up the main features identified from the regional data sets. Thirteen sites were identified and 33 boreholes were drilled by the Department of Water Affairs and Forestry in order to evaluate this approach. The results compared very well to the holes that existed in the area prior to this investigation:

- 40 existing holes – total blow test yield/air lift = 5.4 l/s
- 33 new holes – total blow test yield/air lift = 74 l/s

Although not all the holes or sites were high yielding, the regional approach has been proven to be successful both in the more successful siting of water yielding boreholes, and the yield per borehole. The optimum airborne geophysical data set and flight line spacing has also been determined as 50-75m line spacing airborne magnetic data. Furthermore, for this specific geological setting, the main aquifers were found to be faults and shear zones rather than lithological contacts or weathered basins.

Integrated approach to groundwater exploration on the Lebowa Granite Suite.

deur

Magdalena Combrinck

Studieleier: *Prof. W. J. Botha*

Departement: *Geologie*

Graad: *Magister Scientiae in Eksplorasie Geofisika*

SAMEVATTING

Die hoof doelstelling van hierdie projek was om die persentasie suksesvolle boorgate vir grondwater ontwikkeling te verbeter in 'n omgewing wat bestaan uit kristallyne gesteentes. Die gebied wat vir hierdie studie gekies is, is 'n 10X10 km area in die Lebowa Graniet Suite, wat nedersettings in die Ga-Masemola distrik insluit in die Noordelike Provinsie. Hierdie spesifieke gebied is ongeskik verklaar vir grondwater ontwikkeling, op grond van die feit dat die bestaande boorgate nie genoeg water kon lewer om in die bevolking se minimum vereistes te voorsien nie. Om te verbeter op die bestaande benadering van gelokaliseerde grondwater eksplorasie, wat gemik is daarop om water vir 'n spesifieke nedersetting binnne 'n spesifieke radius te voorsien, is 'n regionale, eksplorasie benadering ondersoek as alternatief. Hierdie benadering het die gebruik van hoë digtheid lug geofisiese data, struktuurkartering en grond geofisika om die belangrikste regionale strukture op te volg, ingesluit. Dertien teikengebiede is geïdentifiseer en 33 boorgate is deur die Departement van Waterwese en Bosbou geboor om hierdie benadering te evalueer. Die resultate vergelyk baie goed met die boorgate wat reeds bestaan het voor die aanvang van die studie:

- 40 bestaande boorgate – totale blaastoets lewering = 5.4 l/s
- 33 nuwe boorgate – totale blaastoets lewering = 74 l/s

Alhoewel die boorgate nie almal hoë lewerings het nie, is bewys dat die regionale benadering nie alleen tot 'n hoër verhouding suksesvolle gate lei nie, maar ook tot hoër lewerings gate. Die optimum lug geofisiese datastel is bepaal as lugmagneties op 50-75m lynspasiëring. Verder is daar ook gevind dat, vir hierdie spesifieke gesteente eenheid, veskuiwings en skuifskeursones eerder as litologiese kontakte of verweringskomme, die beter waterdraers is.

Acknowledgements

I would like to express my sincere gratitude to the following persons and institutions without whom this project would not have been possible:

- *Professor Willem Botha, my promoter and project leader for his guidance, motivation and invaluable support and advice*
- *The Water Research Commission, Council for Geoscience and Geodass SA Ltd for their very generous financial support*
- *The Department of Water Affairs and Forestry for the drilling of boreholes*
- *All the students and friends who in one way or another helped with the acquisition of data; Willem, Antonie, Rian, Timmy, Hammond, Mike, Kobus*
- *My parents and family for their continuing support*

LIST OF CONTENTS

Page

5. Chapter 5: Processing and interpretation of airborne geophysical data applied to the siting of boreholes

6. Chapter 6: Ground follow-up and case studies

LIST OF FIGURES AND TABLES

CHAPTER 1

INTRODUCTION

1.1 GENERAL

The use of geophysical techniques for the location of suitable targets for water supply boreholes is well understood. It is however in the application of these techniques in traditionally poor groundwater potential areas such as the Lebowa Granite Suite of the Northern Province, National Groundwater Information System (NGIS), that the correct interpretation of the geophysical data becomes crucial in planning and developing community water supplies. To this end an integrated multidisciplinary approach is proposed whereby airborne geophysical techniques combined with ground geophysics, geology, orthophotos, topocadastral data and detailed structural geological mapping are used in the siting of boreholes for groundwater development.

A 10x10km target area, situated in the southern district of the Northern Province, figure 1, was chosen for this study. The area has one of the lowest water/capita/day ratios in the country (Environmental Potential Atlas [ENPAT], version 1, 1994). Detailed structural geological mapping, (Hoffman, 1997), and hydro-geological assessments, (Botha, 1997), was undertaken in the area.

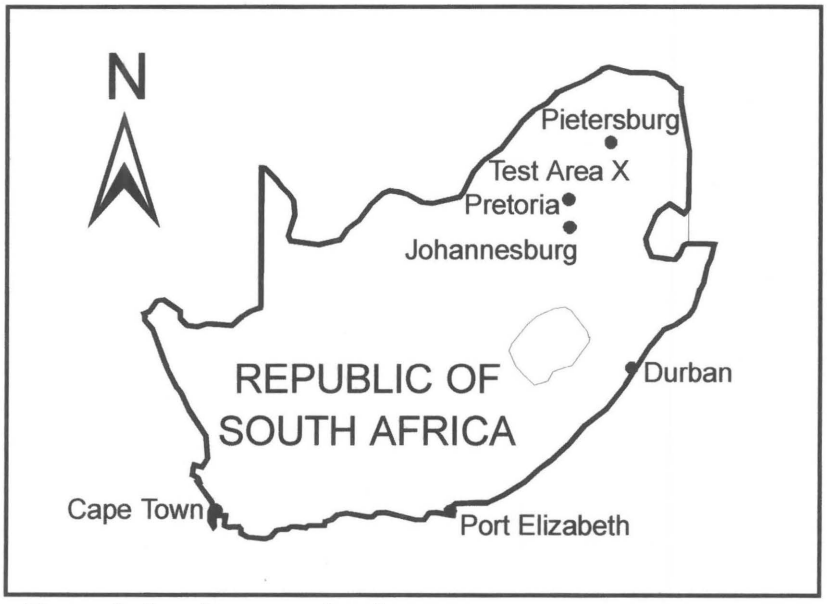

Figure 1: Locality map of study area.

1.2 OBJECTIVES

The objectives of this study are summarized in figure 2:

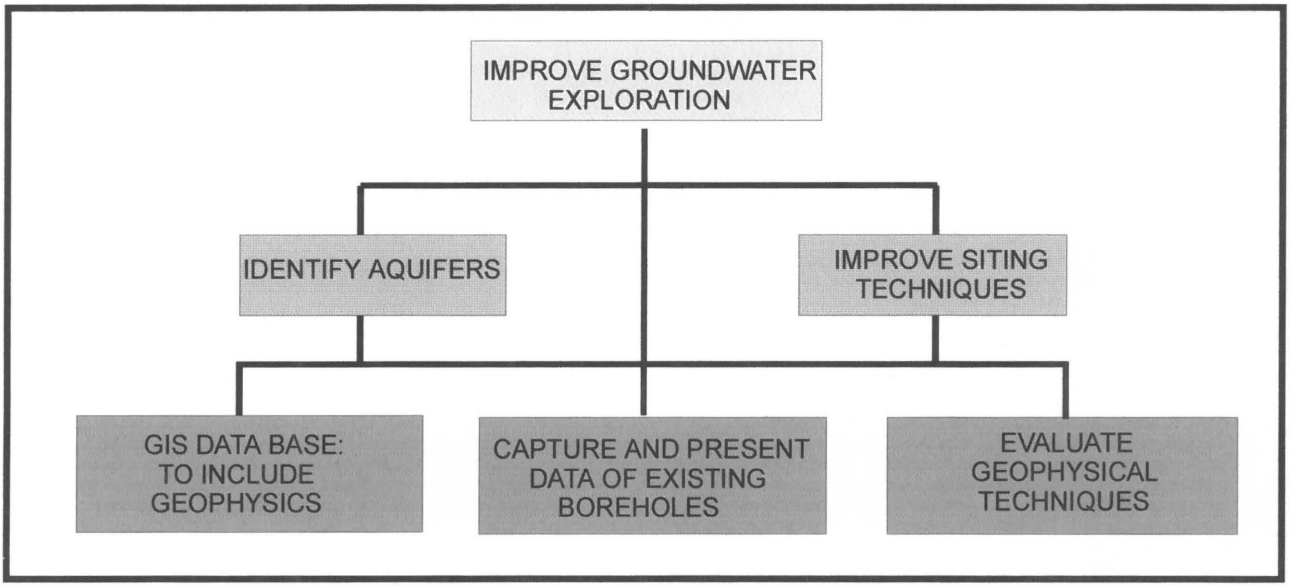

Figure 2: Schematic presentation of the objectives of this study.

The primary objective is to improve the success rate of siting boreholes for groundwater development. This leads to two secondary objectives, that is

- the identification of the aquifers in the study area,
- and the development and evaluation of more efficient geophysical techniques for borehole siting.

Identification of aquifers

This can only be done if the location of boreholes can be accurately placed on maps and the geophysical interpretation used to site the boreholes can be evaluated for its correctness. The most efficient way of undertaking this, was through the use of a GIS, incorporating all relevant data.

Evaluation of different geophysical techniques

Airborne magnetics, frequency domain EM and spectrometric gamma-ray techniques were applied in the study area and targets on the ground were followed up with magnetic and EM

surveys. Ample data therefore exists to determine which data sets play the leading role in improving the selection of groundwater yielding boreholes.

1.3 GEOLOGY AND GEOHYDROLOGY

1.3.1 Geology

The study area is underlain by the Lebowa Granite Suite of the Bushveld Igneous Complex, figure 3.

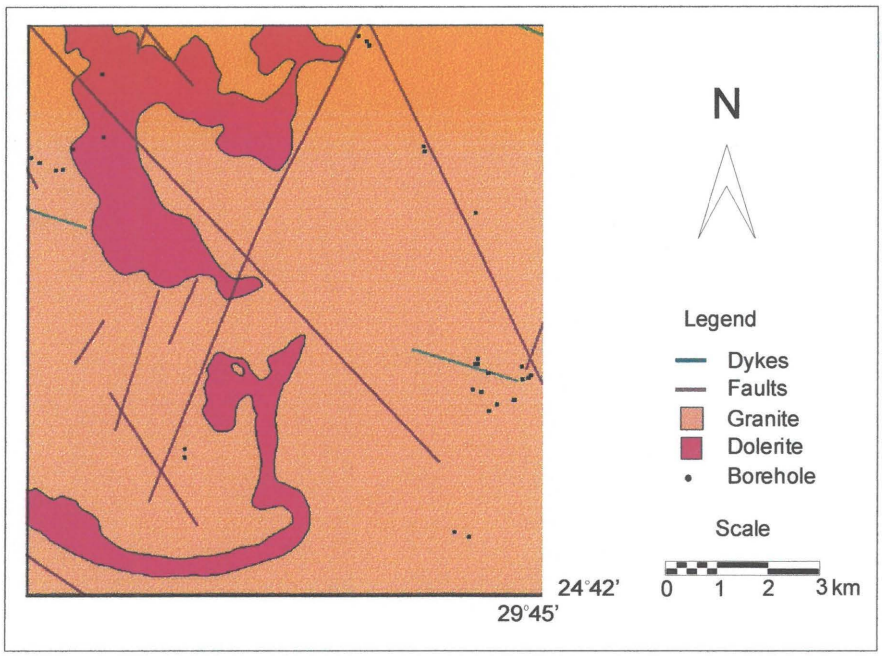

Figure 3: Geology of the study area

The most important lithological unit in the area is the Nebo Granite, a sill-like granitic intrusion, Kent, L.E., 1980. It dips to the west and varies in thickness from 420 m in the south to 2,4 km in the north. Its age is determined as 1920±40 Ma (Tankard, 1982). The granite exhibits a crude stratiform layering with a coarse-grained gray granite at the base, grading up through medium-grained gray and red, then through red granophyric granite, and finally granophyre, although this sequence is not always complete at one location. The most important minerals are quartz, feldspar and minor but variable amounts of hornblende or biotite. Mafic minerals are more abundant in the coarser grained varieties. Accessory minerals are zircon, fluorite (which affect the drinking quality of the water), apatite, sphene, epidote and magnetite. Alteration of the

primary minerals yields biotite, chlorite, saussurite, epidote, hematite and fine aggregates of clay minerals, (Tankard, 1982).

1.3.2 Structural Geology

Discontinuities (joints, shear zones and faults) in the Nebo Granite are prominent in the outcrop areas, where orientations of such structures can be measured. Prominent discontinuities can be followed for several kilometers using field mapping, aerial photographs and satellite images (Botha, 1998).

A total of 761 measurements of different discontinuities were taken, recording the dip and strike orientations (Hoffman, 1996), figure 4. This was plotted on stereo nets from which Rose diagrams were derived.

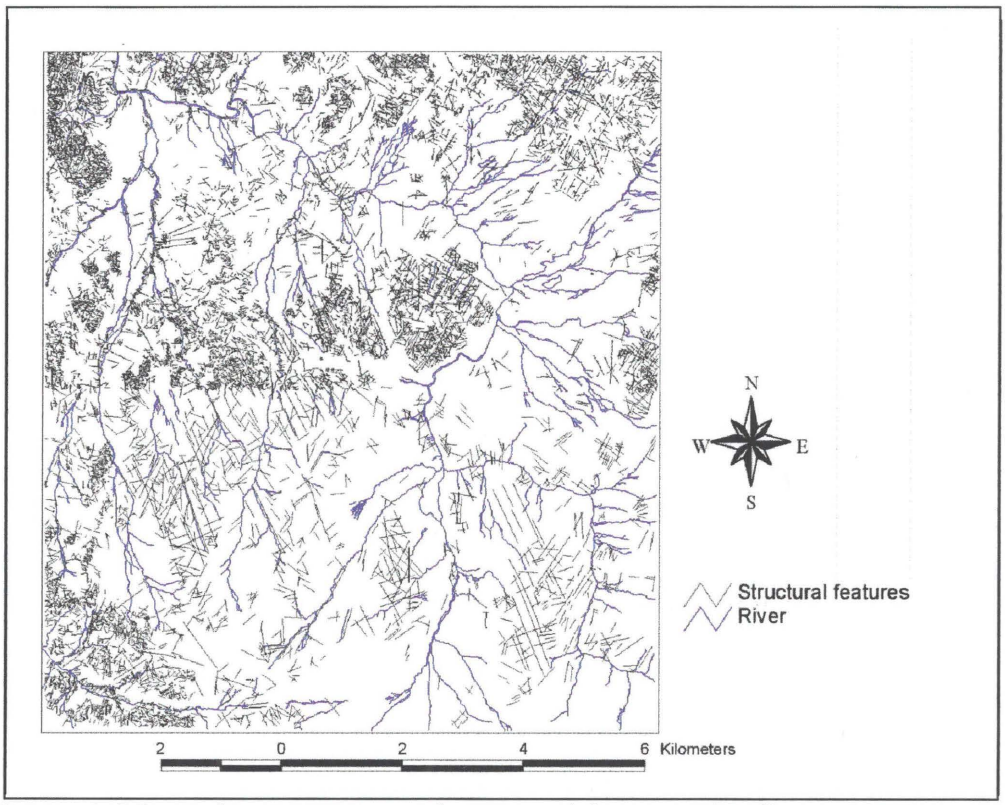

Figure 4: Map indicating measured structural features, (Hoffman, 1996)

Botha (1998) concluded that genetically different fractures occur in the Nebo Granite, namely, cooling fractures, shear zone fractures (faulting) and quartz-rich fractures due to hydrothermal activity (intrusion). Furthermore the shear zones and fractures have a more broken appearance at

the surface than the surrounding granite (evident from outcrops). Fine grained dolerite intrusions show some of the same geological fractures, some having the same orientation as in the granite. This implies that fracturing took place before, during and after Karoo times, (Botha, 1998).

On the basis of the structural orientation measurements it is evident that three different geological settings exist. The geological settings can be divided into the granite north of the dolerite intrusion, the dolerite intrusion and the granite south of the dolerite intrusion. Some strike orientations occur in all three geological settings while others concentrate in the area above, below or within the dolerite intrusions, (Botha, 1998).

The most prominent strike orientations that were mapped, were 40-50° and 140-150° (Hoffman, 1996). The structures mapped in this area correspond to the strike direction of known regional structures occurring on the sub-continent. This implies that the stresses active in the study area originated on a regional scale (Botha,, 1998).

The following hydro-geological conclusions were made by Botha (1998):

- Open fracture zones occur in the Nebo Granite and are caused by regional faulting.
- These fracture zones are caused by brittle deformation, producing potentially high yielding aquifers.
- The regional nature of the fracturing may indicate that groundwater occurring in these structures could originate far outside the study area, e.g. in the Chuniespoort dolomite north of the Bushveld Igneous Complex.

1.3.3 Surface water, recharge and rainfall

The availability of surface water in the area is restricted to non-perennial streams and fountains, most of which are severely contaminated, (Botha, 1998). There are very few dams, reservoirs or any other form of water infrastructure and individuals have to walk up to 15 km per day in order to fetch water for their most basic needs, (Consultburo, 1997).

The mean annual rainfall is 350 mm, while the annual recharge however is calculated as 12 mm, (Vegter, 1995). During droughts the rainfall and recharge is obviously much less and the water supply is inadequate for the needs of the local population. The building of dams have been

proposed, but a feasibility study has shown that for this specific area it is not a viable solution due to the rate of silting, (Haupt, 1997). The alternatives to surface water as source are either long distance pipelines from other areas or the efficient development and management of groundwater. Due to the fact that groundwater development is a more economic resource it is the first alternative that should be investigated and is therefore the subject of this study.

1.3.4 Groundwater aquifers, -level and -quality

The typical aquifers found in hard rock terrains such as covered by the study area are:

- basins in the granite caused by deep weathering, or
- weathered fractured zones associated with faults, dykes, shear zones or changes in lithology, (Larsson, 1981).
- weathered contact zones along intrusive dykes

In this study emphasis was placed on the second type of target as basins in the area are very shallow and sensitive to droughts. Published groundwater levels vary between 5m and 30m depending on topography and recharge, (Vegter, 1995). Available results from this study has shown that contact zones along dykes do not yield water in the study area.

1.4 METHODOLOGY

All available information on existing boreholes was entered into a GIS database. Where available, the geophysical data that were used to site the various boreholes were obtained, checked for accuracy, entered into the GIS database and evaluated as to the applicability of the various techniques. Where the geophysical data could not be found, ground geophysics were done by the research team. The GIS database was then used to assist in the identification of the various possible aquifers on the Lebowa Granites.

Airborne electromagnetic, magnetic and gamma-ray radiometric surveys were completed on the test site. These data sets were interpreted with special emphasis to identify zones of deep weathering, geological contacts, dykes, sills and structural information. From this data, combined with the other data sets already mentioned, target areas were selected for ground geophysical surveys and possible borehole sites. The ground geophysical surveys consisted of magnetic and

electromagnetic profiles. A number of boreholes were then drilled by the Department of Water Affairs and Forestry to evaluate the identified structures.

A number of boreholes were then drilled by the Department of Water Affairs and Forestry to evaluate the identified structures.

CHAPTER 2

THE DEVELOPMENT OF A GIS DATABASE

2.1 EXISTING BOREHOLE DATA

An intensive search was undertaken to locate all existing boreholes in the study area. A total of 38 boreholes were located. Since coordinates obtained from the Department of Water Affairs and Forestry (DWA&F) were inaccurate in the order of several hundreds of meters, accurate coordinates were obtained using a differential GPS. In addition to the 38 boreholes in the study area, information on 100 boreholes sited on the rest of the Nebo area were obtained and used in the quoted statistics in this chapter.

In order to identify the aquifers, and evaluate the siting of existing boreholes, all available data on the boreholes were obtained. The data for each hole consist of some or all the following attributes:

- borehole number
- coordinates
- borehole depth
- depth of static water level
- associated geology
- yield (usually blow test yield)
- method of siting
- equipment, such as handpumps, associated with holes
- geophysical data used in the siting of the hole, if any

Contributors to this information are the National Groundwater Information System (from the DWA&F) and several consulting companies which worked on contract for DWA&F. Unfortunately, this data proved to be insufficient for the purposes of the study due to the following reasons.

The geophysical data (which is considered one of the most important aspects for the evaluation of the siting techniques), could not be located for any of the boreholes in the study area. Furthermore, the coordinates (when given) were not accurate enough to distinguish between several holes in the same area in the field. This made it impossible to use the rest of the DWA&F since the information could not be tied to a specific borehole. The borehole numbers, which uniquely identify each hole, were weathered away in many cases. A number of boreholes were found with no numbers and consequently no information.

The geophysical information associated with the siting of each borehole was considered essential for the evaluation of the aquifer. It was considered quite possible that a low yield borehole can be considered not viable due to an incorrect interpretation of the geophysical information rather than a lack of water in a lineament. Due to the lack of availability of this data, it was decided to do geophysical profiles at all the existing holes where cultural noise allowed for such a survey. At each site two perpendicular profiles of 200m length were completed with one of the profiles as close as possible to being perpendicular to one of the main structural directions, to maximize the geophysical response of possible structures on which the holes were drilled.

2.2 BOREHOLE DATA REPRESENTATION (Arcview 3.1)

The study required a large number of multidisciplinary data sets to be compared. The most efficient way to do this is by means of a Geographical Information System (GIS). The software chosen was Arcview 3.1 for the following reasons:

- it is PC based
- it is already widely in use in the geophysical and groundwater community
- it is compatible with other databases (e.g. dBase, Arc-Info)
- it can be customized to have a user friendly interface giving easy access to all data

Arcview 3.1 makes use of *views* and *themes* with specific *attributes* to graphically represent data. In order to evaluate and compare the different data sets, they all had to be converted to a format acceptable by Arcview 3.1.

The different borehole data attributes are entered in a spreadsheet format and can be entered and edited directly in Arcview 3.1 or be imported from Excel, Quatro Pro, dBase or any equivalent spreadsheet program. It can in fact even be imported from an ordinary text file created in a DOS editor or Notepad. As soon as this table is created in Arcview 3.1, the data can be used to create themes, which can be graphically displayed in views.

For this database the coordinates of the boreholes are used as unique identifiers and each borehole is represented as a point on a map-like display (the view), using these coordinates. By choosing the **information** button, and clicking on a borehole all the attributes, in table format, of that borehole can now immediately be viewed. This is illustrated in figure 5.

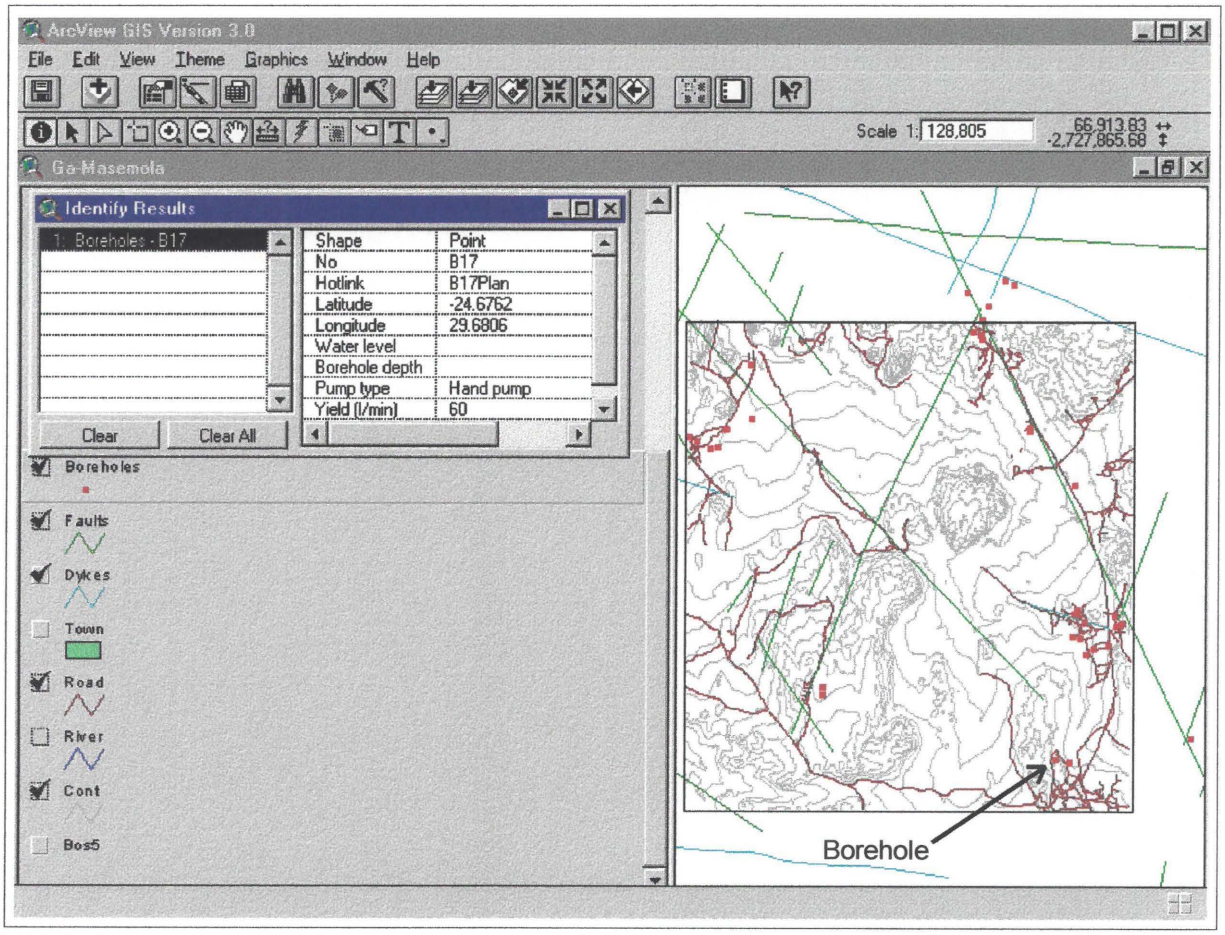

Figure 5: An ArcView screen image showing the boreholes overlain on topography and structure.

To have easy access the geophysical profiles at each borehole use was made of the **hotlink** function, which enables the user to recall any other view or image with a click of the mouse. For this specific study two views were created and "hotlinked" to each borehole. The first is a plan view showing the profiles relative to the borehole, the profile directions, the methods used and

any significant landmarks or cultural noise sources. The next step is a view showing the geophysical profiles with borehole positions. (These were created in Corel Draw, and imported into Arcview 3.1 as TIFF files. Graphs can also be drawn in Arcview 3.1, but it was decided that the options were a bit limited for the information to be conveyed in a single view.) Figure 6 shows the two data presentations that are hotlinked to Arcview.

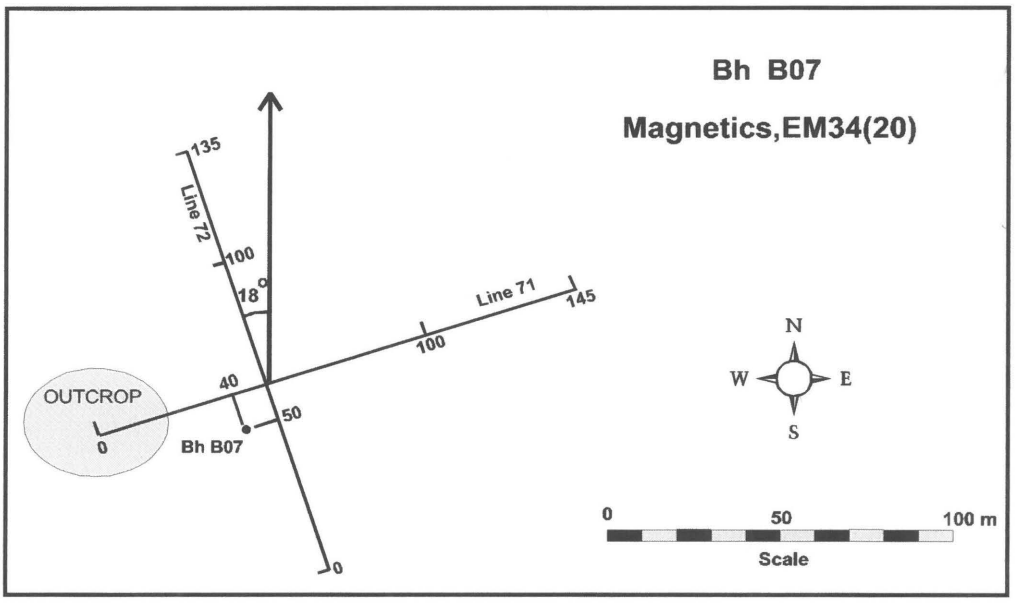

Figure 6(a): A map view of the profiles surveyed at a borehole

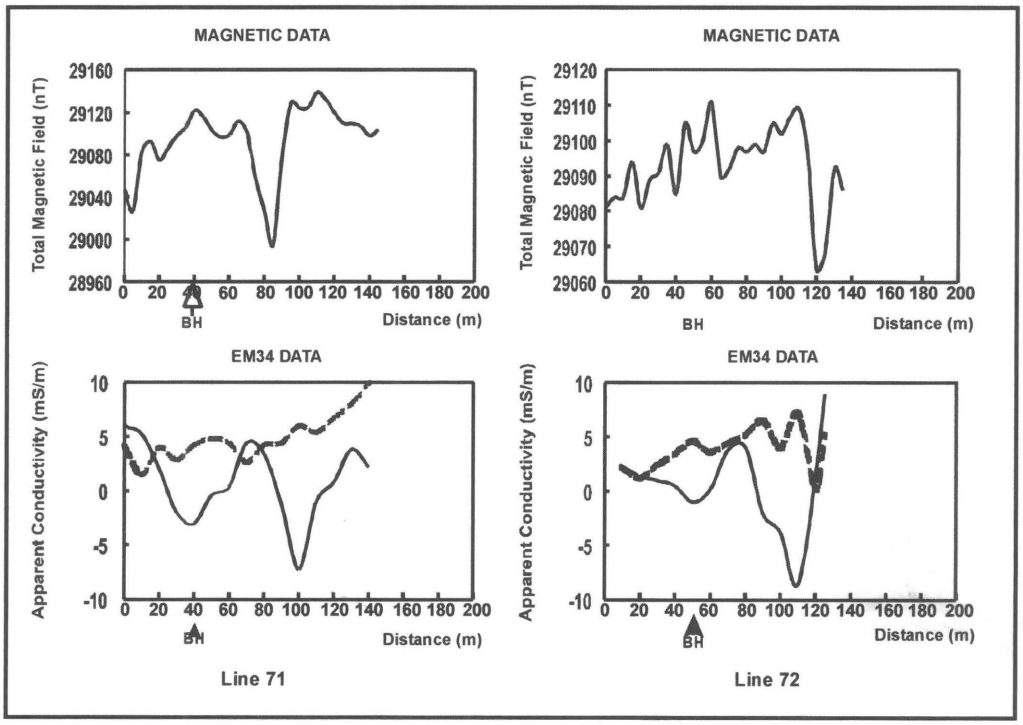

Figure 6(b): A view of the profiles surveyed at each borehole.

Once all the data is in the database it is very easy to use and extremely fast. It is now possible to simultaneously view all relevant information associated with a borehole, as shown in figure 7.

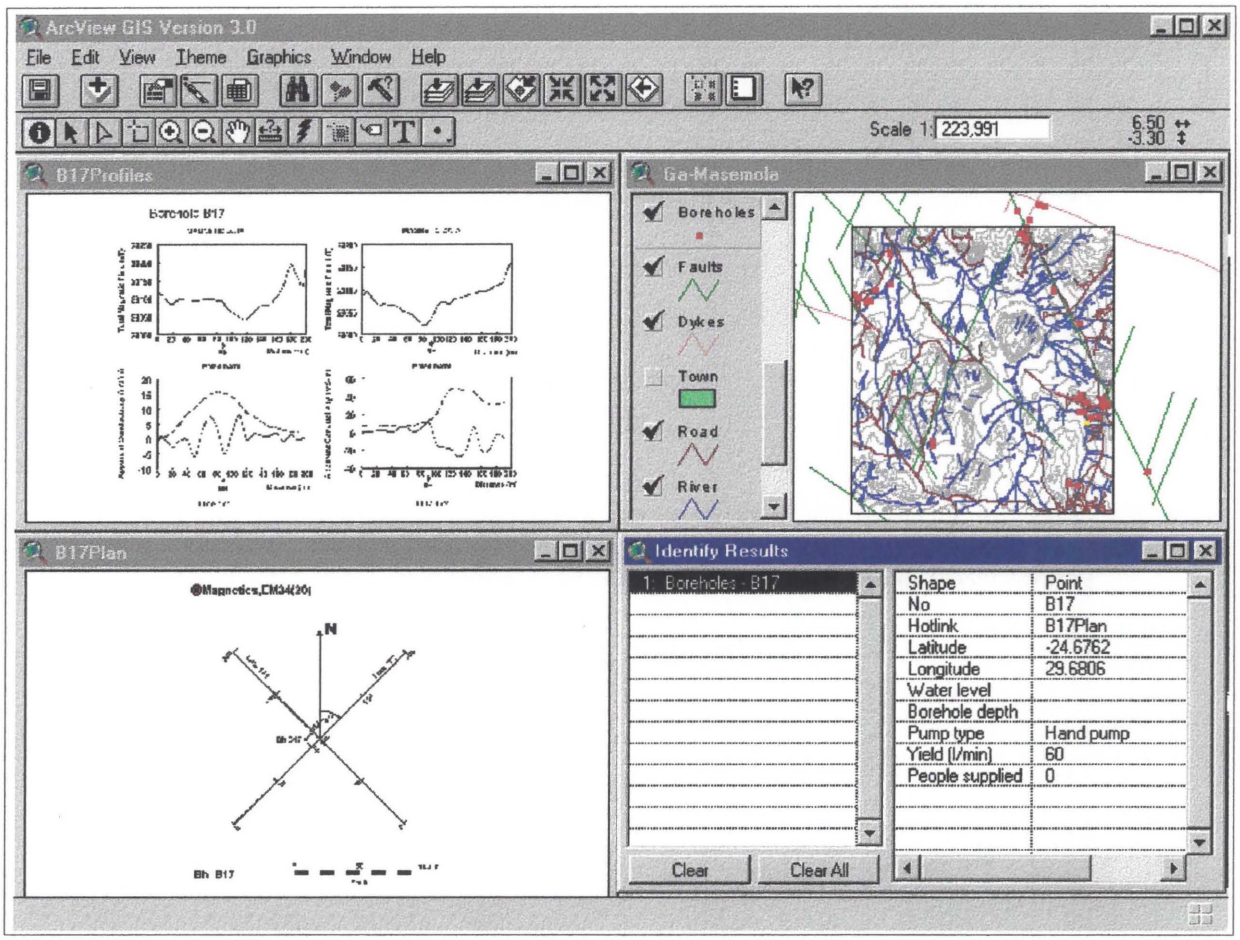

Figure 7: A screen view showing all relevant data associated with a borehole.

2.3 Remarks:

- Like all databases, it takes a considerable amount of time to do the physical data capturing, especially if the original formats are not compatible with Arcview 3.1.

- Queries and legends

  Some of Arcview 3.1's features that should be mentioned due to their special applicability for this study, are the **query** function and the **legend** editor. The legend editor enables the user to apply a variety of customized colour coded legends to a theme based on any of the attributes in the original data table. The query function enables the user to apply any kind of logical query (<, =, >, AND, OR, etc.) or combinations thereof to the data and will show all the boreholes for which the query is TRUE in yellow. An example of this is to find all

boreholes that have been sited on magnetic anomalies AND have a yield higher than the average yield. This can then give an indication of the success of this specific method.

CHAPTER 3

GEOPHYSICAL TECHNIQUES TRADITIONALLY APPLIED TO BOREHOLE SITING

3.1 INTRODUCTION

This chapter contains a brief overview of geophysical techniques that are often routinely used in the siting of boreholes for groundwater development. One will often find that a specified technique is favoured in a certain area based on the field of expertise of the operator rather than on the physical properties of the target. When choosing a technique, it is essential to consider the physical properties of the target and the host rock and where possible, to use a combination of techniques.

3.2 DIRECT CURRENT RESISTIVITY SOUNDINGS AND PROFILING

These methods, also described as galvanic resistivity methods, are used to measure the earth's resistivity. Current is driven through one pair of electrodes (galvanic contacts) and the potential established in the earth by this current is measured with a second pair of electrodes (potential electrodes). This principle can be used to study variations in resistivity with depth (vertical sounding) or to study lateral resistivity variation (horizontal profiling), (Van Nostrand and Cook, 1966).

The instrumentation used is usually relatively inexpensive, consisting basically of:

- a power source (DC or very low frequency alternating current)
- two or more current electrodes (usually made of steel)
- two or more potential electrodes (usually made of copper)
- lightweight cables
- multimeters for measuring current and voltage.

The method is based on Ohm's Law, the general form of which can be given as:

$$\mathbf{E} = \rho\mathbf{j} \qquad (3.1)$$

where

$\boldsymbol{E}$ = electric field vector

$\boldsymbol{j}$ = current density vector

ρ = resistivity

For a three dimensional volume of material, as shown in figure 8, the resistance R, defined by Ohm's law as the ratio between potential difference and current, is proportional to the dimensions of the volume of material, that is :

$$R \propto \frac{L}{A} \tag{3.2}$$

where

A = area perpendicular to **j**

L = length in the direction of **j**

R = resistance ($=\Delta V/I$)

ΔV = potential difference over L

I = current

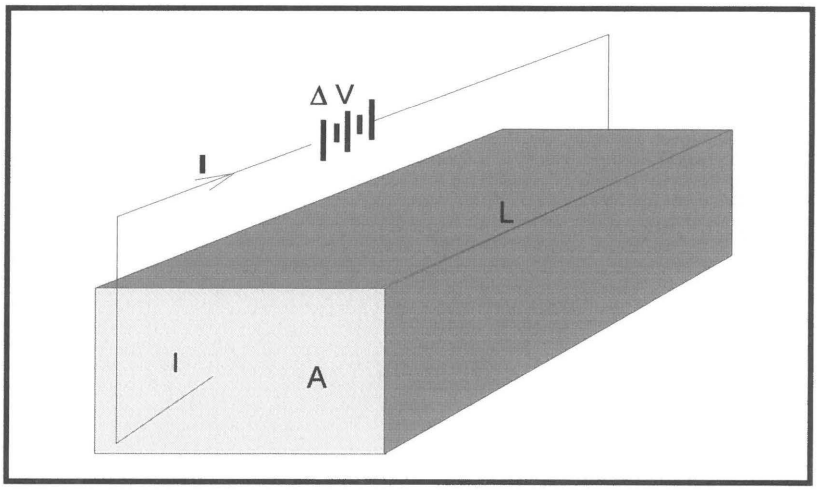

Figure 8: A volume of material defining the units used in equation 3.2

The proportionality constant is defined as the resistivity ρ, with:

$$\rho = \frac{AR}{L} \tag{3.3}$$

From this, the resistivity is seen to have the dimensions of length and resistance, with SI units of Ωm (ohm.meter).

When doing resistivity measurements in the field, however, the medium being measured is often not a homogeneous, isotropic earth. In such a case a known current is passed through the earth and the resulting potential distribution caused by this, is observed using the potential difference (ΔV) measurements between two electrodes. This potential is then compared to the potential that would have been observed in a homogeneous, isotropic earth. The ratio of the measured potential to the theoretical potential, for the special case of the theoretical potential equal to unity, is called the *apparent resistivity* and is the fundamental parameter used in this technique, (Keller and Frischknecht, 1966).

Although there are many different configurations for electrode geometry and spacing, the two most commonly used, are the Slumberger and Wenner configurations. Both these configurations/arrays require four electrodes, as illustrated in figure 9.

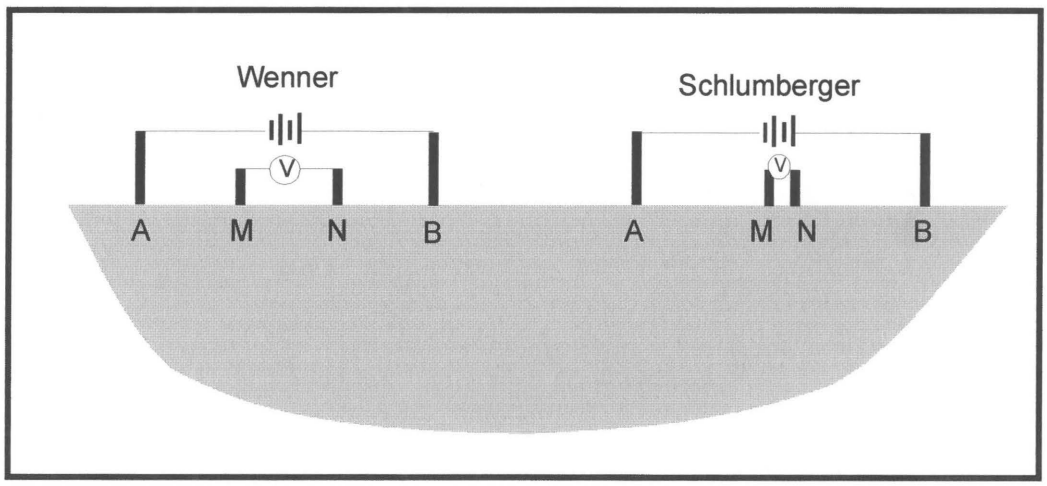

Figure 9: Schematic presentation of the Wenner and Schlumberger configurations of electrodes.

For the Wenner array all electrodes are at equal distances appart. For the Slumberger array the current electrodes are at a spacing, say 2**a**, from one another and the potential electrodes are at a spacing b < **a**/5, from one another, their center at distance **a** from the current electrodes. When using these arrays a geometrical factor (K) must be calculated and applied to determine the apparent resistivity. For the different arrays these factors are given as:

$$K = \pi \frac{AM.AN}{MN} \quad \text{..... Schlumberger} \qquad (3.4)$$

and $$K = 2\pi a \quad \text{..... Wenner} \qquad (3.5)$$

The apparent resistivity, ρ_a, is then given by:

$$\rho_a = \frac{K.\Delta V}{I} \qquad (3.6)$$

The apparent resistivity values can be interpreted to give either a resistivity profile with depth or to map lateral variations in resistivity. The method can be applied to map:

- weathered basins (using depth soundings)
- vertical structures such as faults and lithological contacts (using profiling). The method is however not recommended for vertical structures since it is more sensitive to resistive targets and the profile generated by a vertical target can be relatively complex to interpret, (Botha, 1975).

A serious disadvantage of applying the resistivity technique is that good physical contact is needed between the current electrodes and the earth in order to force a large enough current into the earth. In the specific study area, this is very difficult due to the many outcrops that make it impossible to do long profiles or deep soundings.

3.3 FREQUENCY DOMAIN ELECTROMAGNETIC TECHNIQUES (FDEM)

The FDEM induction techniques are best suited for detecting steeply dipping good conductors at shallow depths. This makes it ideal for detecting weathered structures such as faults and fractures, (Telford, 1990).

Electromagnetic systems are based on the principles that all electrical currents have magnetic fields associated with them and that all time varying magnetic fields will induce current in a conductor. A time varying magnetic field is generated by driving an alternating current through a

wire loop or antenna. If any conductive material is present in the associated magnetic field, currents normal to the direction of the magnetic field will be induced in the conductor. These induced currents, in turn, create their own associated magnetic fields that, together with the primary field associated with the original transmitter, forms part of the total magnetic field. This resultant magnetic field is then measured in terms of the voltage induced in the receiver loop, (Keller and Frischknecht, 1966).

In the FDEM nethods, measurements can be made of the in-phase and quad-phase (out of phase) components of the total magnetic field. The EM34, designed to operate at low induction numbers ($r/\delta << 1$), measures the ratio of the quadrature component of the secondary magnetic field ($Q\mathbf{H}_s$) to the free space primary magnetic field ($\mathbf{H}_p$). The instrument is designed to measure the response due to the leading term in the half-space expression of the half-space response for the normalized quadrature component, (horizontal coplanar configuration), (McNeil, 1980). This term can be written as:

$$Qh_z \approx \frac{1}{2}\left(\frac{r}{\delta}\right)^2 = \frac{\omega\mu_0\sigma r^2}{4} \qquad (3.7)$$

It follows from equation 3.7 that Qh_z is directly proportional to the terrain conductivity and the receiver is calibrated in terms of apparent conductivity,(McNeil, 1980).

The EM34 is a moving source (transmitter) - moving receiver type instrument. It consists of a transmitter coil and receiver coil, both small enough to be easily handled by a two man team. It has three standard coil separations, 10m, 20m and 40m, corresponding to three different frequencies and different depths of investigation , Table 1.

Coil separation	*Frequency*	*Depth of investigation (Horizontal coils)*	*Depth of investigation (Vertical coils)*
10 m	6400 Hz	15 m	7.5 m
20 m	1600 Hz	30 m	15 m
40 m	400 Hz	60 m	30 m

Table 1. Investigative properties associated with different EM34 coil separations.

If measurements are taken with the horizontal coil configuration the EM34 can be seen as a quadrature-phase HLEM (Horizontal Loop Electromagnetic) system. It is capable of detecting steeply dipping plate-like structures with a low conductivity-thickness product in resistive ground. If the target thickness is much less than the intercoil spacing a characteristic HLEM response as shown in figure 10, will be mapped. These anomalies can be interpreted to yield conductance, depth and dip, (McNeil, 1983).

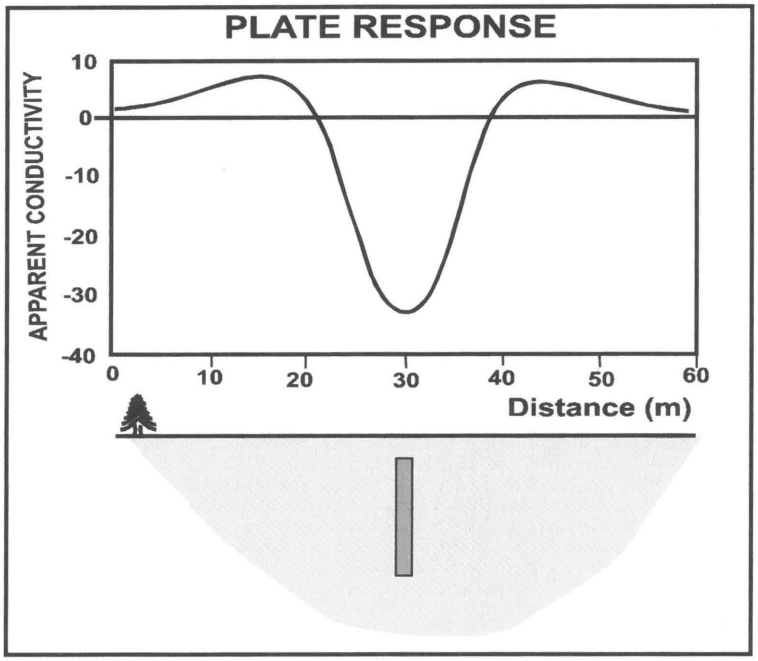

Figure 10: A typical horizontal loop response over a vertical conductor.

The EM34 system allows easy and rapid measurements, is sensitive to changes in conductivities in the order of 5 or 10 percent and the data can be interpreted fast and accurately. The maximum coil separation of 40m limits the depth of investigation to 60m, but in the study area this was found to be sufficient.

3.4 MAGNETICS

The earth's magnetic field, from an exploration geophysicist's perspective, is composed of three parts:

- the main field (internal origin)
- a small field with external origin

- spatial variations of the main field which are caused by local magnetic anomalies in the near-surface crust of the earth.

The main field varies relatively slowly and can be shown to have an internal origin using spherical harmonic analysis. The present theory is that the source of this field is convection currents of conducting material circulating in the liquid outer core. The field closely represents that of a bar magnet with the two poles being close to, but not exactly on, the geographical north and south poles of the earth. This field contributes to more than 99% of the total magnetic field, (Telford, 1990).

The relatively small external field is caused by electric currents in the ionized layers of the upper atmosphere. Time variations of this part are much more rapid than for the main field. Variations are caused by solar and lunar variations as well as magnetic storms which correlate with sunspot activity, (Telford, 1990).

Local changes in the main field result from variations in the magnetic mineral content of near-surface rocks often indicating the presence of dykes and/or faults/shear zones. These anomalies do not persist over great distances and are the main targets of the groundwater explorationist.

The magnetometer used for the ground geophysics in this study is a proton-precession magnetometer. This instrument depends on the measurement of the free-precession frequency of protons that have been polarized in a direction approximately normal to the direction of the earth's field. The protons induce a voltage that is a function of the precession frequency ν. The magnetic field can then be determined from:

$$F = \frac{2\pi\nu}{\gamma_p} = \left(23.487 \pm 0.002 nT/Hz \right)\nu \qquad (3.8)$$

where

F = total field intensity in nanoTesla

ν = precession frequency

γ_p = gyromagnetic ratio of the proton

Only the total field intensity (F) can be measured and the sensitivity is approximately 1 nT. The field procedure consists of taking a measurement at equal intervals along a profile. The values are presented as profile plots of amplitude versus distance. The shape of the magnetic profile is a function of the geometrical shape of the causative body, the direction of the profile, the inclination and declination of the main magnetic field at that position and whether or not the body has remanent magnetization. These factors are taken into account by most standard software packages like MAGIX from INTERPREX. Using such software, a possible geological model can be derived from the data. The derived model is however non-unique and therefore has to be correlated with other techniques or known geology.

In this study the magnetic method is used to delineate the doleritic intrusions (either as dikes or sills) into the granite. These magnetic features are used as marker horizons. Faults are detected as displacements in these marker units. Once detected, these faults are then mapped in detail using the EM techniques. Due to the relative short nature of the traverse undertaken, magnetic base station data were not collected to remove diurnal magnetic variations.

3.5 ORTHOPHOTOS

Although the use of orthophotos is not a truly geophysical technique, it proves invaluable in the search for groundwater. Important information that can be derived from these 1:10 000 maps are:

- important topographical features and relationships
- rivers, fountains, springs and catchment areas
- available infrastructure such as roads, existing dams and villages
- accurate positioning in the field when searching for target structures
- delineation of structural features such as faults and shear zones visible on the surface
- information assisting in planning of ground surveys
- vegetational trends

CHAPTER 4

INTEGRATING MULTIDISCIPLINARY DATA SETS USING A GIS

4.1 INTRODUCTION

Due to the multidisciplinary nature of the study, a mechanism was needed to incorporate data sets of different origin, different spatial attributes and different formats. Two PC based programs were used to accomplish this. The first is Arcview 3.1 and the second is Oasis Montaj 4.1 from Geosoft. Oasis was used for its data processing capabilities especially with respect to the airborne geophysical data. All relevant maps and profiles generated in Oasis are exported to Arcview 3.1 so that the end user of the database will only need Arcview.

The following data sets were incorporated into the database:

- Geology and large scale topocadastral data
- Small scale topocadastral Data
- Ground Geophysical and borehole Data
- Structural Geology
- Airborne Geophysics
- Orthophotos

The origin, format and relative contribution of each set will be discussed briefly in the rest of this chapter.

4.2 GEOLOGY AND LARGE SCALE TOPOCADASTRAL DATA

The geology and large scale topocadastral data of the test area and surroundings came from BOSGIS. This is a GIS database developed by the Bushveld Research Institute at the Geology Department, University of Pretoria. A subset of this data is shown in figure 3. This data came in Arcview format and could be incorporated directly into the present database. The data it contains was digitised from 1:250 000 geological maps of the Council for Geoscience which is not as high in resolution as most of the other data sets, but due to the relative simple nature of

the geology, it proved to be sufficient for the purpose of the study. The large scale topocadastral data unfortunately did not have the resolution required and were not used extensively in the study. The geological data are used during interpretation of the geophysics, the development of a model for the study area and on selecting possible targets.

The data consist of:

- the major lithological units - Nebo Granites and Dolerite intrusions for the area under investigation (polygon themes)
- faults, dykes and lineaments (line themes)

Due to the resolution problem however, these features could not be located accurately enough to serve directly as targets for ground geophysics. The main structural directions were identified from them, and some of these structures have been correlated with other data sets and placed more accurately on that basis.

4.3 SMALL SCALE TOPOCADASTRAL DATA

Once the test area was identified, small scale topocadastral data was digitised from the 1:10000 orthophotos. This was done on contract by GISLab at the University of Pretoria. This data also came in Arcview 3.1 format and contains the following themes, figure 10:

- villages (polygon themes)
- rivers (line themes)
- roads (line themes)
- contours at 20 m intervals (line themes)

These data sets are used to determine topographic influences, accessibility options, recharge possibilities and structural correlations, e.g. where rivers apparently follow linear features such as faults. The contour theme data were also used to create a Digital Terrain Map (DTM) to highlite topographical and structural features (Botha, 1997).

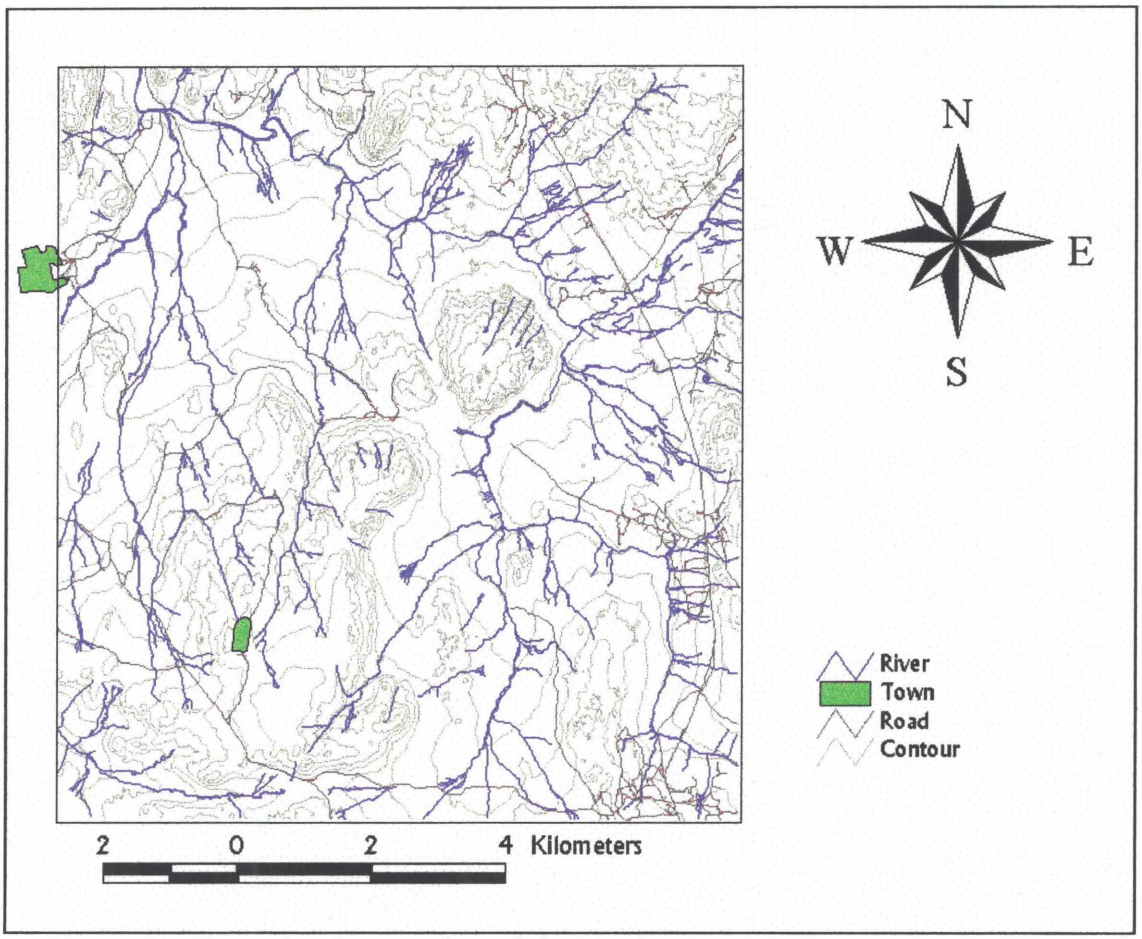

Figure 11: Example of topocadastral data in Arcview 3.1.

4.4 GROUND GEOPHYSICAL AND BOREHOLE DATA

The data format and the presentation of ground geophysics and borehole information were discussed in 2.2. Superimposing these data sets over other data sets allows one to decide whether a borehole can be associated with an identifiable structure on any of the other data sets. This information can then guide the groundwater exploration program. Deductions that can be made using the GIS approach are:

- which structures have groundwater development potential

- where would be the best place to explore and exploit these in terms of accessibility, needs of local population, recharge, future management and pollution/environmetal dangers
- which techniques would be best suited for finding and identifying the structure
- what typical response should be expected when using such a method
- where would the optimal drilling position be on an associated geophysical anomaly

It would also assist in further hydrogeological, engineering and environmental studies.

4.5 STRUCTURAL GEOLOGY

The detailed structural geology of the study area was mapped by Hoffman (1997) as part of a Bsc. (Hons) project, digitized and incorporated into the Arcview 3.1 database (Figure 11).

Figure 11: Map showing structural features (Botha, 1997).

From this data the main structural directions were calculated in much more detail and possible target features such as prominent faults and shear zones were identified. As can be expected, this data shows a very good correlation with the airborne geophysical data. There are, however, certain features visible which are not prominent on the airborne geophysical data and vice versa. This only serves to illustrate the point that there is no one ultimate technique in groundwater exploration and that a combination of different disciplines prove to be essential. The success of the structural data set is of course dependant on the amount of outcrops visible to the geologist. In the investigation area there were an abundance of these, making a very thorough study possible. The format of this data are line themes in Arcview 3.1.

4.6 AIRBORNE GEOPHYSICS

The airborne data consist of total field magnetic data, DIGHEM frequency domain EM data at three frequencies and radiometric data.

The airborne geophysical data are in Oasis Montaj format due to the fact that all the processing and interpretation were done using the Oasis software. In order to view this data in Arcview 3.1 it has to be exported from Oasis and imported to Arcview 3.1. This is done in raster format

(e.g. a TIFF file). This data can then be combined with other data sets, provided these other data sets are in vector format. This is due to the fact that two raster format data sets occupying the same space are not transparent. Only the top one can be seen and information on the bottom one cannot be accessed. Furthermore, seeing that there are no attributes connected to these data sets, queries cannot be performed on them and digital values for the data cannot be accessed in Arcview 3.1.

The information conveyed, however, through the raster image is sufficient to allow spatial correlations to be made with the other data sets. In this respect Oasis Montaj can be used with much more accuracy, since these data sets can be combined by making use of linked cursors in different windows following either the grid images or profiles as shown in figure 12.

This data are used to delineate structural features and lithological units. Correlated with one another and the other data sets they prove invaluable in identifying the main structural features as well as giving information on the state of weathering of these structures. The magnetic data can also be downward continued to give an "expected profile" at any position on the ground. This proves especially helpful when looking for a specific structure during the ground follow-up stage (figure 13).

4.7 ORTHOPHOTOS

The 1:10 000 orthophotos were scanned and imported into the Oasis Montaj software. This data are also in the raster format but provide very useful information when siting target areas for further ground follow-up work. This data set is invaluable in planning a ground survey, allowing one to consider the strike direction of the target, as well as accessibility and possible obstacles such as dense vegetation or topographical features. Orientation in the field is much easier and optimal survey line lengths, directions and positions can be decided before visiting the site. This, in turn, saves time and money once the ground follow-up has to be done.

In some cases the targets are of such a nature that a drilling position can be sited from the airborne data without the need of ground geophysics. Accurate positioning in the field can be done from the orthophoto where there are prominent landmarks nearby. Another very helpful

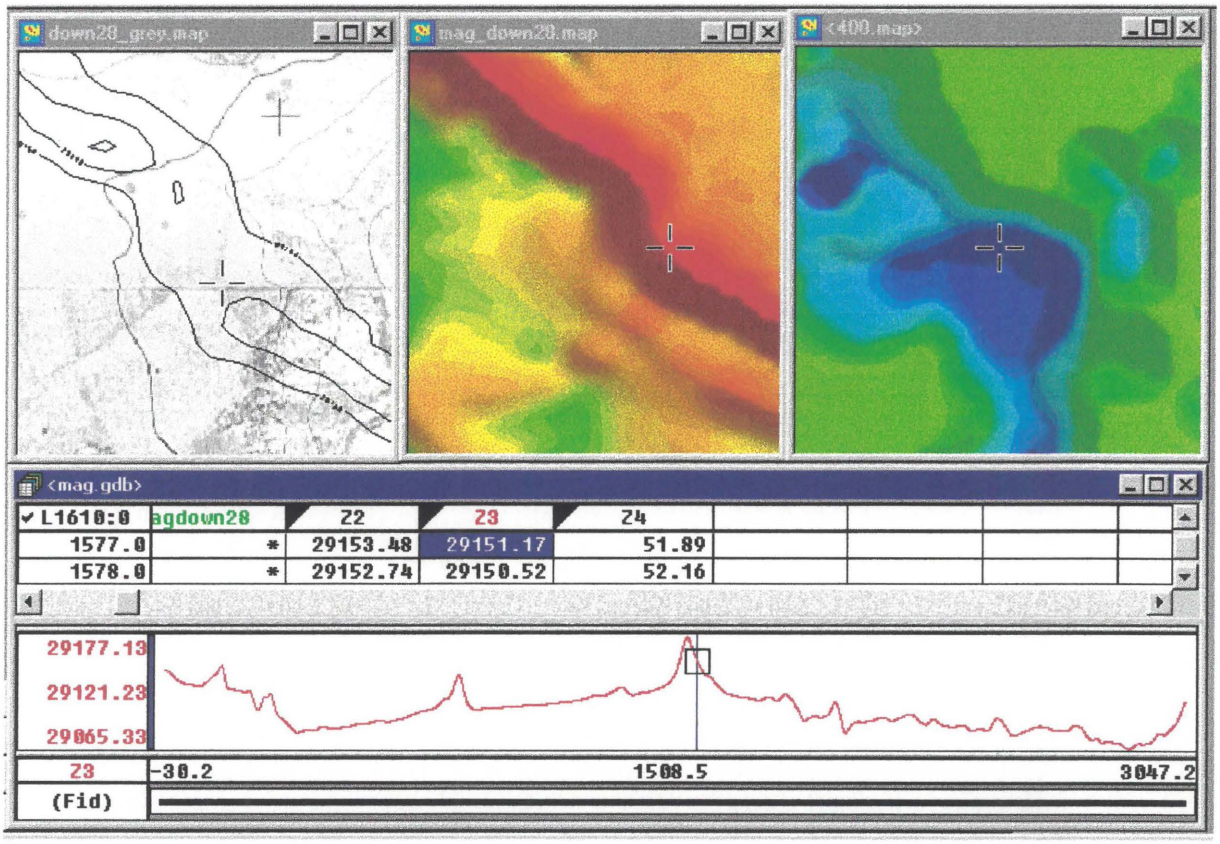

Figure 12: Window from Oasis Montaj showing different data sets of the same area (orthophotos, magnetic and EM34 data with magnetic profile), all linked by the same cursor.

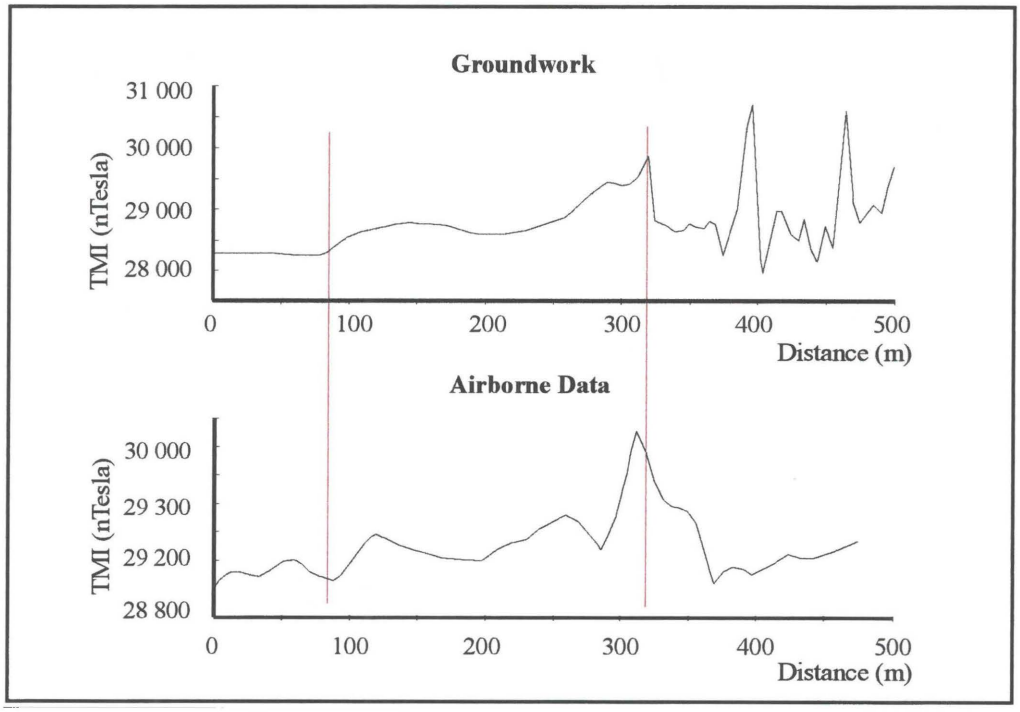

Figure 13:Comparison between downward continued airborne magnetic data and data acquired through groundwork along the same profile.

feauture provided in the Oasis Montaj software is the ability to superimpose the contour data on the orthophotos. This enables the ground geophysicist to locate targets in the field and helps to decide when the target structure has been identified and mapped.

4.8 SUMMARY

The GIS approach allows one to compare any two or more data sets with one another and identify spatial correlations. When a feature of interest is therefore identified on any one data set it can be compared to the other data sets and from that the most effective technique to find and/or map this feature can be decided. The software futher allows one to readily obtain the exact coordinates of an identified feature.

Furthermore, all available geophysical data previously used in the area, as well as all the information on existing boreholes can easily be accessed. Not only can potential targets for groundwater exploration be identified, but management decisions such as which areas have to be developed first due to the greatest shortage of water, or which areas have the highest risk of pollution, can be made with easier and faster access to relevant information.

This type of database can of course be developed to include other data sets as well without losing or changing any of the original data, and if there are changes in the original sets they can be updated as well. This must be seen as a dynamic system, developed to aid any groundwater related scientist to make better informed decisions in either exploration or management.

CHAPTER 5

PROCESSING AND INTERPRETATION OF AIRBORNE GEOPHYSICAL DATA APPLIED TO THE SITING OF BOREHOLES

5.1 INTRODUCTION

Three airborne geophysical techniques were investigated namely:

- Frequency domain electromagnetism
- Total field magnetics
- Radiometrics (consisting of Thorium, Uranium, Potassium and Total count measurements)

The survey coverage consisted of 1177 line kilometers, including 31 line kilometers for tie-lines. Flight lines were flown in an azimuthal direction of 0°/180° with a line separation of 100 metres. The helicopter (Bell 206L-3 turbine helicopter) flew at an average airspeed of 136km/h, with an EM bird height of 30m, magnetic bird height of 40m and spectrometer at 60m (Pritchard, 1997). The airborne data were digitised using a 10Hz sampling frequency. This implies an average ground station spacing of approximately 7m.

5.2 AIRBORNE ELECTROMAGNETIC DATA

5.2.1 DIGHEM data aquisitioning

The EM system used was the DIGHEM^{V} model. The DIGHEM system is an airborne frequency domain electromagnetic system utilizing both co-planer and co-axial configurations. Data from the co- axial coil configurations are used to supplement the co-planar data. The system utilizes the multi-coil coaxial/coplanar technique to energize conductors in different directions. There are five coil pairs, three co-planar (horizontal) and two co-axial (vertical with axes in flight direction). An in-phase and quadrature phase channel is recorded from each transmitter-receiver coil pair. It is a towed bird type system with a symmetric dipole configuration. The coil separation is 8m for the 400Hz, 900Hz, 5500Hz and 7200Hz, and 6.3 meters for the 56kHz coil-pair, (Pritchard, 1997). The coil orientations and frequencies are given in Table 2.

Five in-phase and five quadrature channels are recorded as well as two monitor channels.

Coil orientation	*Nominal frequency*	*Actual frequency*
Co-axial	900 Hz	1 141 Hz
Co-planar	425 Hz	389 Hz
Co-axial	5 500 Hz	5 355 Hz
Co-planar	7 200 Hz	7 209 Hz
Co-planar	56 000 Hz	55 890 Hz

Table 2: Coil orientations and frequencies of Dighem system (Pritchard, 1997).

The targets for this system, (as for all EM systems) are conductors. The DIGHEM responses fall into two general classes, discrete and broad. The first class encompasses sharp, well-defined anomalies from discrete conductors such as sulphide lenses and steeply dipping sheetlike conductors (e.g. graphite sheets). The second class consists of wide anomalies from conductors having a large horizontal surface (e.g. conductive overburden and flatly dipping sheetlike conductors). The conductive earth (half space) model can be suitably classified with the broad conductors, and is the model used for creating resistivity contour maps (figures 14 to 16), (Sengpiel, 1983).

The application of the DIGHEM system to groundwater exploration is motivated on the basis that weathered material usually is more conductive than its unweathered counterparts. Since weathered rock material allows increased groundwater movement, conventional wisdom associates weathered structures with possible aquifers. Zones of deep weathering, especially if they are coincident with large structural features, were the important features being investigated in this study and the DIGHEM data were used to locate and delineate such structures in the area under investigation.

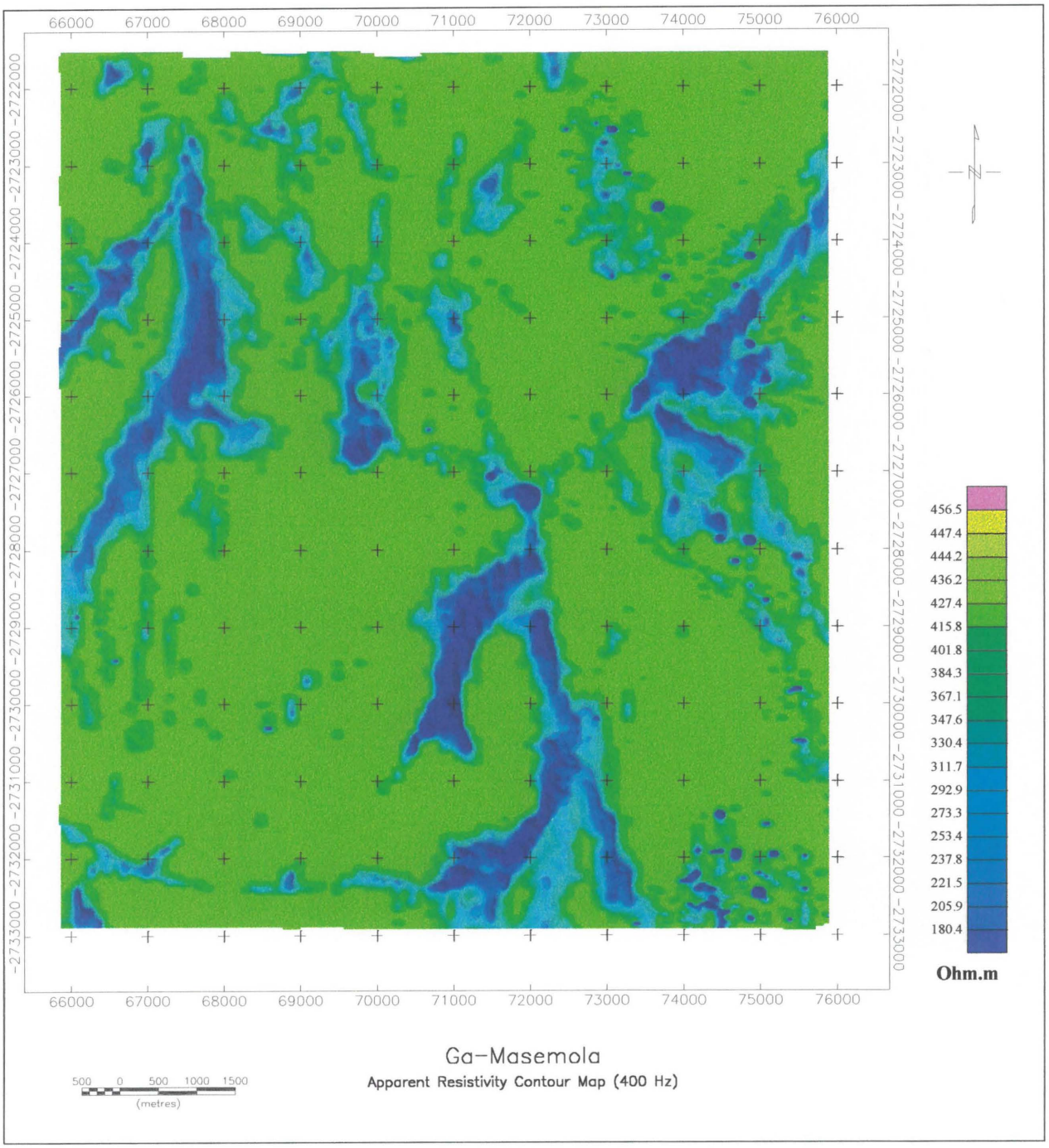

Figure 14: DIGHEM resistivity contour map for 400Hz frequency. (Blue indicates high conductivity.)

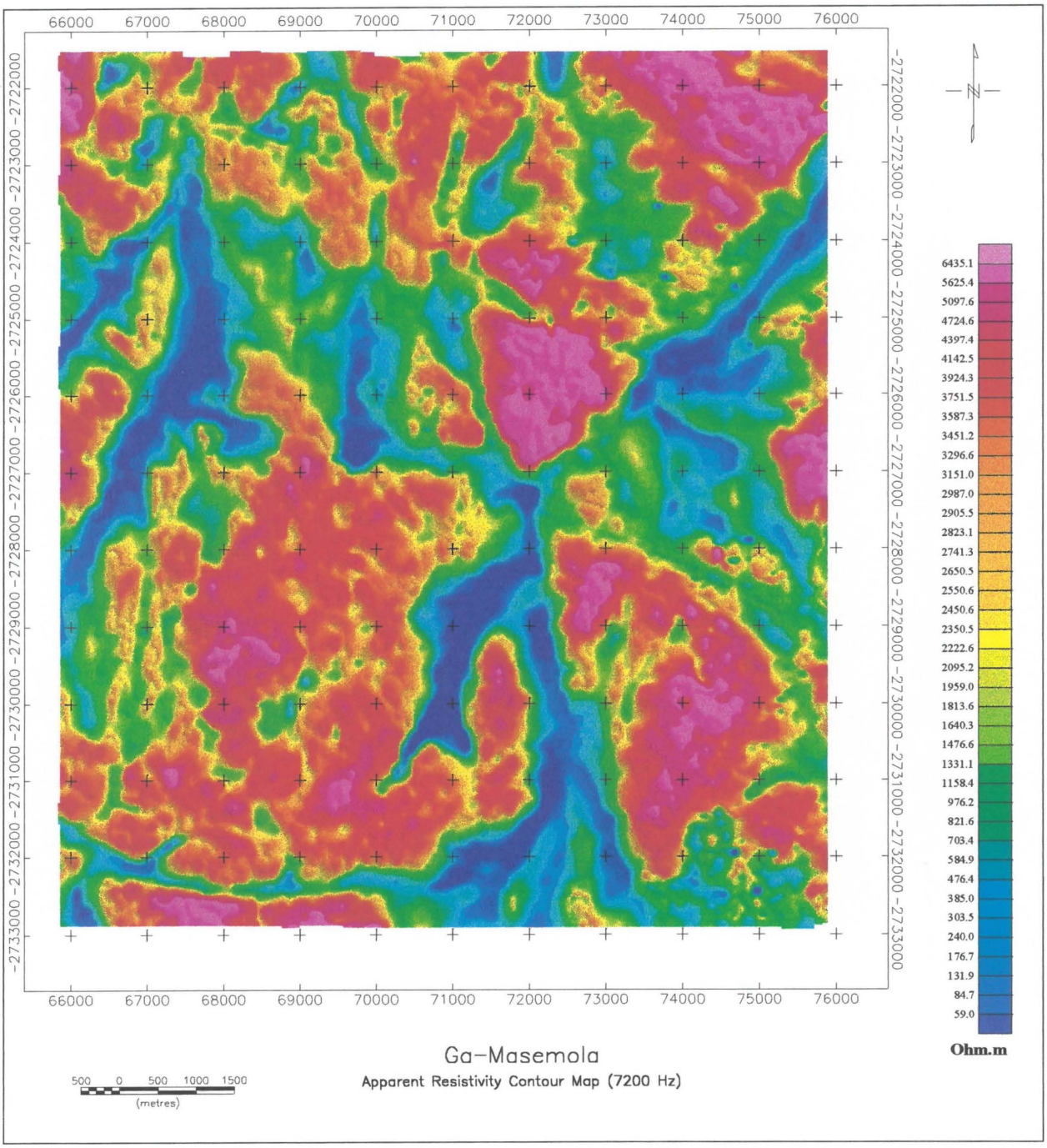

Figure 15: DIGHEM resistivity contour map for 7200 Hz frequency.

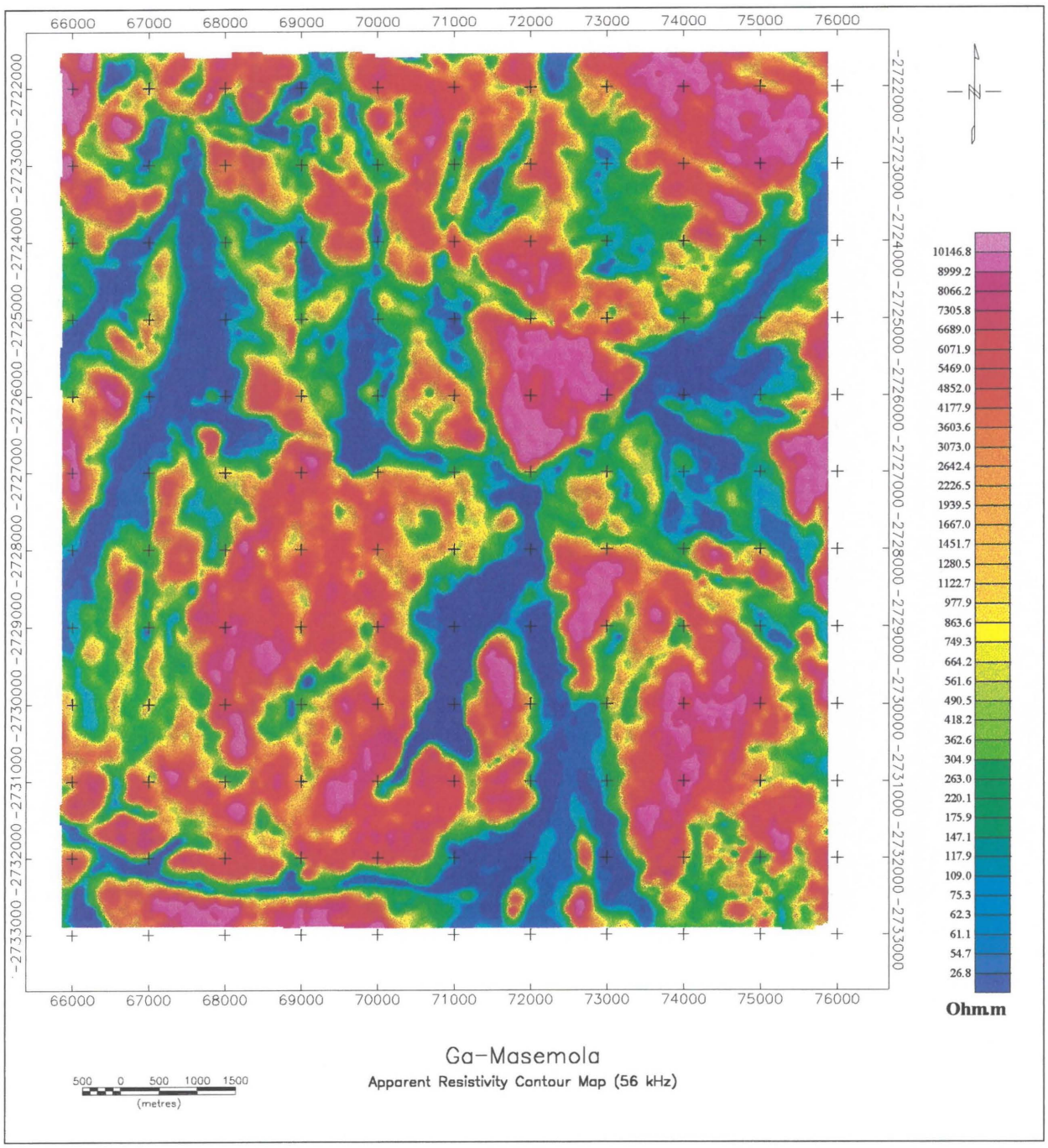

Figure 16: DIGHEM resistivity contour map for 56 kHz frequency.

5.2.2 Interpretation of the DIGHEM data

The focus of the interpretation was to identify regional structures such as faults or any other conductive features that could be correlated with zones of extensive weathering and therefore possible aquifers. The lowest frequency data (400Hz in this case) provides the deepest conductivity information according to the skin depth relation δ (Telford, 1990):

$$\delta = \left(\frac{2}{\omega \mu \sigma} \right)^{\frac{1}{2}} \qquad (5.1)$$

with:

ω = angular frequency

μ = magnetic permeability

σ = apparent conductivity

The deep structures were the main targets since they are ostensibly less sensitive to droughts.

The apparent resistivity contour maps were used, together with contour maps of the quadrature phase response (figures 17 and 18), to identify and map conductive linear target features. The quadrature phase contour maps enhance the smaller conductivity features that are not readily visible on the resistivity maps and also provide a more detailed delineation of the structures. Furthermore, the 900 Hz co-axial data show targets perpendicular to the flight line direction more clearly.

The main targets were traced with thick black lines on the 400 Hz apparent resistivity map. Smaller features were filled in with thin blue lines by making use of the 400 Hz, 7200 Hz and 56 kHz maps. The dotted red lines show features that were defined more clearly by making use of the quadrature phase contour maps. The results of this interpretation are shown in figure 19.

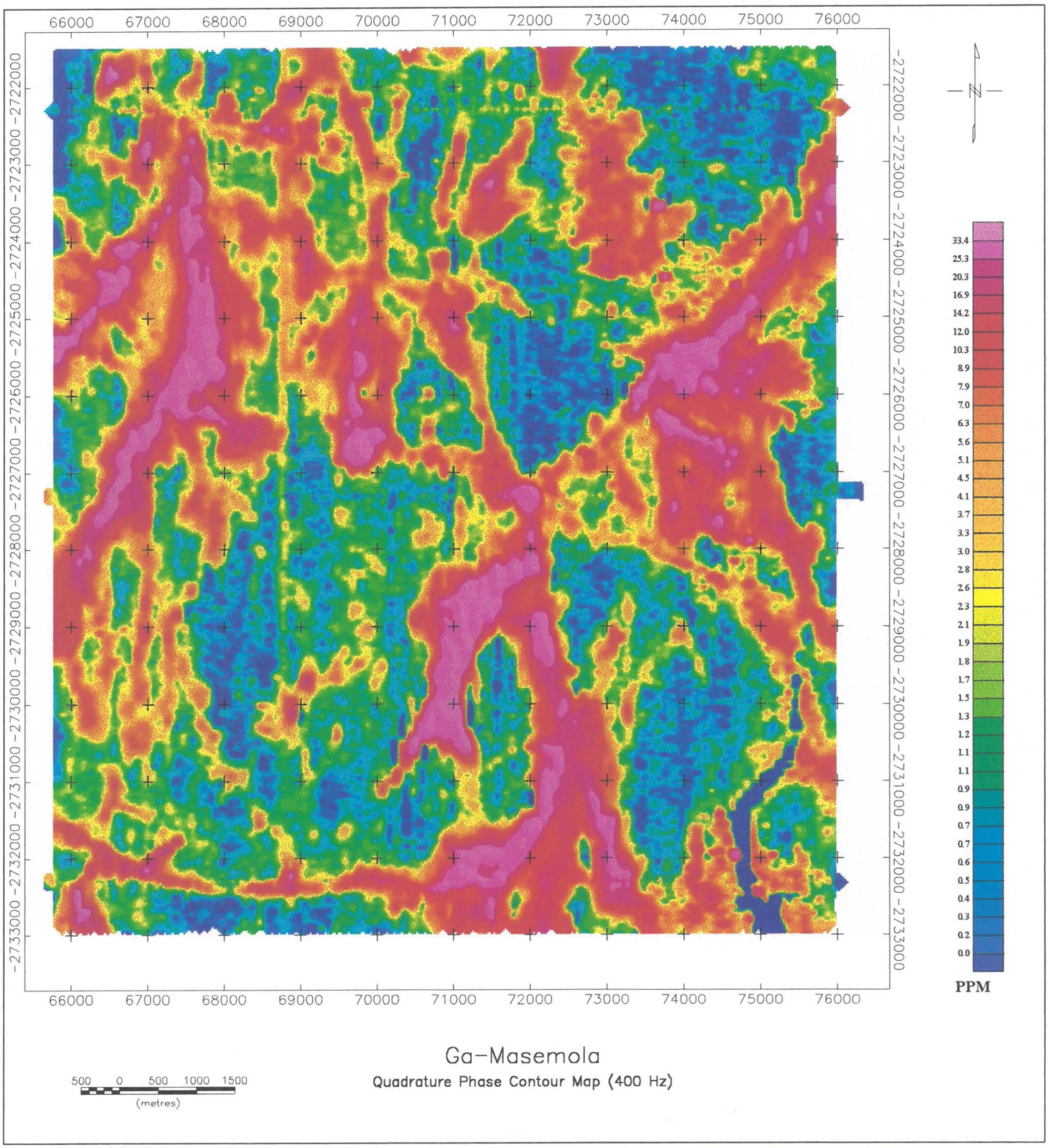

Figure 17: Contour map of the quadrature phase component (400 Hz, co-planar).

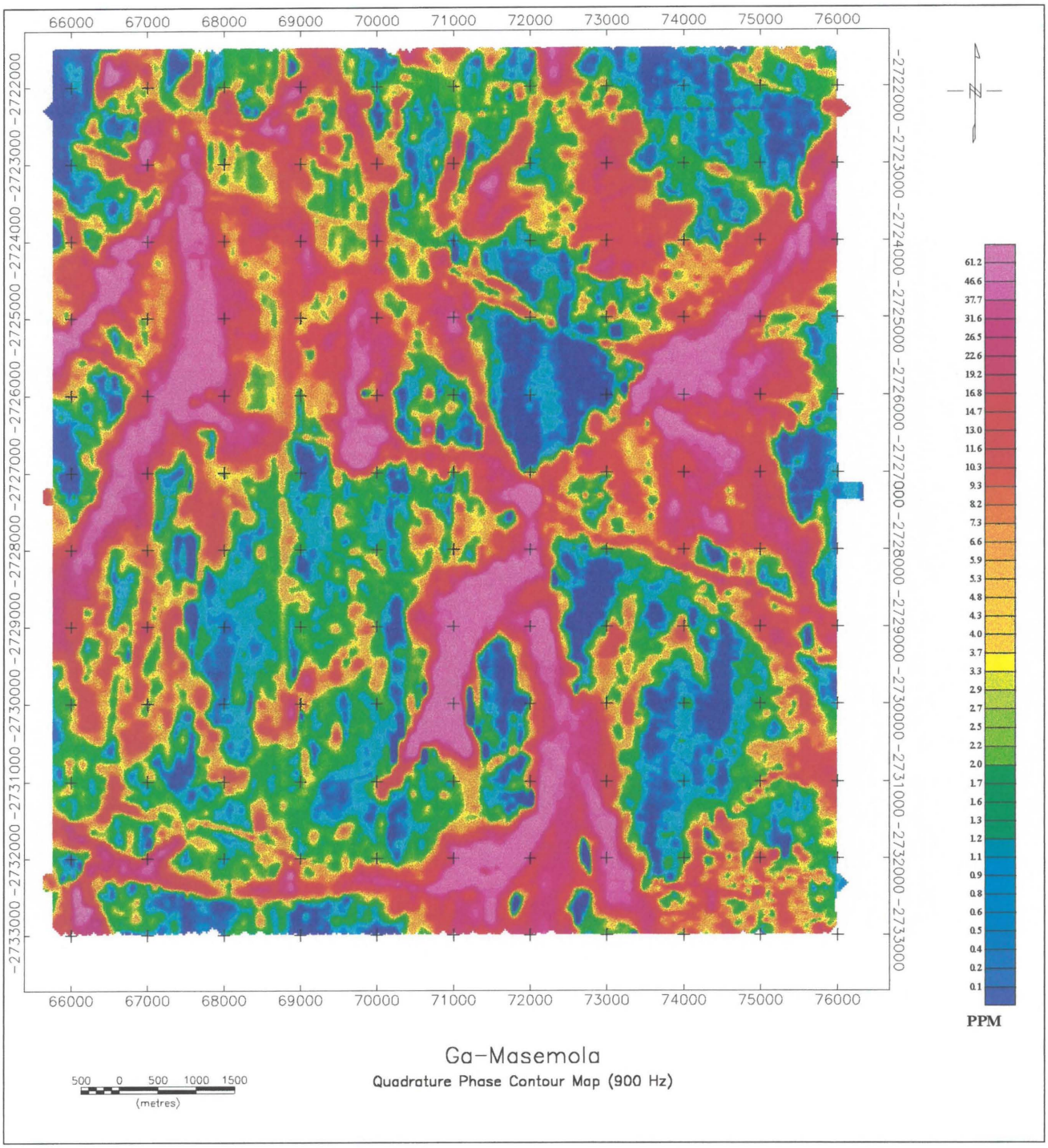

Figure 18: Contour map of the quadrature phase component (900 Hz, co-axial).

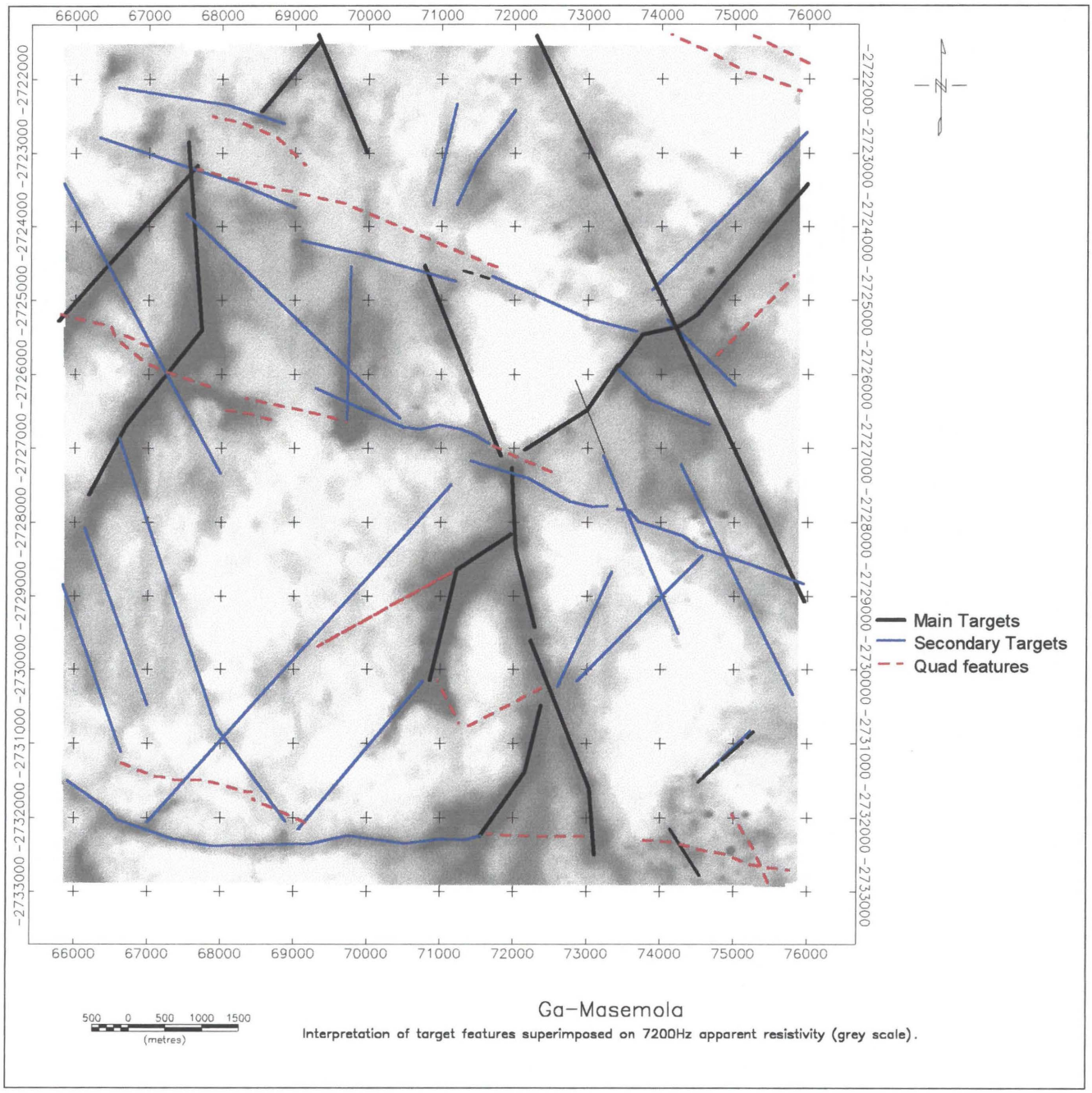

Figure 19: Interpreted structural features.

5.3 AIRBORNE MAGNETIC DATA

5.3.1 Magnetic data acquisitioning

The magnetometer used was a Scintrex H8 Cesium Vapour type with sensitivity of 0.005 nT. A sampling rate of 10 Hz was achieved and this sensor was also towed in a bird 20 m below the helicopter (± 40m above the ground).

A digital recorder containing a clock synchronized with that of the airborne system, was operated together with a base station magnetometer to record, and permit subsequent removal of diurnal variations of the earth's magnetic field. The base station magnetometer was a Geometrics G856-X, proton precession instrument with a sample rate of 30 seconds, (Pritchard, 1997).

The airborne magnetic data are used to identify and map different lithological units and structural features. Different lithological units give different responses due to differences in magnetite content. Faults can be inferred from a displacement in a magnetic unit. By modeling profiles taken from the airborne data sets other important parameters such as depth, dip and depth extent can also be determined. These profiles also serve as an important "datalink" between the airborne and ground follow-up data (figure 13).

5.3.2 Magnetic data processing and interpretation

By overlaying a simplified version of figure 3 (geology of the study area) on the total magnetic field map, a definite correlation can be seen with the shallow magnetic features and the geology (figure 20). The high magnetic values (red) clearly represent the dolerite sills and dikes as expected, due to the noticeable higher magnetite content in dolerite, relative to granite, (Telford, 1990). On the magnetic data it is clearly seen that the dolerite sill extends to the east and intruded into the granite. There are also east-west striking dolerite dikes in the eastern half of the area. It should be noted that the magnetic amplitude variation in the study area is small, varying between 28900nT and 29400nT.

Several filters were applied to the magnetic total field data to highlight certain features.

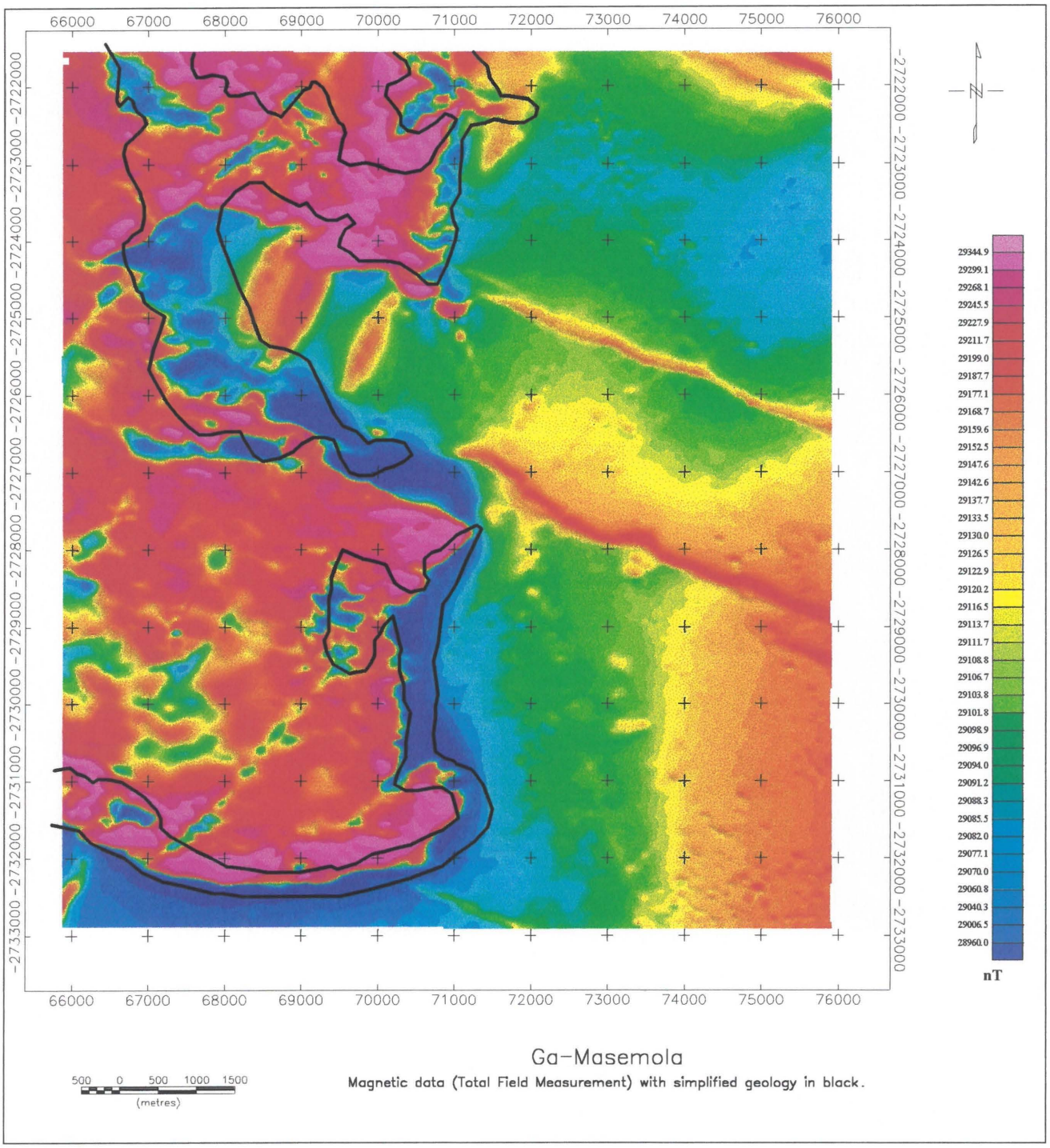

Figure 20: Magnetic total field with simplified geology superimposed

5.3.2.1 Analytical signal

Nabighian (1972) has shown that for two-dimensional bodies a bell-shaped symmetrical function can be derived which maximizes exactly over the top of a magnetic contact. The three-dimensional case was derived in 1984 also by Nabighian. This function is the amplitude of the analytical signal. The only assumptions made are uniform magnetization and that the cross-section of all causative bodies can be represented by polygons of finite or infinite depth extent. This function and its derivatives are therefore independent of strike, dip, magnetic declination, inclination and remanent magnetism, (Debeglia and Corpel, 1997).

The 3-D analytical signal A, of a potential field anomaly can be defined (Nabighian, 1984) as:

$$A(x,y) = \left(\frac{\partial M}{\partial x}\right)\hat{x} + \left(\frac{\partial M}{\partial y}\right)\hat{y} + \left(\frac{\partial M}{\partial z}\right)\hat{z} \qquad (5.2)$$

with :

M = magnetic field.

The analytical signal amplitude can now be calculated (Debeglia, 1997) as:

$$|A(x,y)| = \sqrt{\left(\frac{\partial M}{\partial x}\right)^2 + \left(\frac{\partial M}{\partial y}\right)^2 + \left(\frac{\partial M}{\partial z}\right)^2} \qquad (5.3)$$

This filter was applied to the airborne magnetic total field data, yielding figure 21. Comparing this with figure 20 (total field), the difference is most obvious along the edge of the dolerite sill in the southwestern quarter. Using the superimposed geology as standard, it is seen that the analytical signal amplitude maximizes over the edge of the sill. In interpreting the data, the edges of three-dimensional bodies and the centers of two-dimensional bodies were delineated using the peak values of the analytical signal amplitude.

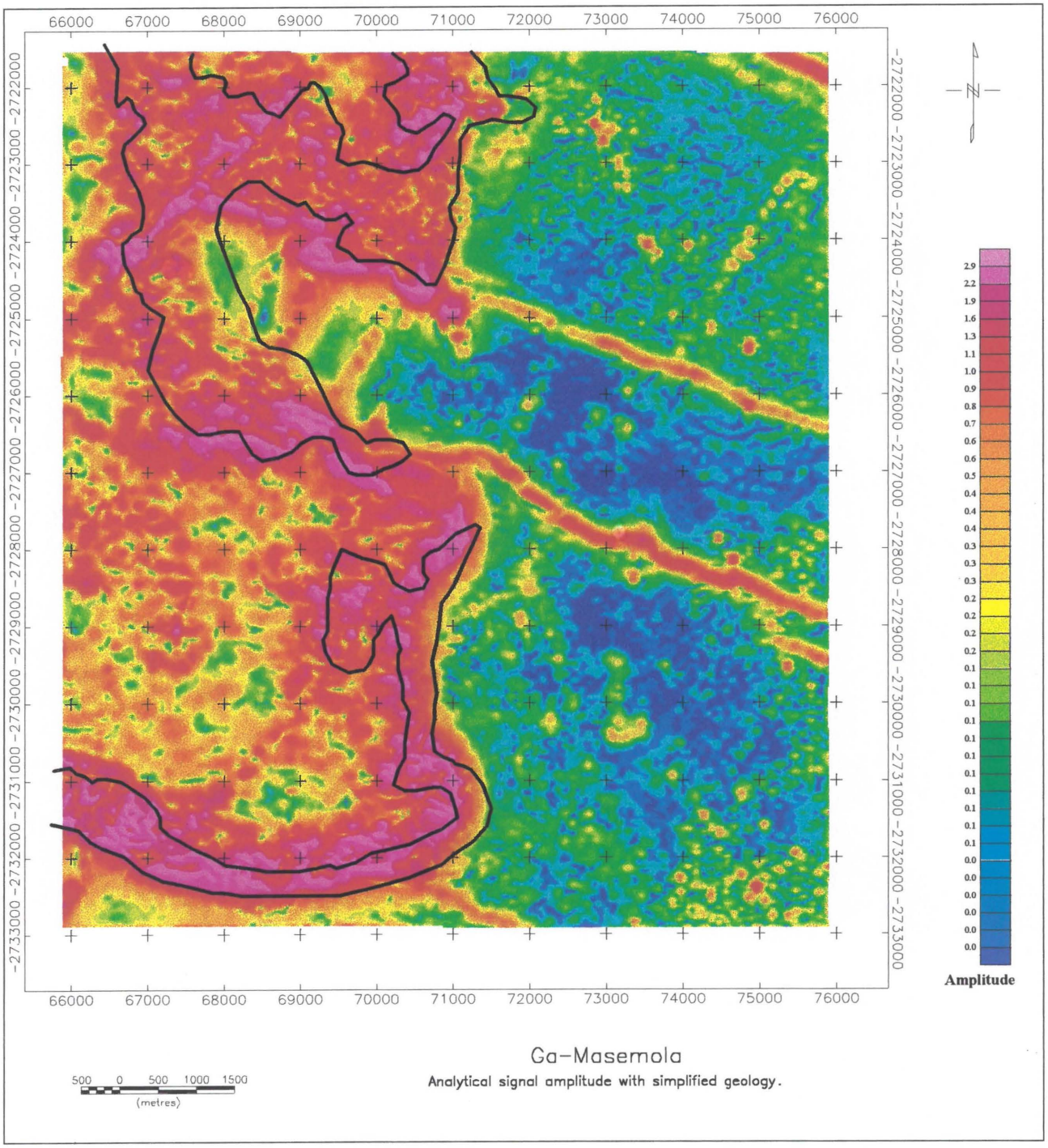

Figure 21: Analytical signal amplitude.

{In the discussions below, the following parameters are used. (Geosoft Inc., 1996):

μ	*X wavenumber (complex, radians/m)*
ν	*Y wavenumber (complex, radians/m)*
$r = \sqrt{\mu^2 + \nu^2}$	*Wavenumber (radians/m)*
$\theta = \tan^{-1}(\mu/\nu)$	*Wavenumber direction*

}

5.3.2.2 Reduction to the magnetic equator

Reduction to the magnetic equator is used in regions of low latitude to center the peaks of anomalies over the causative bodies. This allows for more accurate interpretation of the data under certain physical conditions. Unlike the analytical signal filter, this procedure is subject to the influences of remanent magnetization. The filter expression is given as, (Geosoft Inc., 1996):

$$L(\theta) = \frac{-\cos^2(D-\theta)}{\left[\sin I + i.\cos I.\cos(D-\theta)\right]^2} \qquad (5.5)$$

with:

I	geomagnetic inclination
D	geomagnetic declination

The result of this filter is shown in figure 22. Features striking northeast are more clearly delineated on this map, especially in the western half of the area.

5.3.2.3 Reduction to the magnetic pole

A reduction to the pole transform (figure 11) will provide a symmetrical anomaly over a vertically dipping, non-remanent body and is again used to improve interpretability under certain conditions. At low latitudes, however, an amplitude correction is required to prevent north-south signals from dominating the data. This filter can be described as (Geosoft Inc., 1996):

$$L(\theta) = \frac{1}{\left[\sin(I_a) + i\cos(I).\cos(D-\theta)\right]^2} \qquad (5.6)$$

with:

I geomagnetic inclination

I_a inclination for amplitude correction ($I_a > I$)

D geomagnetic declination

For two-dimensional structures the anomaly peaks correlate very closely with the analytical signal peaks, indicating that the effect of remanent magnetism is relatively small.

5.3.2.4 Downward continuation

Downward continuation is used to enhance features at a specified depth/level (lower than original acquisition level) by bringing the plane of measurement closer to the sources. The procedure is susceptible to high frequency noise. This data is especially useful for ground follow-up work when downward continued to ground level. The expression (Geosoft Inc., 1996) is:

$$L(r) = e^{hr} \qquad (5.7)$$

with:

h distance in meters, to continue downward.

Figure 24 shows the airborne data downward continued to ground level (h=38m). This map enhanced features in the low amplitude eastern half of the area, and gives an overall sharper image with more detail on the shallow features.

5.3.2.5 Upward continuation

Upward continuation attenuates high frequency data while enhancing the deeper basement anomalies (figure 25). Depending on the distance (h) used to upward continue the data, it can

also be used to define a regional or background field. Upward continuation is described (Geosoft Inc., 1996) as:

$$L(r) = e^{-hr} \qquad (5.8)$$

with:

h distance in meters, to continue upward.

5.3.2.6 Vertical Derivatives

The first vertical derivative (figure 26) is used to enhance the shallow geologic sources in data and often is useful in delineating high frequency features more clearly where they are shadowed by large amplitude, low frequency anomalies. The expression (Geosoft Inc., 1996) is:

$$L(r) = r^n \qquad (5.9)$$

with:

n order of differentiation

This map shows much more detail in the eastern half of the area than any other map, and also enhances magnetic low features that are superimposed on magnetic high structures.

5.3.2.7 Attenuating low frequency anomalies

From the perspective of prospecting for groundwater bearing structures the features at depths less than 150m are important and it is necessary to isolate their response for interpretation. This can be done in several ways. One approach is to use the upward continued data as a background or regional data set. By subtracting the upward continued grid file from the original data the anomalies caused by shallow features are enhanced, (figure 27).

The maps created through the application of these filters were used interactively in Oasis Montaj to do an interpretation of the data. Magnetic units, dykes, faults and various lineaments were identified and mapped (figures 28 and 29).

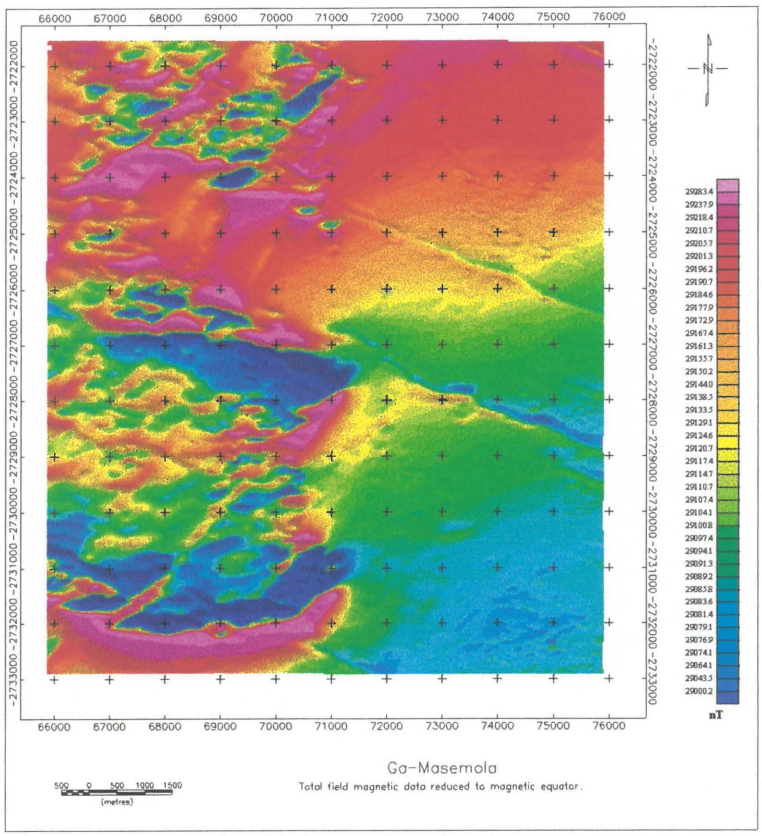

Figure 22: Total field data reduced to the magnetic equator.

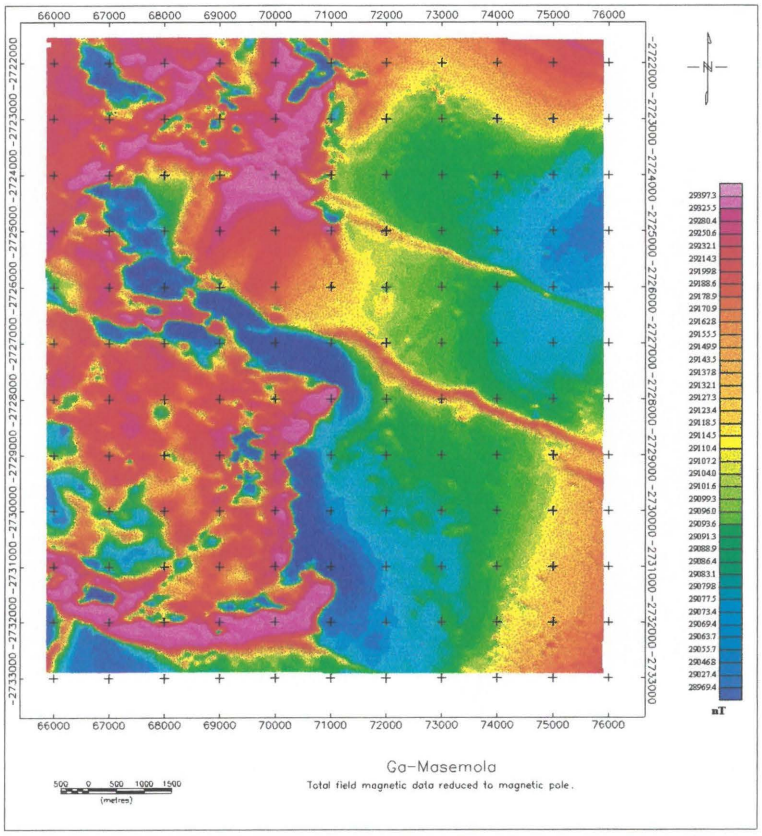

Figure 23: Total field data reduced to the magnetic pole.

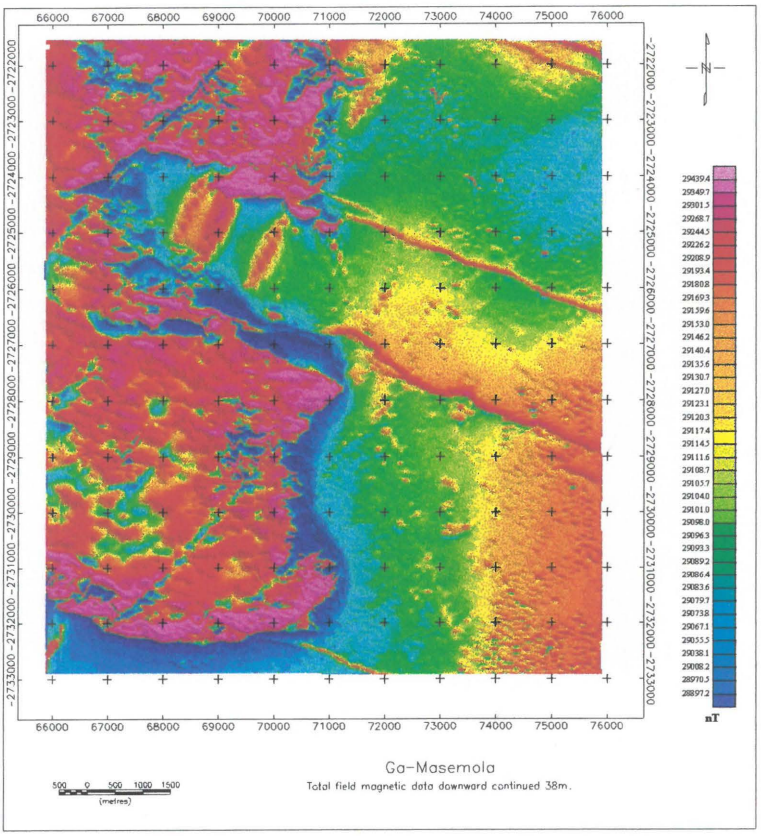

Figure 24: Total field data downward continued 38m.

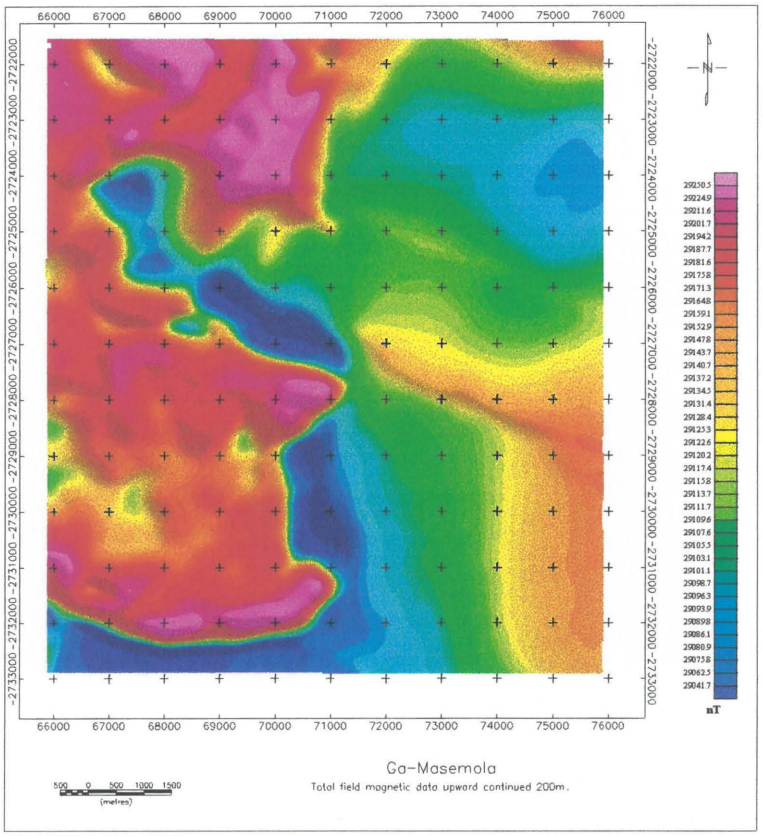

Figure 25: Total field data upward continued 200m.

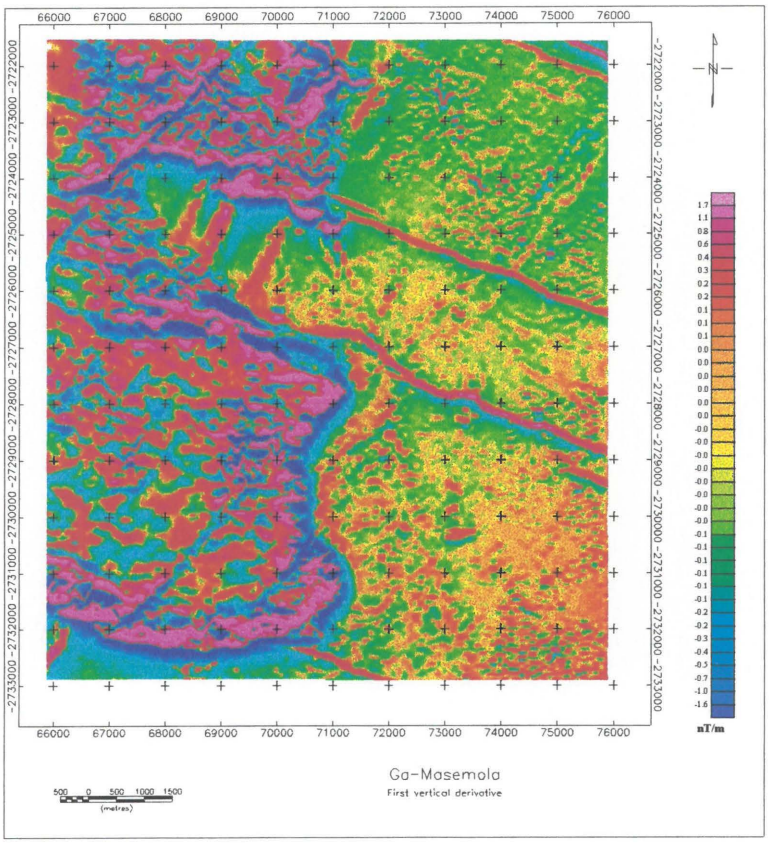

Figure 26: First vertical derivative

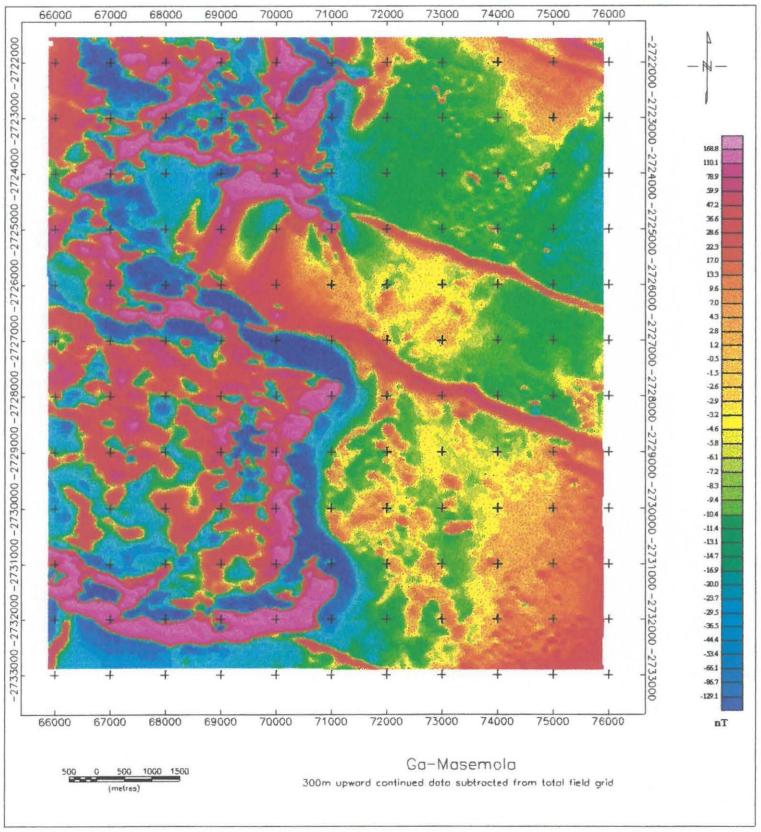

Figure 27: Map showing the residual after the 300m upward continued data is subtracted from the total field data.

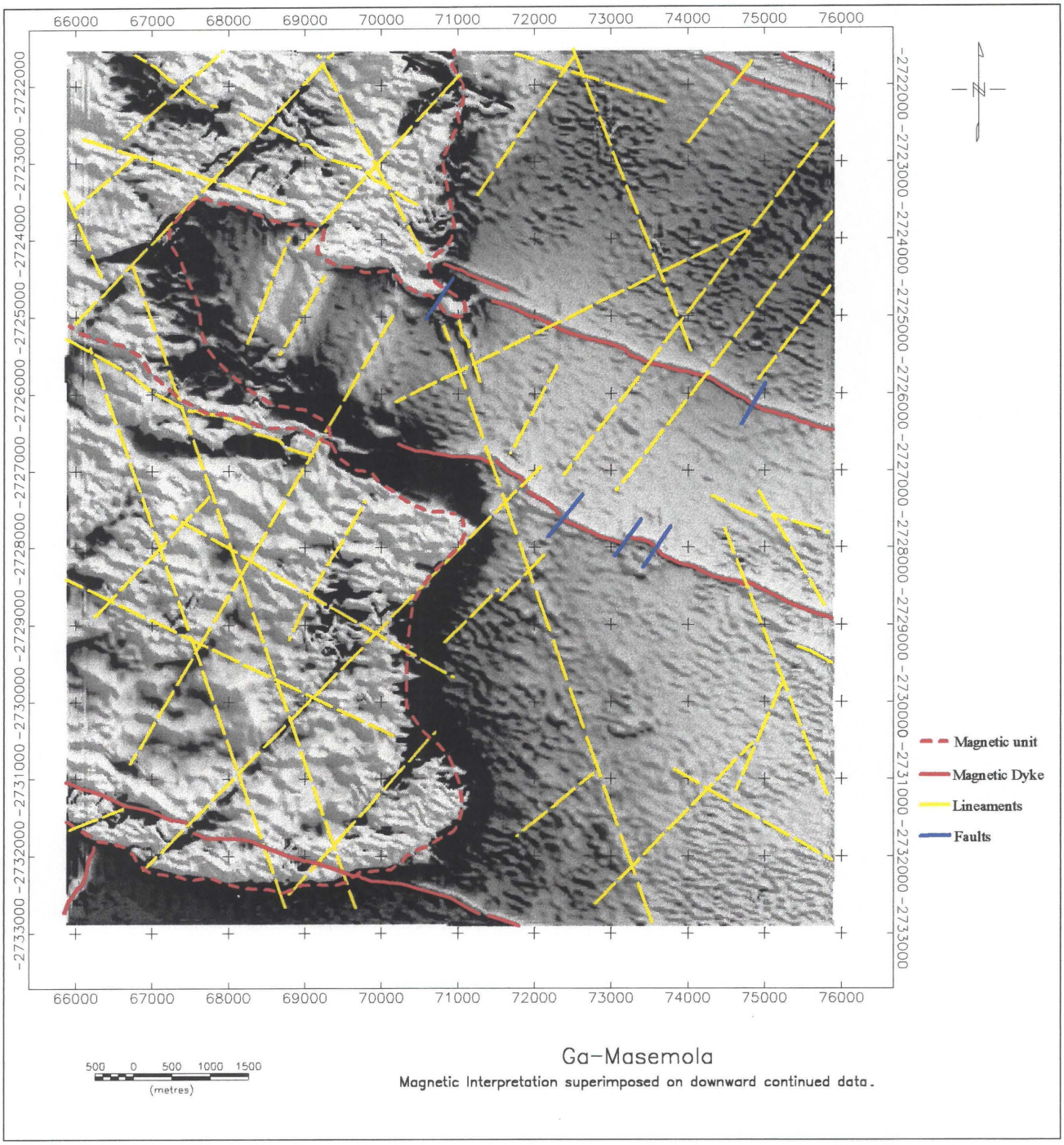

Figure 28: Magnetic interpretation superimposed on downward continued data.

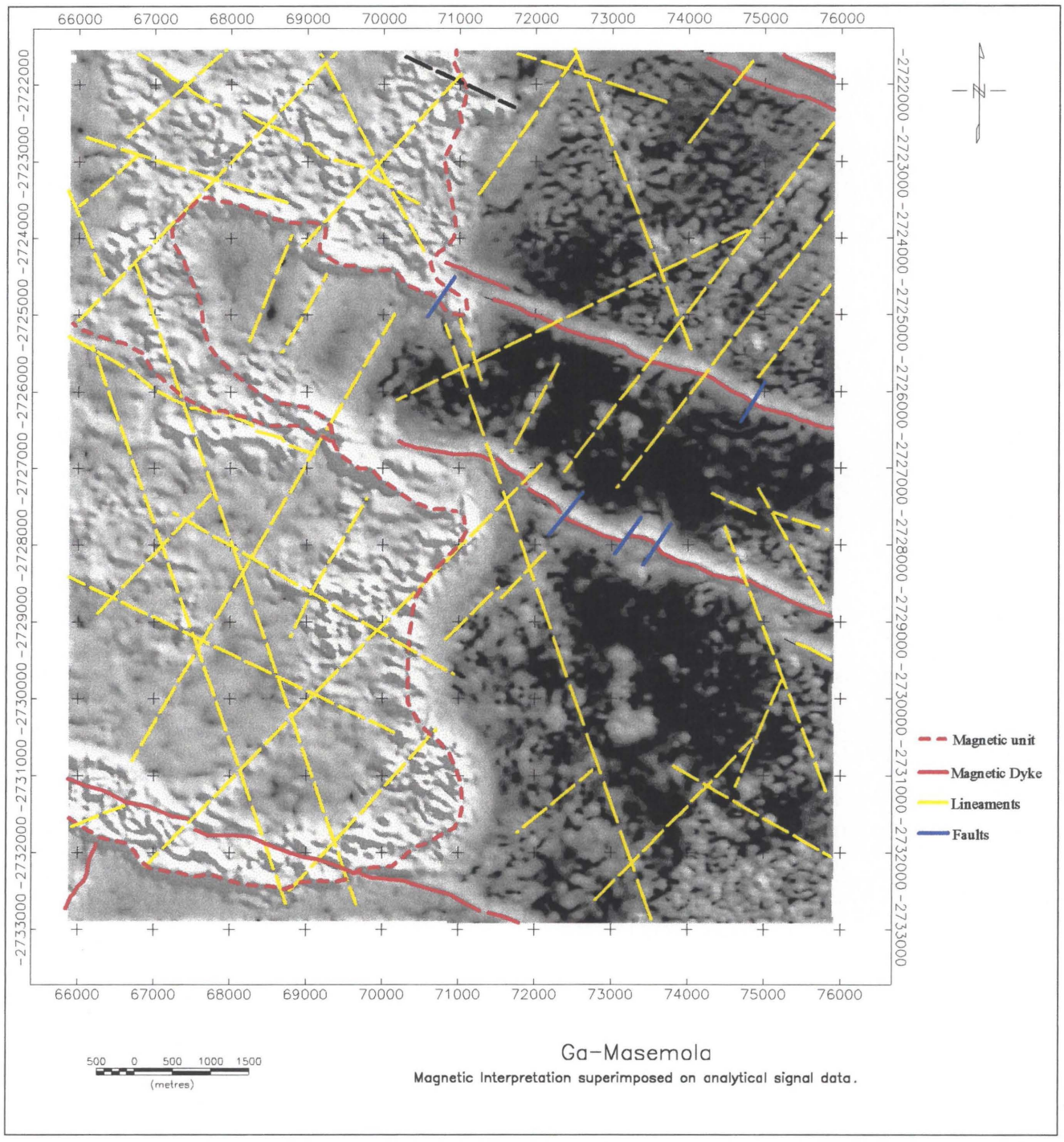

Figure 29: Magnetic interpretation superimposed on analytical signal data.

5.3.2.8 Euler deconvolution

Three dimensional Euler deconvolution is an algorithm which can be applied to magnetic or gravity survey data that are in grid form. The algorithm solves for source positions and depths by deconvolution using Euler's homogeneity relation and geological constraints imposed through the use of a structural index (SI) (Reid, 1990).

From Thompson (1982) the Euler's homogeneity relation is given as:

$$(x-x_0)\frac{\partial T}{\partial x}+(y-y_0)\frac{\partial T}{\partial y}+(z-z_0)\frac{\partial T}{\partial z}=N(B-T) \qquad (5.10)$$

where (x_0, y_0, z_0) is the position of a magnetic source whose total field T is detected at (x,y,z). The total field has a regional value of B and the degree of homogeneity (N) may be interpreted as a structural index, which is a measure of the rate of change with distance of a field (Thompson, 1982). The corollary is that the method cannot yield any dip information (Reid, 1990).

When implementing the algorithm three important parameters have to be specified. These are the maximum depth tolerance to allow, the window size and the structural index. The maximum depth tolerance to allow (given in percentage), controls which solutions are accepted (i.e. solutions with error estimates smaller than the specified tolerance) (Geosoft Inc., 1995). The window size determines the area in terms of grid cells used to calculate the Euler solutions. For high resolution data and shallow targets window sizes of 3X3 to 6X6 are common, while larger window sizes are used for regional data and to define basement structures (Reid, 1990). The structural indices (SI) depend on the source geometry and are summarized in the following table.

SI	*Magnetic field*
0.0	Contact
0.5	Thick step
1.0	Sill/dyke
2.0	Pipe
3.0	Sphere

Table 3: Summary of structural indices for simple models in a magnetic field (Geosoft Inc. 1995).

The results of the Euler solutions are plotted as small circles that are colour coded for depth. A given geological structure will show up on maps created with different values for SI and correspondingly different depths. In order to decide which value of SI to accept, the map on which the symbols (circles) are clustered the closest together are assumed to give the best fit. An index that is too low gives depths that are too shallow and vice versa. Lower indices have lower relative precisions and the parameters obtained from these data are therefore also less precise (Reid, 1990).

Three maps were created using a depth tolerance of 15%, 5X5 window size and SI values of 0, 0.5 and 1 respectively. The results are shown in figures 30-32. The data is seen to correspond very well with interpretations made from the previously mentioned maps. The dykes are extremely well matched on the SI=1 and SI=0.5 maps. Furthermore it is noticed that the prominent magnetic unit (sill) in the western half of the area is associated with depths up to 170m which is much deeper than the other features. The above SI values were chosen because faults, sills and dykes were the target features. As mentioned in the previous paragraph, small indices lead to lower precision and therefore the maps have a noisy character. However, when the solutions are restricted to yield a less clustered map, the structural trends become less visible.

5.4 AIRBORNE RADIOMETRIC DATA

Almost all the γ-ray radiation measured from rock and overburden originates in the upper 0.5 meters of the earth. Radioelement counts are the rates of detection of the gamma radiation from specific decaying particles corresponding to products in each radioelement's decay series. Radiometric data applied to groundwater exploration are used to discriminate between lithological units and to identify faults. Faults can exhibit radioactive highs due to increased permeability that allows Radon migration, or as lows due to structural control of drainage and fluvial sediments that attenuate gamma radiation from the underlying rocks (Pritchard, 1997). Changes in radioelement concentrations due to chemical alteration can also define faults.

The spectrometer used in this survey was a GR-820, 256 multichannel, Potassium stabilized model manufactured by Exploranium. It has an accuracy of 1 count/second. The spectrometer employs four downward looking crystals (recording the radiometric spectrum from 410KeV to

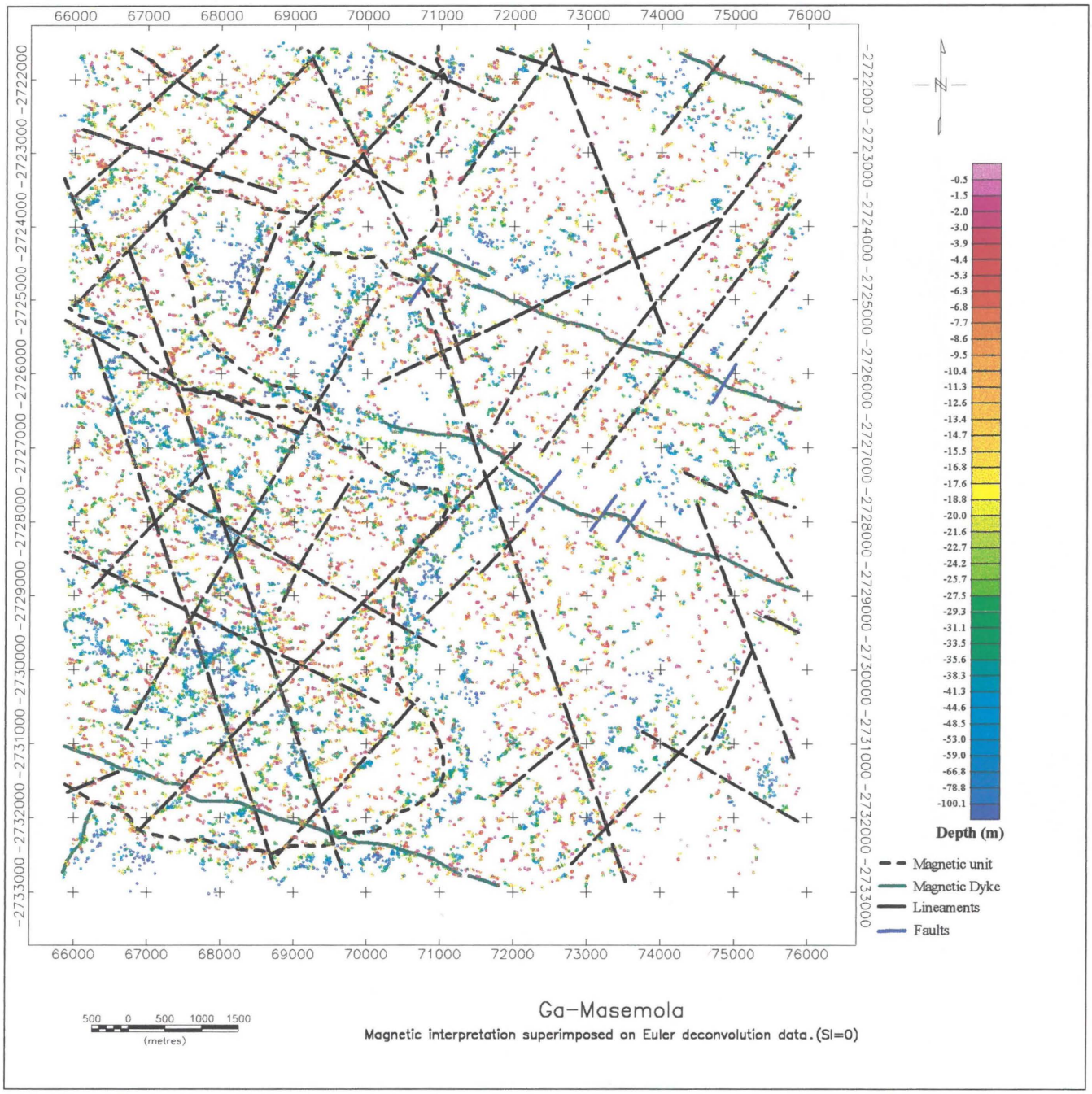

Figure 30: Magnetic interpretation superimposed on Euler deconvolution data. (SI=0)

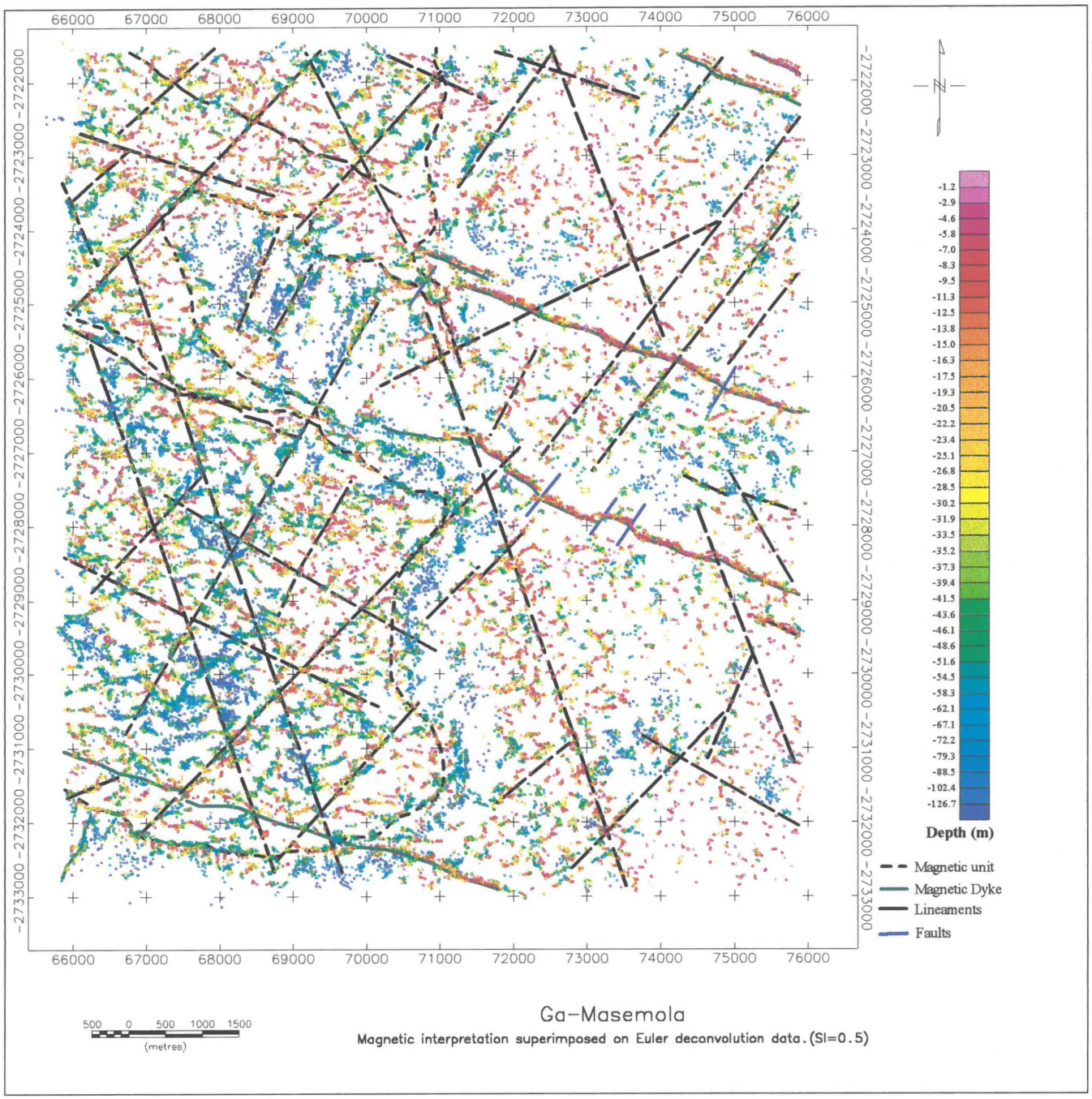

Figure 31: Magnetic interpretation superimposed on Euler deconvolution data. (SI=0.5)

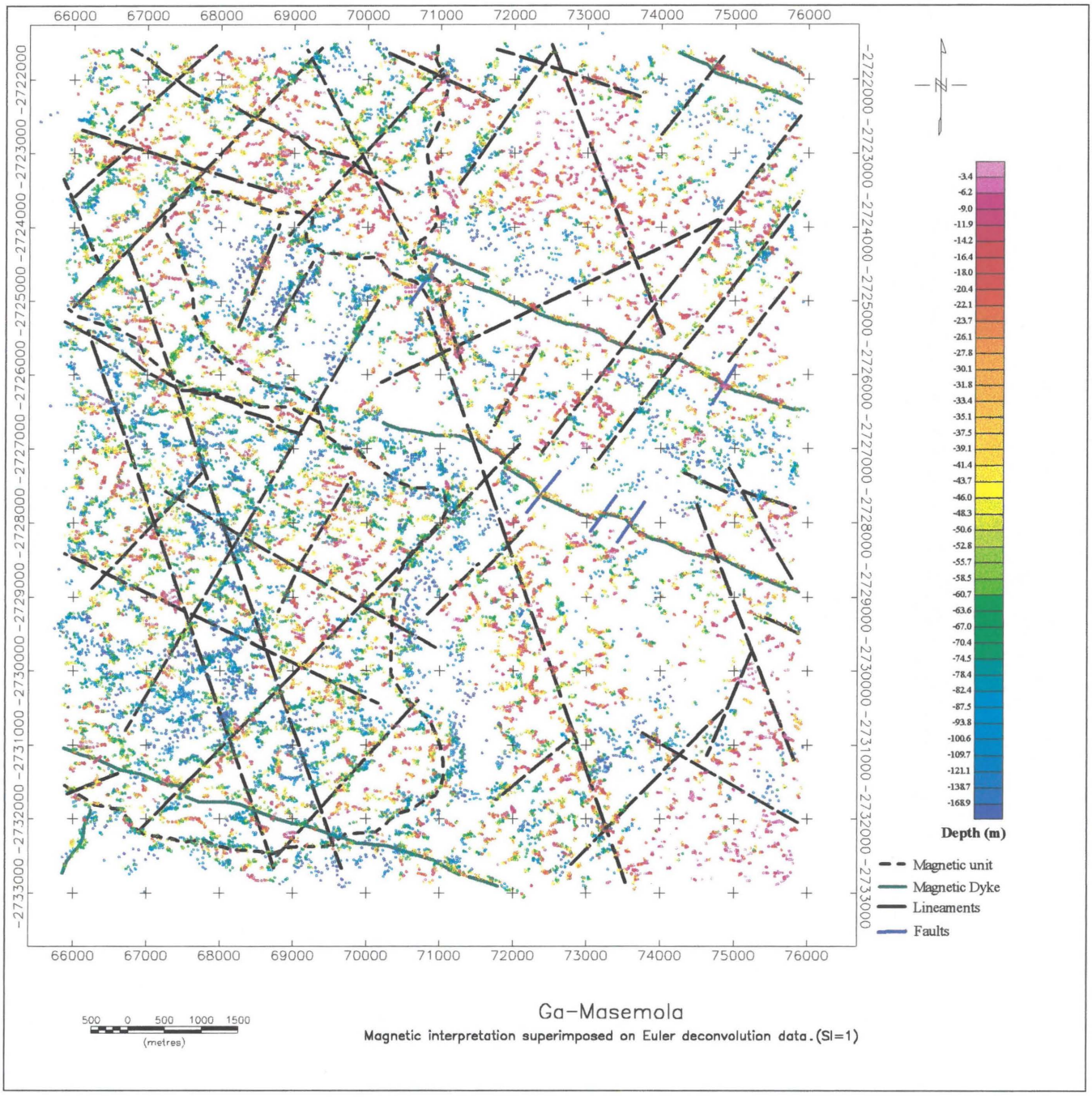

Figure 32: Magnetic interpretation superimposed on Euler deconvolution data. (SI=1)

3MeV over 256 discrete energy windows, as well as a cosmic ray channel detecting photons with energy levels above 3 MeV) and one upward looking crystal (to measure and correct for primarily the Radon contribution). From this data the standard Total Count, Potassium, Uranium and Thorium channels are extracted. The GR-820 provides raw or Compton stripped data that has been automatically corrected for gain, base level, ADC offset and dead time (Pritchard, 1997).

The data is presented as a ternary image (figure 33) with Thorium in yellow, Potassium in magenta and Uranium in cyan.

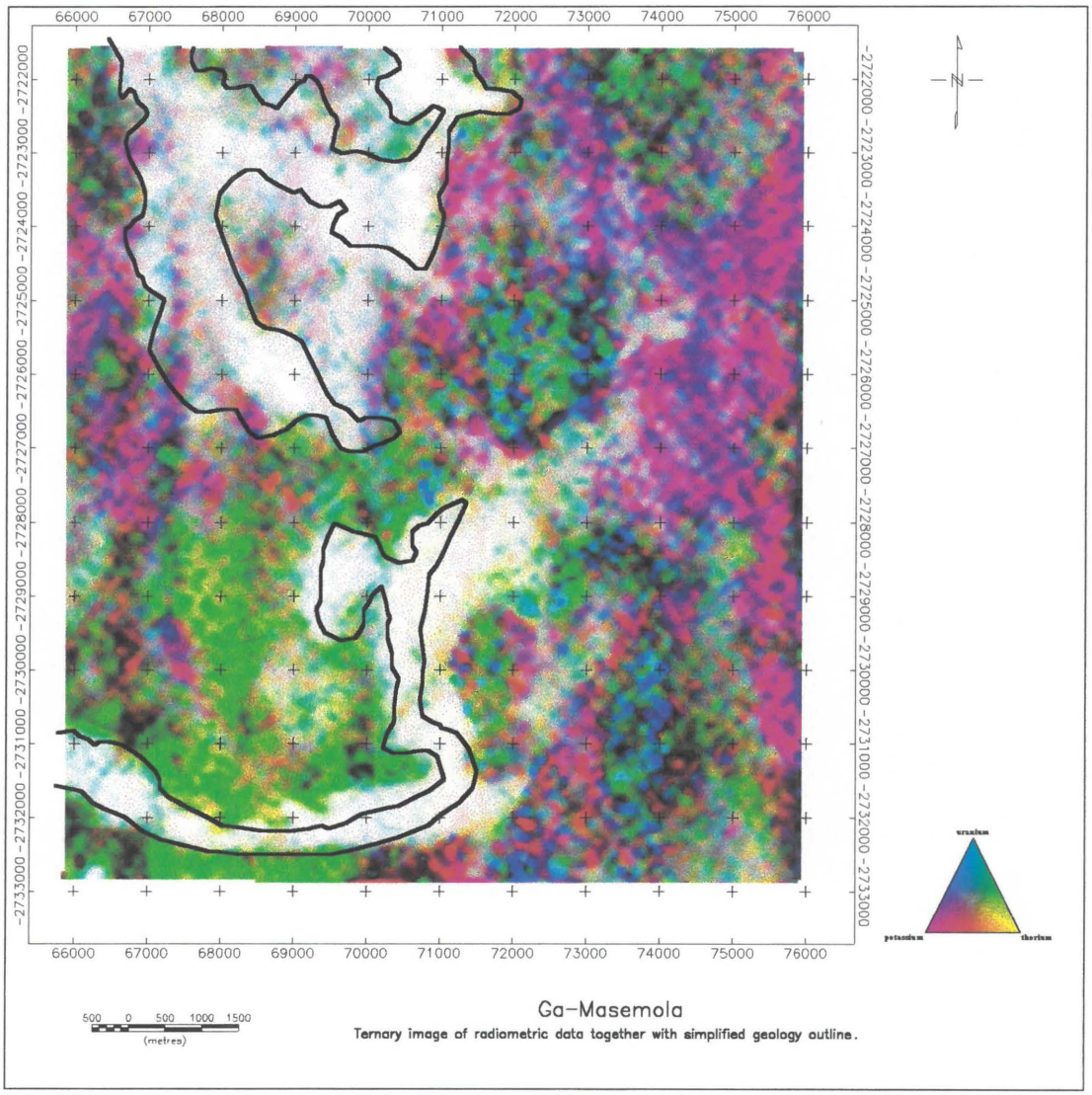

Figure 33: Ternary image of radiometric data with simplified geology outline.

The data can be clearly correlated with the geological outcrops. The white areas indicate the dolerite while the magenta and green indicate higher totalcount concentrations indicative of the granites in the region. Some of the major structural features can be identified on this map, especially in the eastern half.

5.5 ANCILLARY EQUIPMENT

The following ancillary equipment were used to aid in the survey (Pritchard, 1997):

- radar altimeter (0.3 m sensitivity measuring the vertical distance between the helicopter and the ground)
- barometric altimeter (0.1 m accuracy at sea level)
- analog recorder
- digital data acquisition system
- tracking camera
- navigation system (12 channel, simultaneous receiver; 1 m accuracy in differential mode)
- field workstation

5.6 DETERMINATION OF OPTIMUM DATA ACQUISITION PARAMETERS

The initial approach to this project was to obtain all possible relevant data at 100m line spacing. After interpretation of the data it was necessary to determine the most cost-effective set of data that would yield the same information that was obtained from the initial set. In order to do this the following was investigated:

- optimum line spacing
- optimum data set
- optimum ground follow-up

5.6.1 Optimum line spacing

The optimum line spacing was determined by reprocessing the 100m line spacing data using every second, every third and every fourth line. This corresponds to 200m, 300m and 400m line spacings respectively. The optimum line spacing would then be the largest one on which the interpreted structures can still be distinguished clearly. A comparison of the total field data sets is shown in figure 34. At first glance there seems little to choose between the 100 m and 200 m line spacing data. Based on the fact that this study is focused on the granites and that our main targets are faults rather than dykes, sills and dolerite-granite contacts, the measure of resolution was chosen as a north-west striking feature in the eastern half of the area (underlying sites N, L, E and I in figure 35). This feature is much more clearly visible on the EM data and was confirmed by drilling to be a fault in granite (no dolerite visible in drill samples) which yielded water at 3l/s (blow test yield). On the 200m line spacing this feature is barely visible (provided that its position is already known!). Even when applying filters to the 200m data that enhanced this feature on the 100 m data, it cannot be distinguished with certainty.

Unfortunately the data could not be processed at 150m line spacing interval without resampling the data and introducing possible artifacts. Based on the available data however, the recommended line spacing for future surveys is 100 m although even 50 m line spacing should be considered.

5.6.2 Optimum data set

Comparing the different data sets, it is noted that almost all of the prominent electromagnetic features (especially on the 400Hz frequency) are evident on the magnetic data as well. The radiometric data resembles the geological map very well and also confirm the major features visible on the other data sets, but doesn't add any exclusive features to the overall structural interpretation. Taking into account the cost of each data type, the information conveyed by each method and the specialized type of interpretation (mapping faults and fracture zones with weathering shallower than 200m), the magnetic data is by far the most cost effective data set to acquire without loss of information. High density magnetic data is therefore recommended as the best option for an economically viable regional groundwater exploration program.

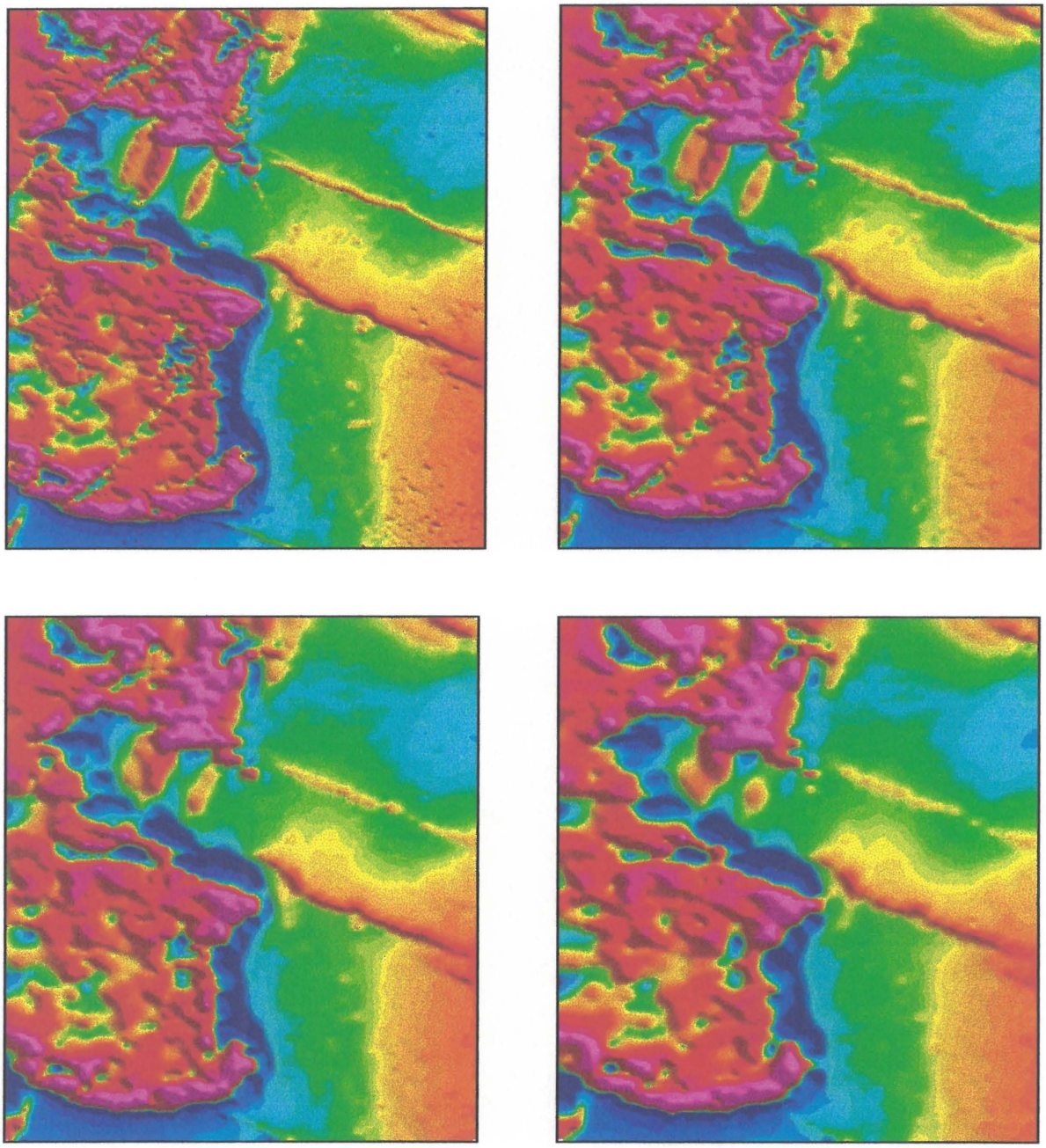

Figure 34: Total field magnetic data processed at 100m (top left), 200m (top right), 300m (bottom left) and 400m (bottom right) flight line spacing.

5.6.3 Optimum ground follow-up procedure

The ground follow-up procedure will be discussed in more detail in a later section. Suffice it to say that by using maps in digital format overlain on one another, field anomaly prediction from the airborne data and sophisticated navigation equipment (real time differential, one piece unit GPS), the fieldwork can be reduced to less than 1 hour per site. This does not include the mobilisation and travel time, which depends on the roads and distances to be negotiated. In our investigation area (which has a curious lack in abundance and quality of roads!) two to three sites could be surveyed per day (by two persons) depending on how close the sites were to each other.

Although certain features can be investigated where they cross roads or villages, this is not always possible and a good first hand knowledge of the investigation area is strongly recommended as many hours can be wasted due to the inaccessibility of sites.

CHAPTER 6

GROUND FOLLOW-UP AND CASE STUDIES

6.1 GROUND FOLLOW-UP PROCEDURE

From the interpretation of the airborne data, a number of target areas have been identified. Ground follow-up was undertaken to map the target areas in greater detail in order to site drilling positions.

The groundwork consisted of magnetic and frequency domain electromagnetic (EM34) profiles. The directions of the survey lines were determined from the airborne geophysical anomalies. The target positions were found in the field with the aid of a global positioning system (GPS) and the 1:10 000 orthophotos. Due to the high resolution of the airborne data and the convenience of overlaying the geophysical anomalies onto the orthophotos (figure 12), the fieldwork could in most cases be limited to a 400m long profile or less. Because the target strike direction is known beforehand from the airborne data, one profile usually proved sufficient to site a borehole. The magnetic surveys consisted of total field measurements at 5m station spacings while the EM34's 20m and 40m coil spacings were used where possible, with 10m and 20m station spacings respectively. The 40m coil spacing configuration yielded very noisy data in areas of low conductivity (<5 mS), and was therefore only included in areas with relatively higher conductivities.

A typical ground follow-up of an airborne target was completed on average in 4 hours. The most difficulties arose from locating access routes to get equipment and a drill rig on site, through dense vegetation (especially thorn trees) in some areas. Once the geophysical measurements were taken, the data were depicted along profiles and interpreted. Because the main target features were already identified from the airborne measurements, the interpretations consisted only of determining a width, dip and exact field location of the target structure. The areas that were chosen as investigation sites from the airborne data interpretation are shown in figure 35. Maps and profiles detailing all the groundwork that were done as well as the sited borehole positions associated with each target, are shown in figures 36-59.

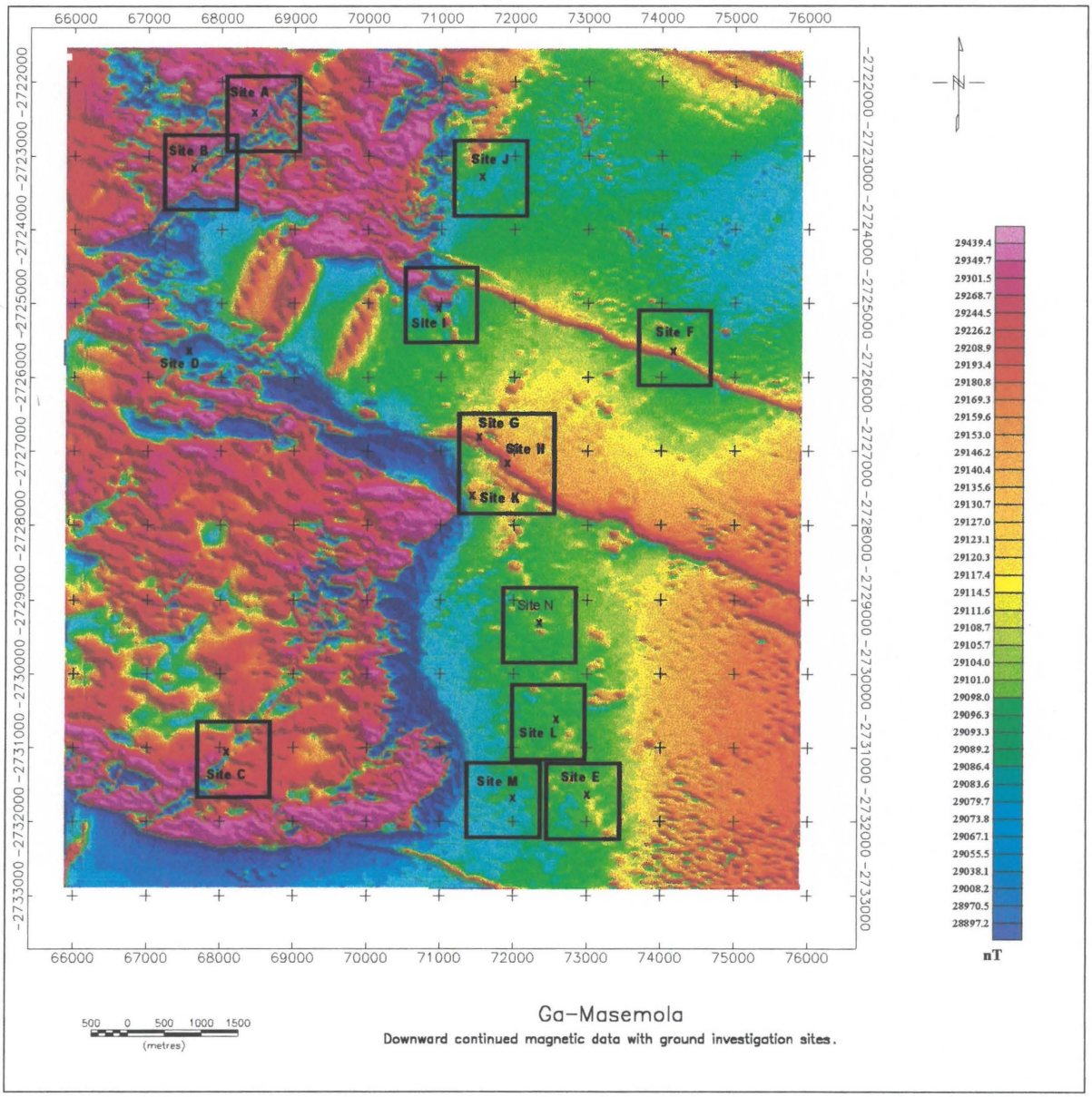

Figure 35: Downward continued magnetic data with ground investigation sites.

6.2 LOCATION MAPS AND GROUNDWORK PROFILES

Site A

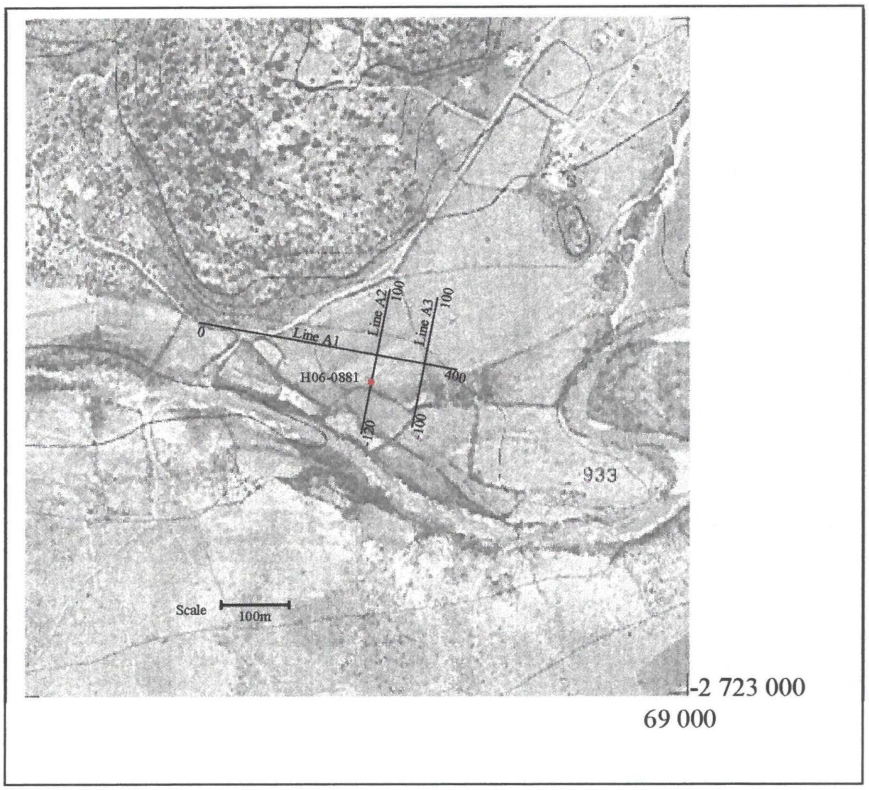

Figure 36a: Location map with field profiles and borehole position (Orthophoto series, 1983)

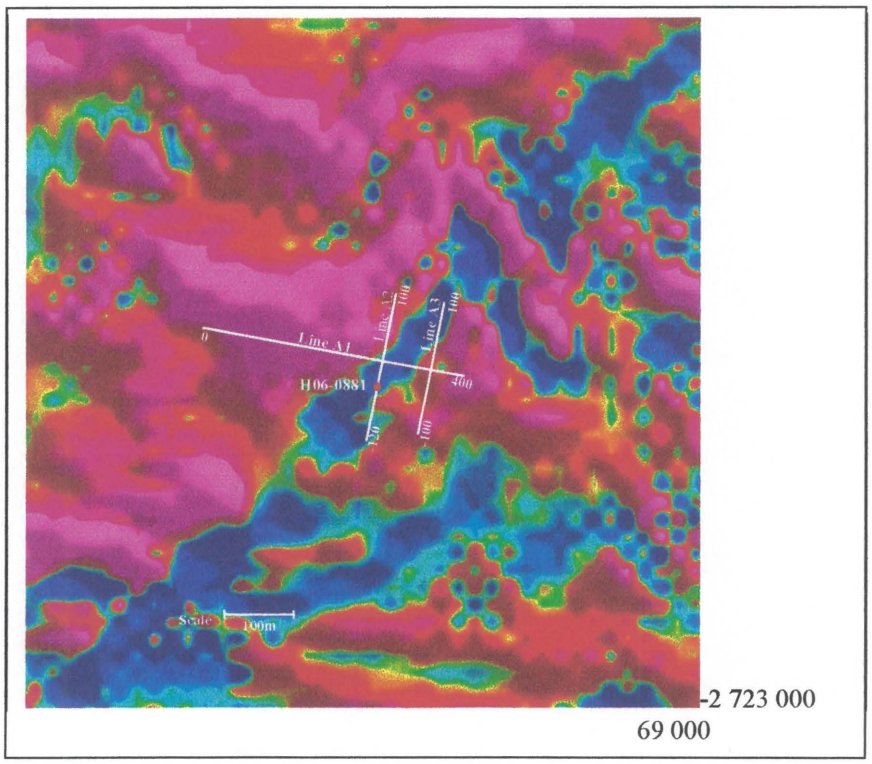

Figure 36b: Airborne magnetic data for the same area as shown above.

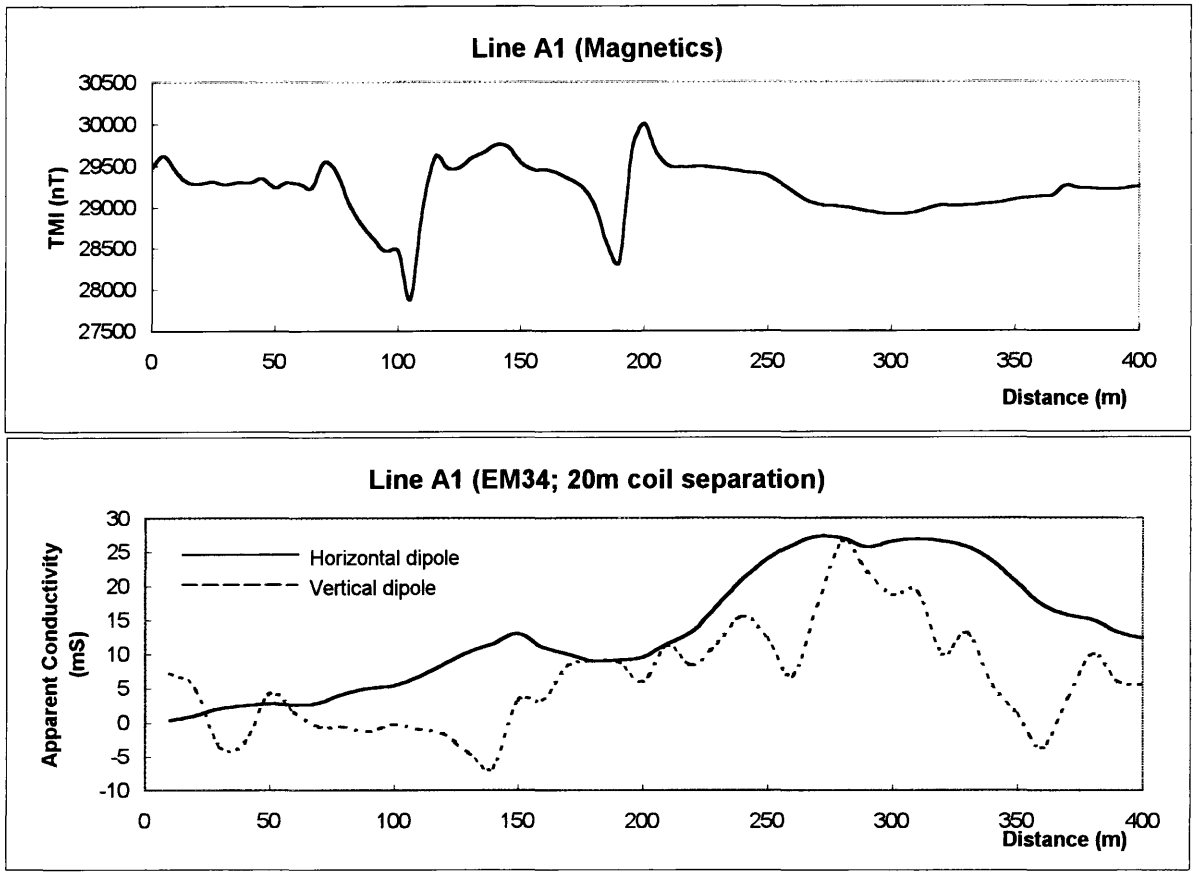

Figure 37a: Profiles for line A1.

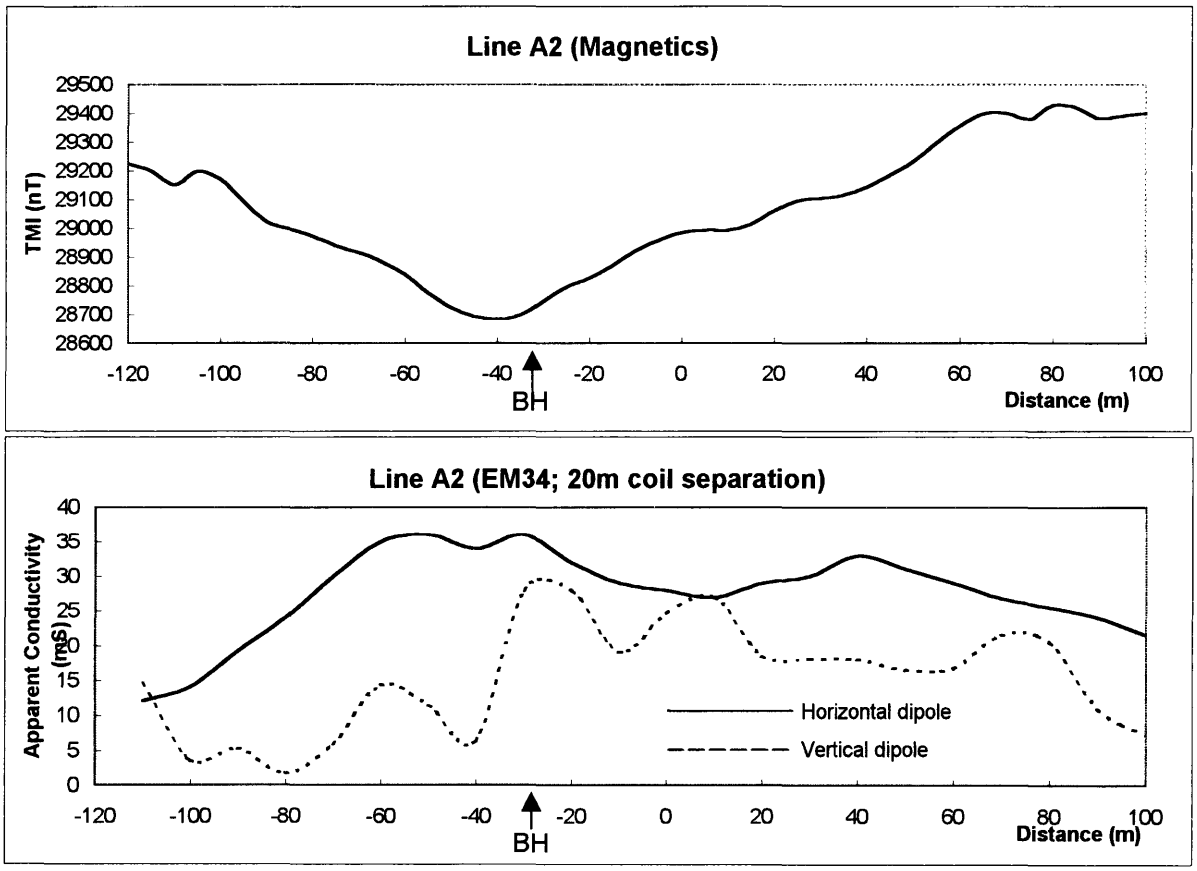

Figure 37b: Profiles for line A2.

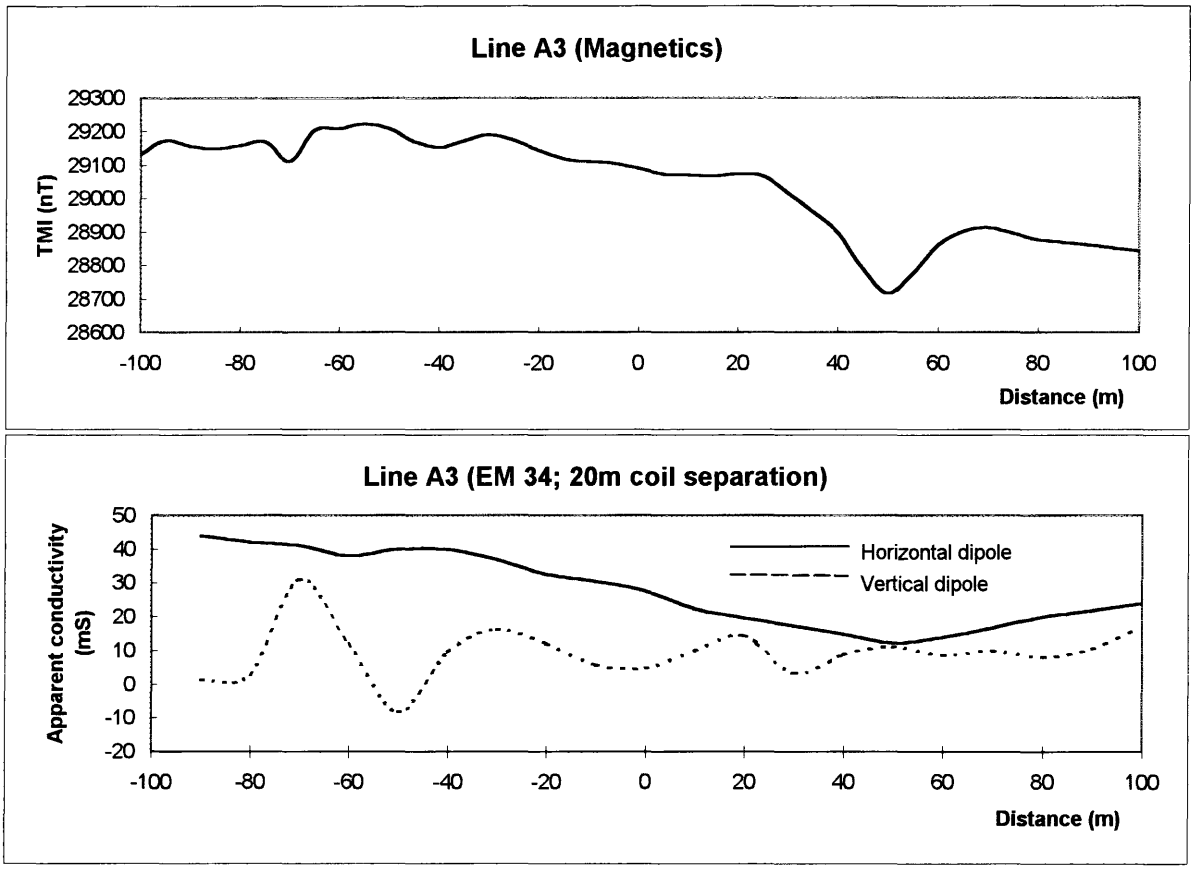

Figure 37c: Profiles for line A3.

Site B:

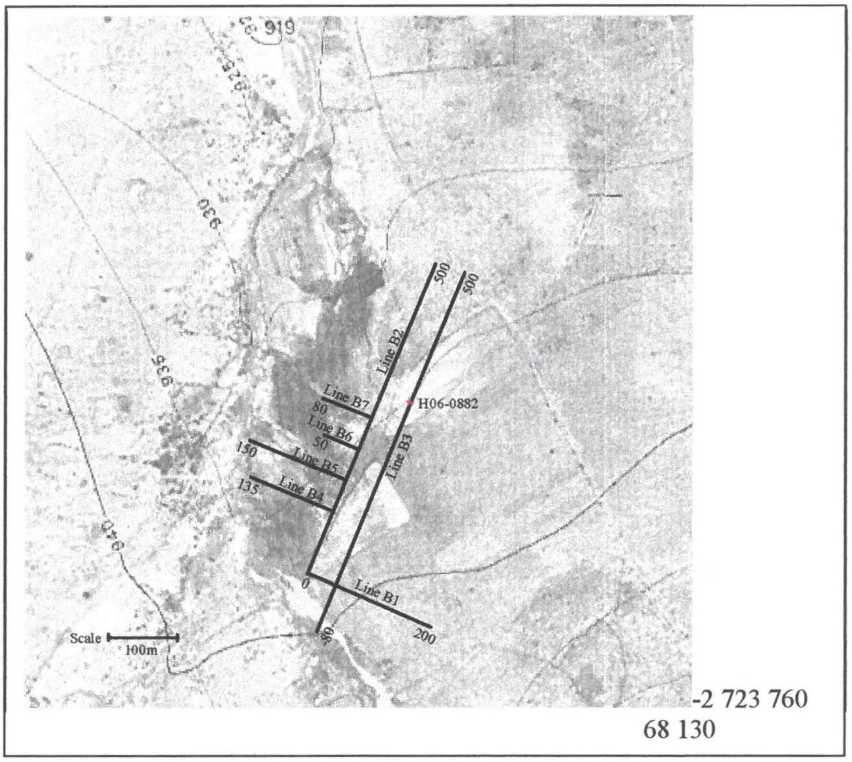

Figure 38a: Location map with field profiles and borehole position (Orthophoto series, 1983)

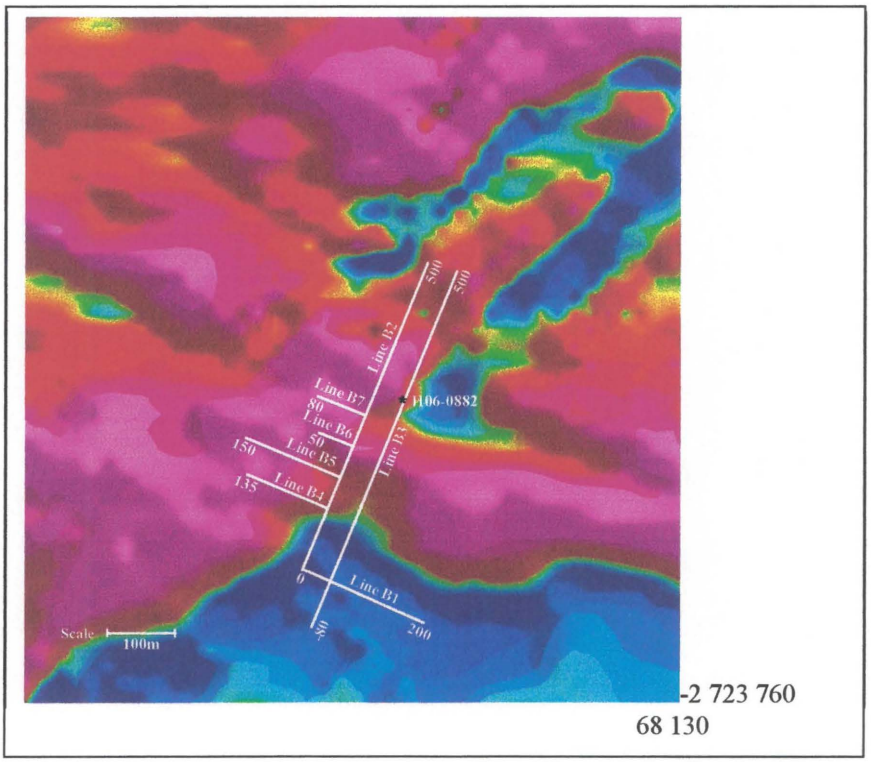

Figure 38b: Airborne magnetic data for the same area as shown above.

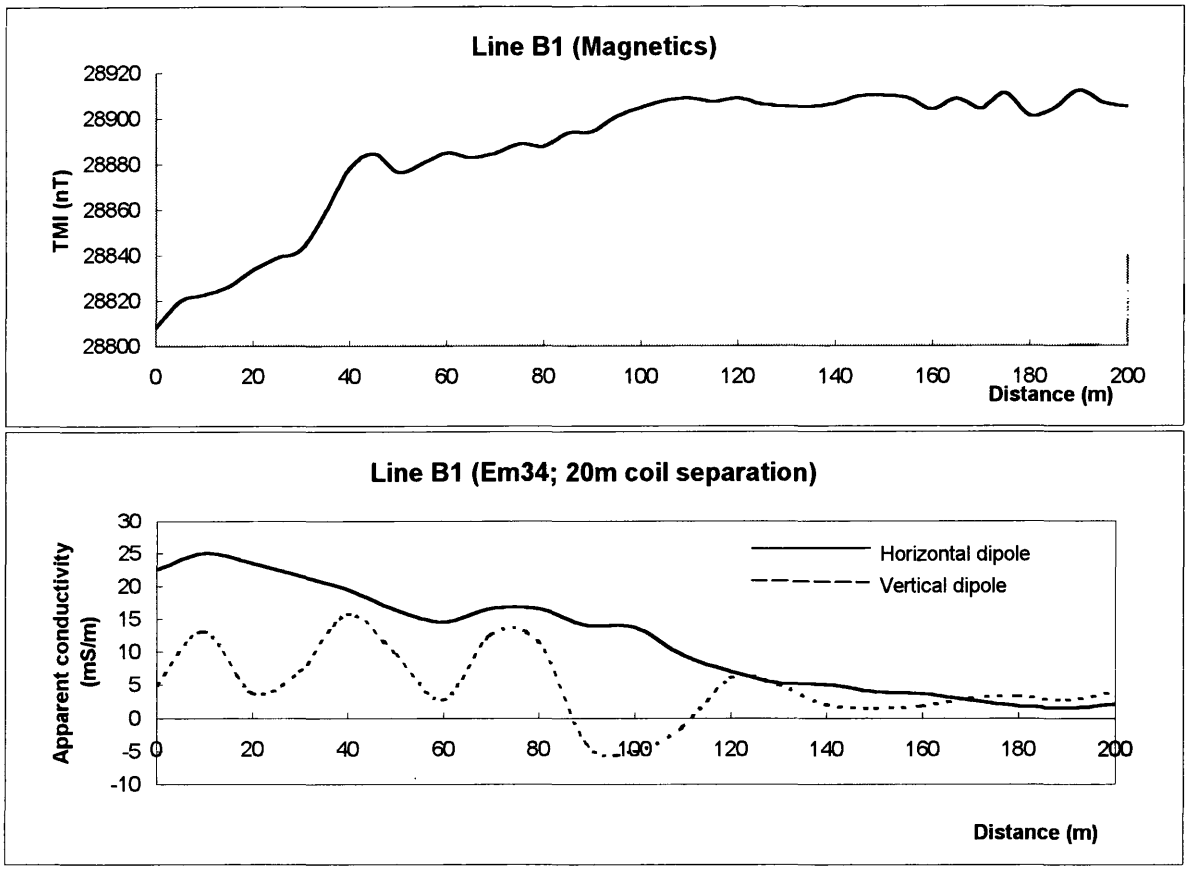

Figure 39a: Profiles for line B1.

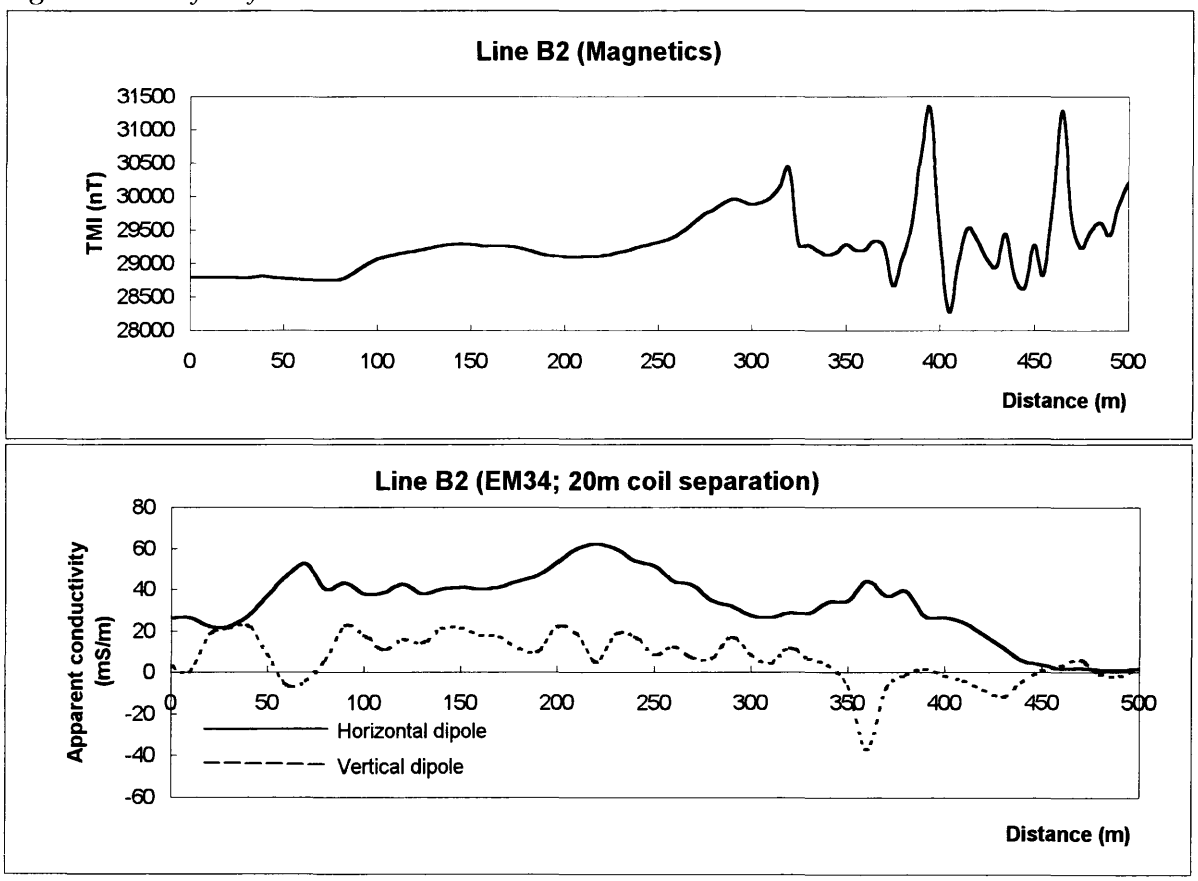

Figure 39b: Profiles for line B2.

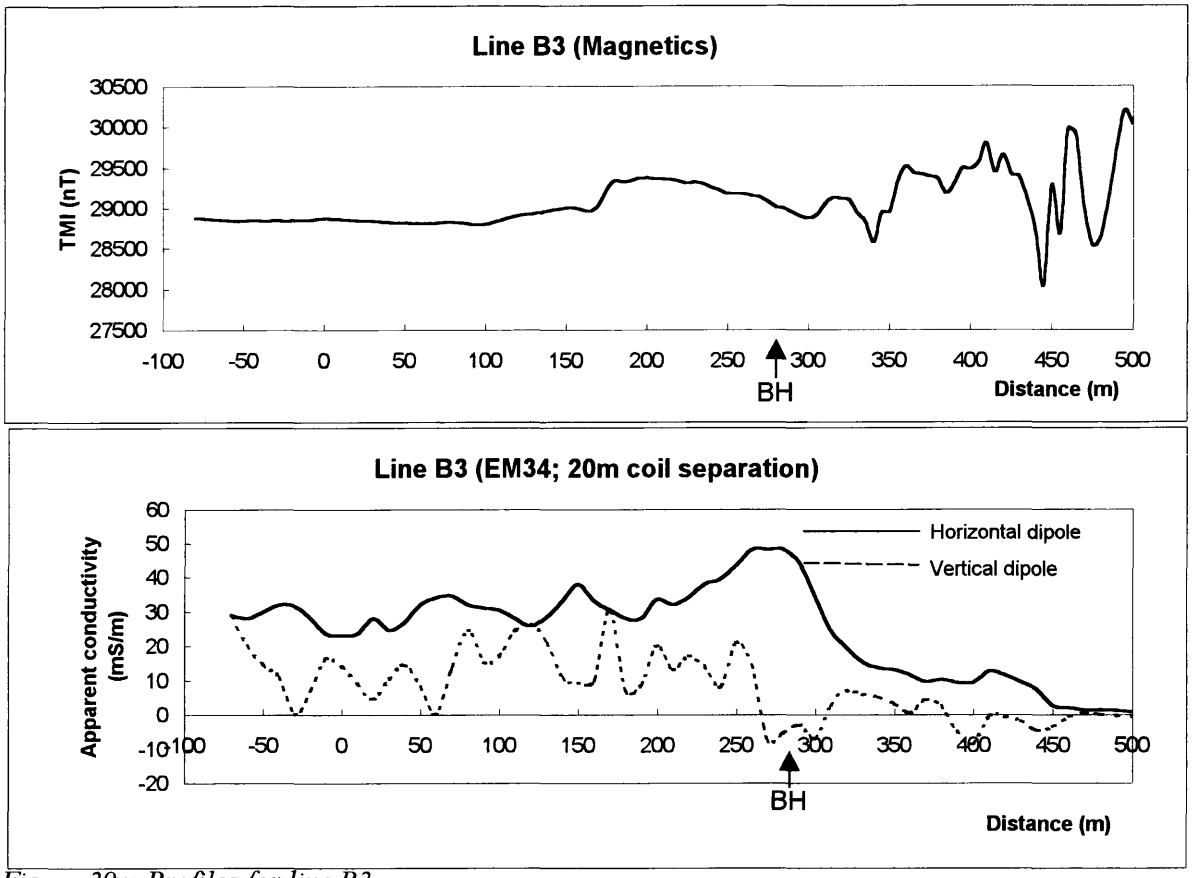

Figure 39c: Profiles for line B3.

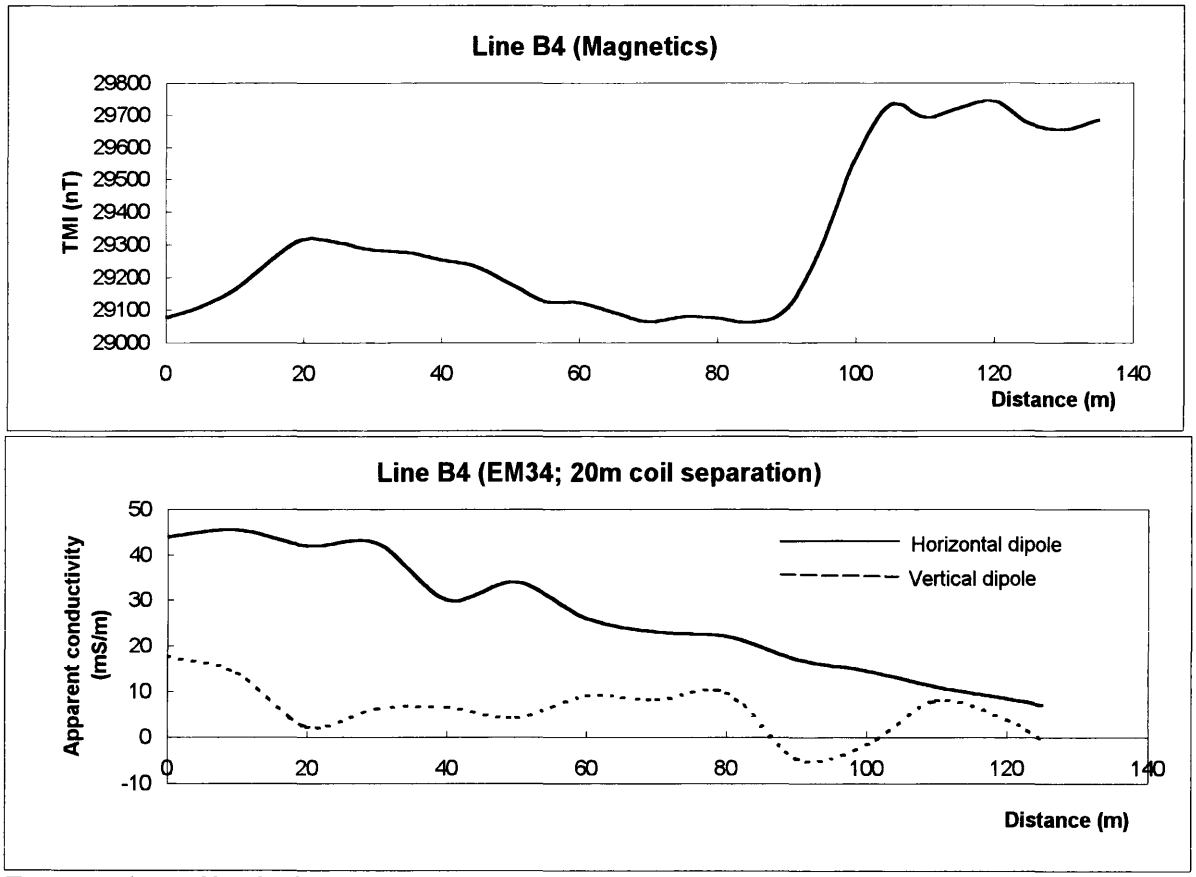

Figure 39d: Profiles for line B4.

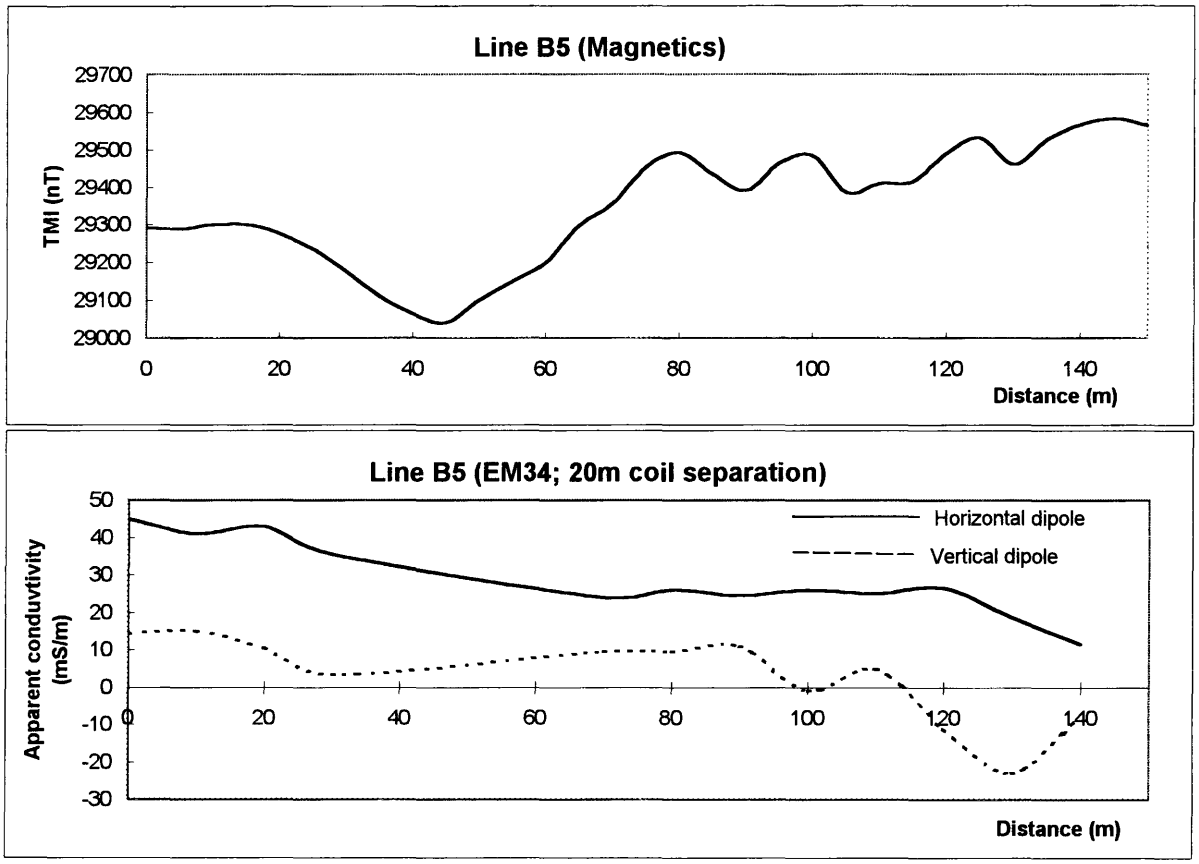

Figure 39e: Profiles for line B5.

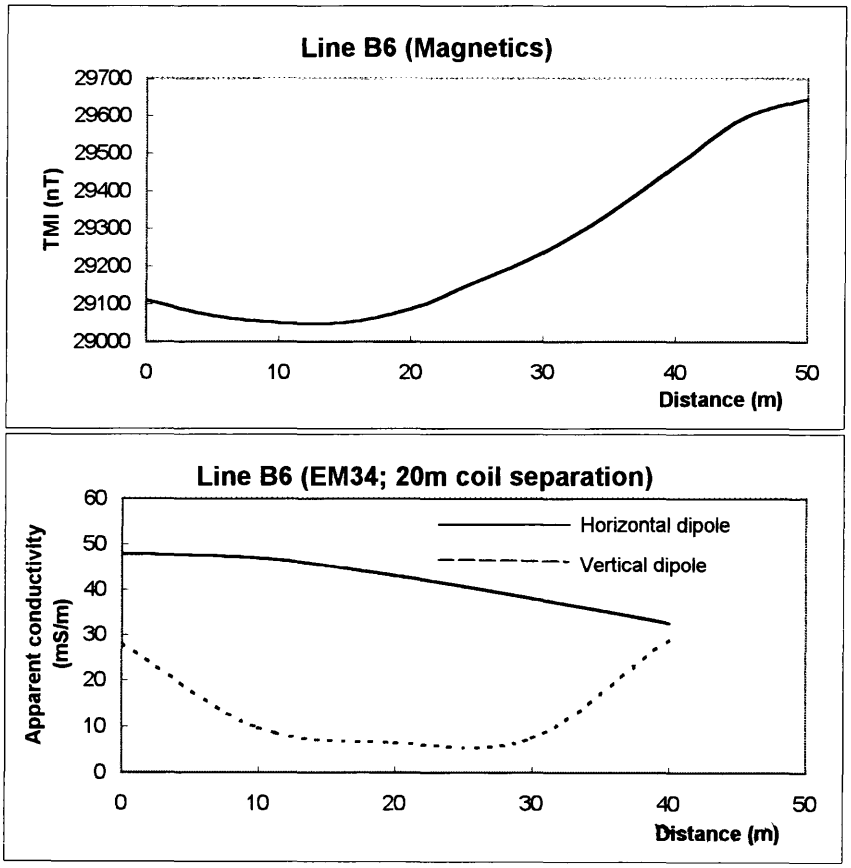

Figure 39f: Profiles for line B6.

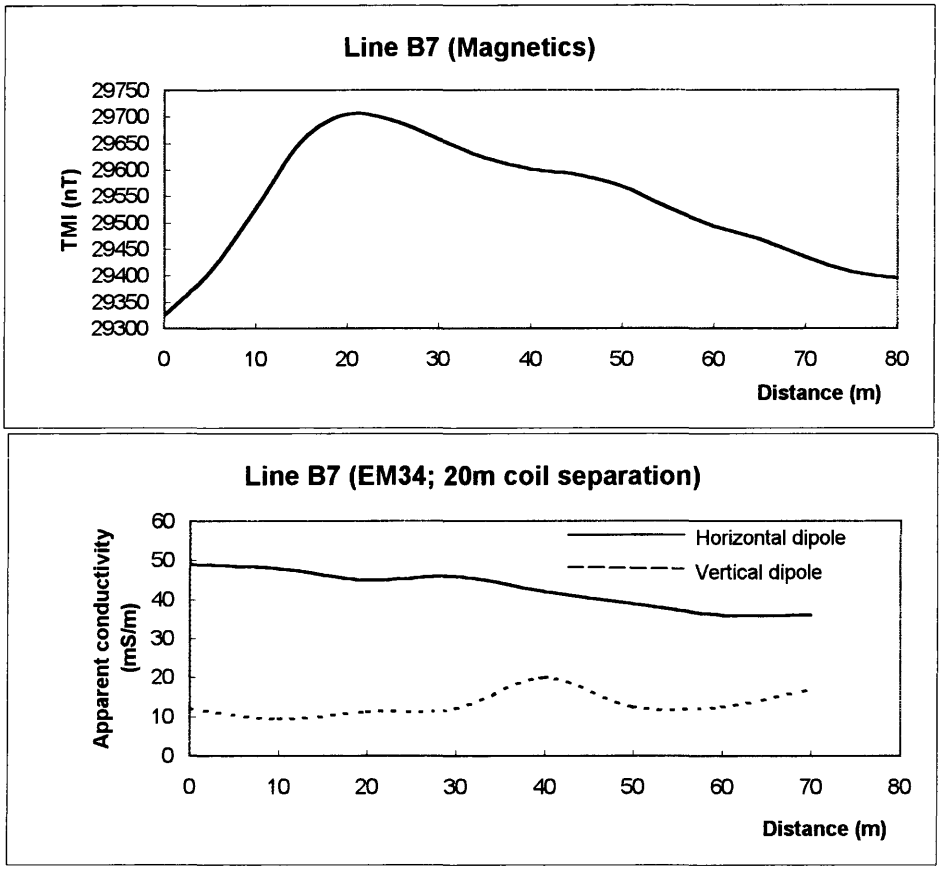

Figure 39g: Profiles for line B7.

Site C:

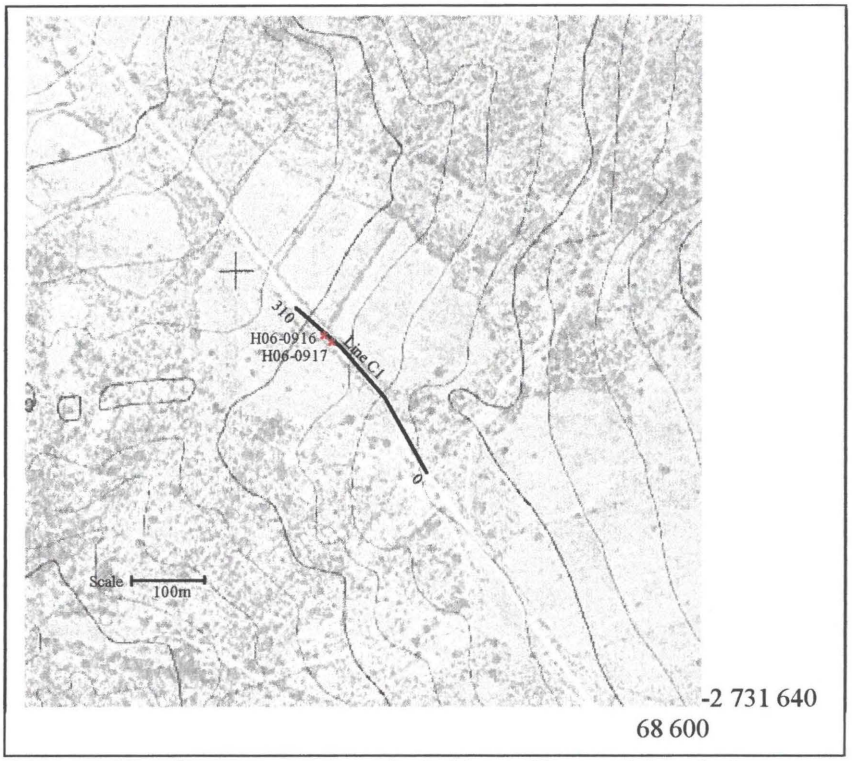

Figure 40a: Location map with field profiles and borehole position (Orthophoto series, 1983)

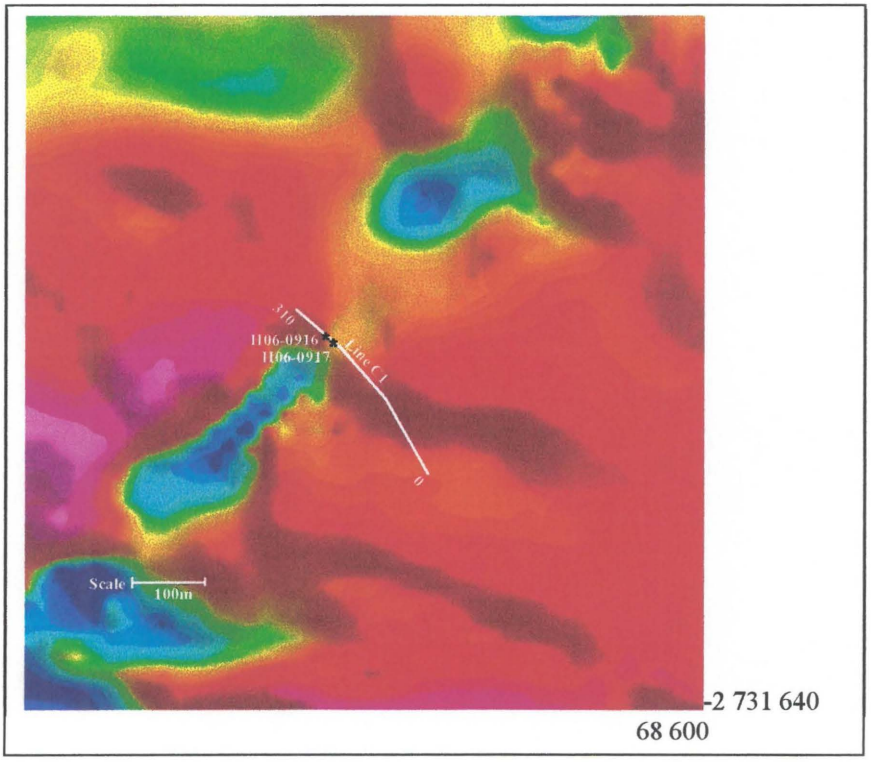

Figure 40b: Airborne magnetic data for the same area as shown above.

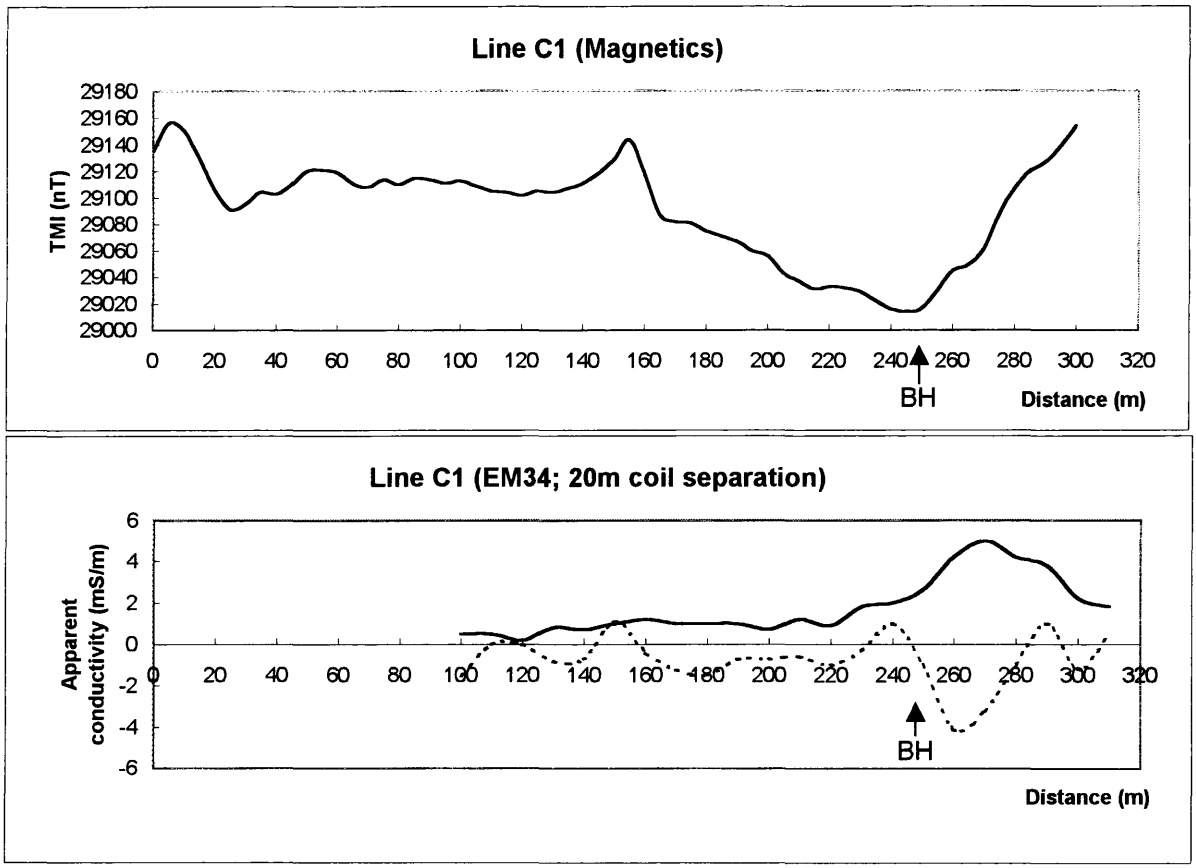

Figure 41: Profiles for line C1.

Site D:

No fieldwork done because the terrain was inaccessible

Site E:

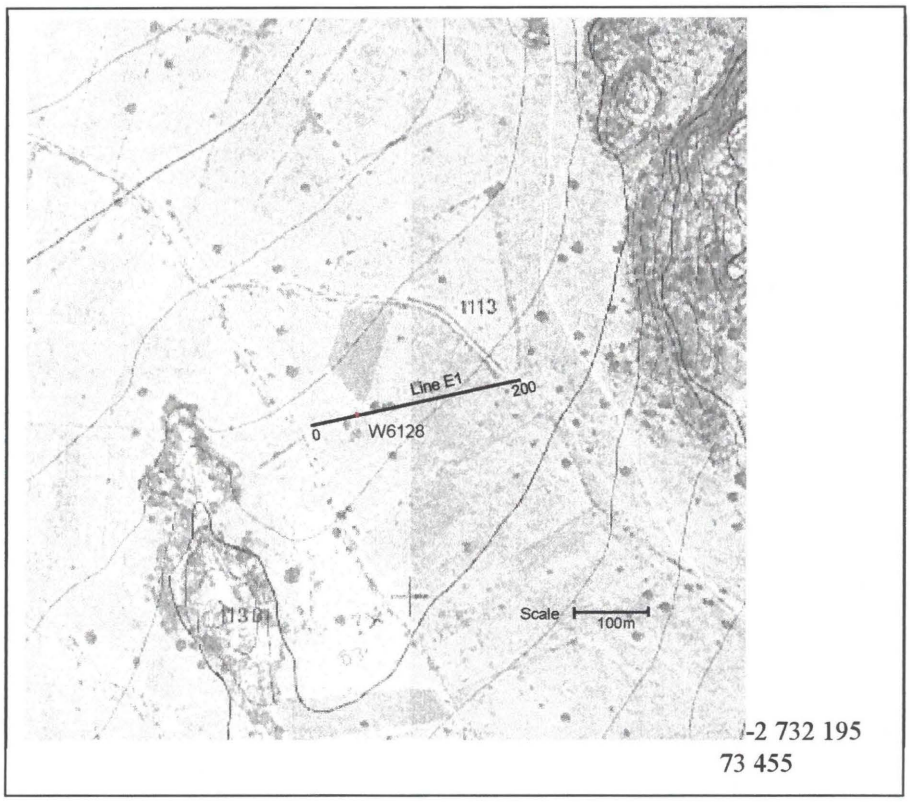

Figure 42a: Location map with field profiles and borehole position (Orthophoto series 1983).

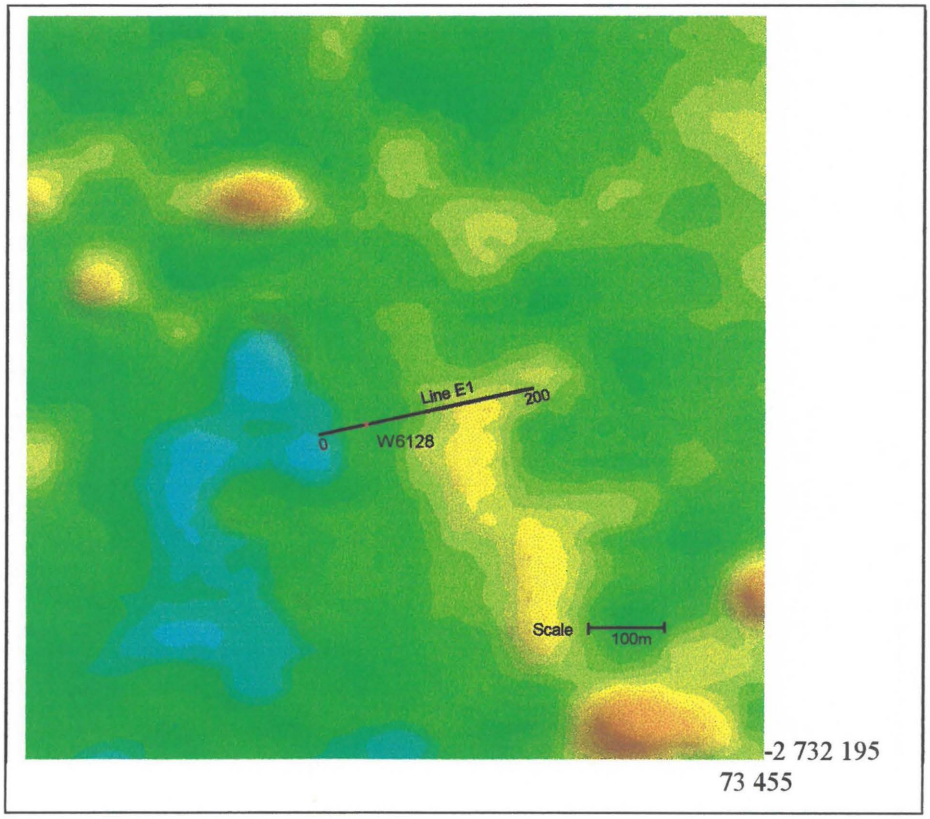

Figure 42b: Airborne magnetic data for the same area as shown above.

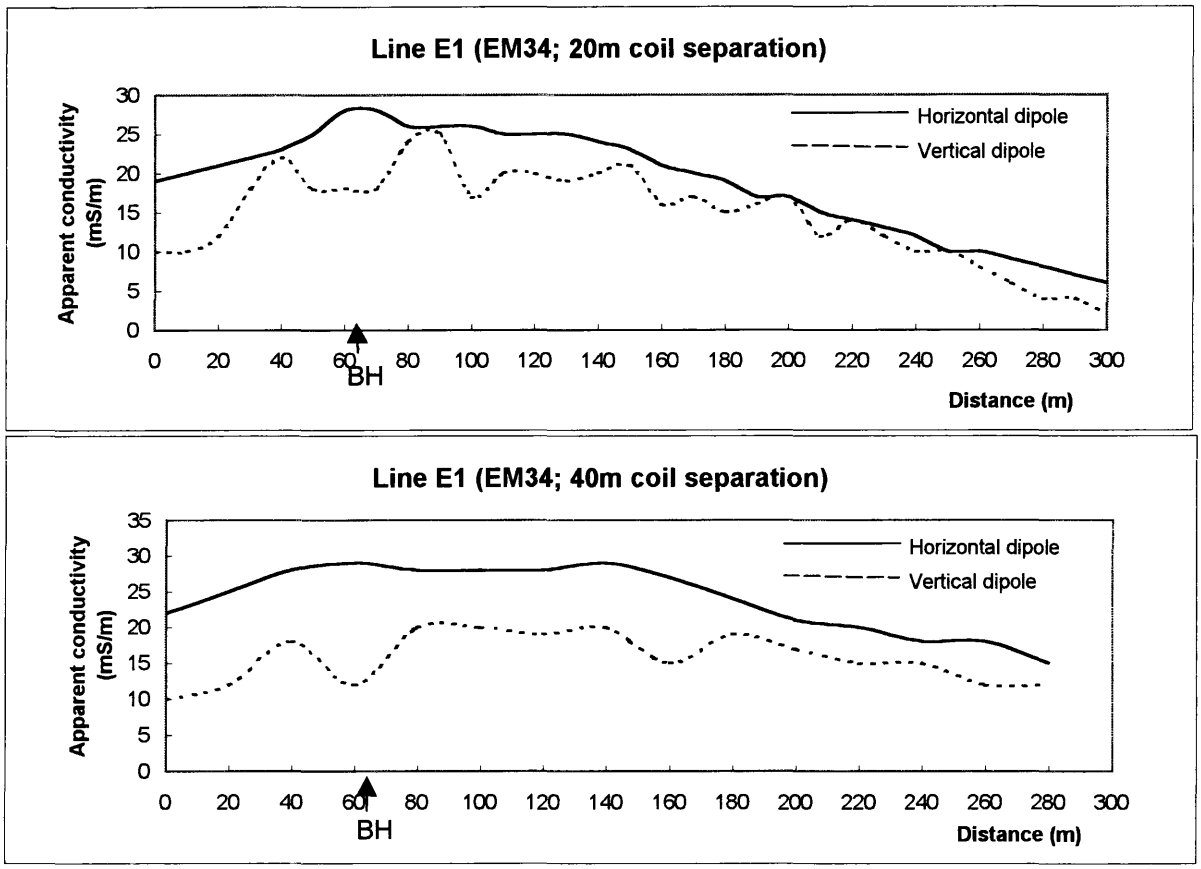

Figure 43: Profiles for line E1.

Site F:

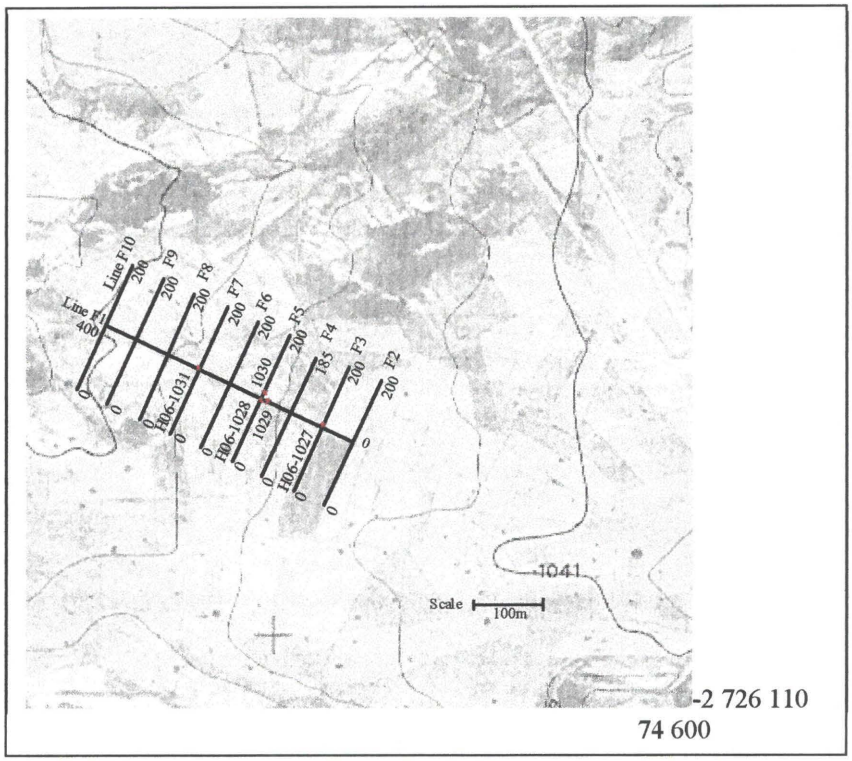

Figure 44a: Location map with field profiles and borehole position (Orthophoto series, 1983)

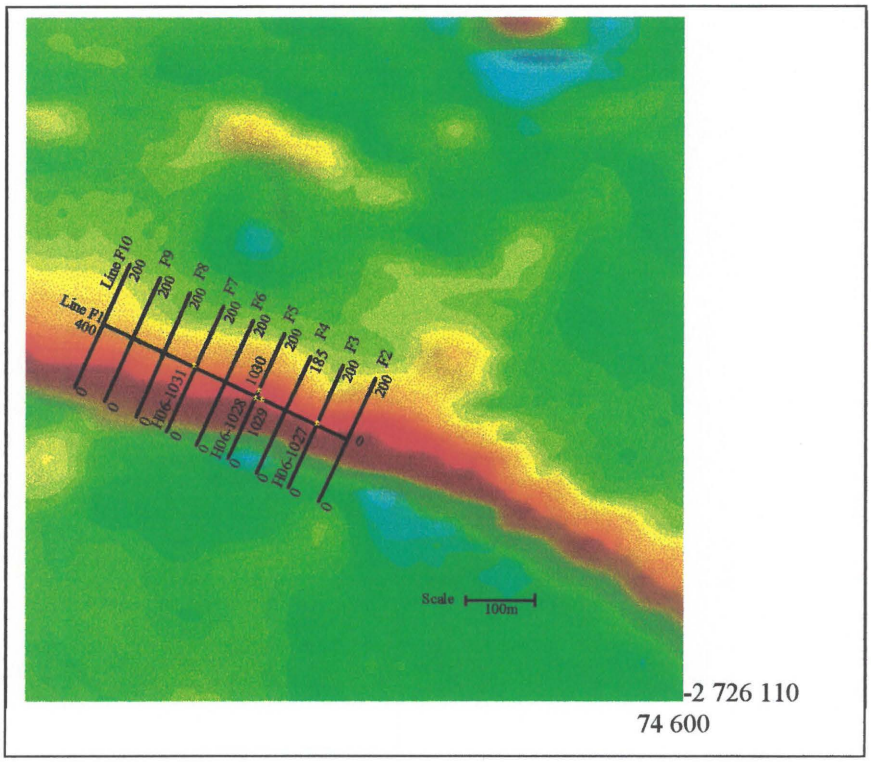

Figure 44b: Airborne magnetic data for the same area as shown above.

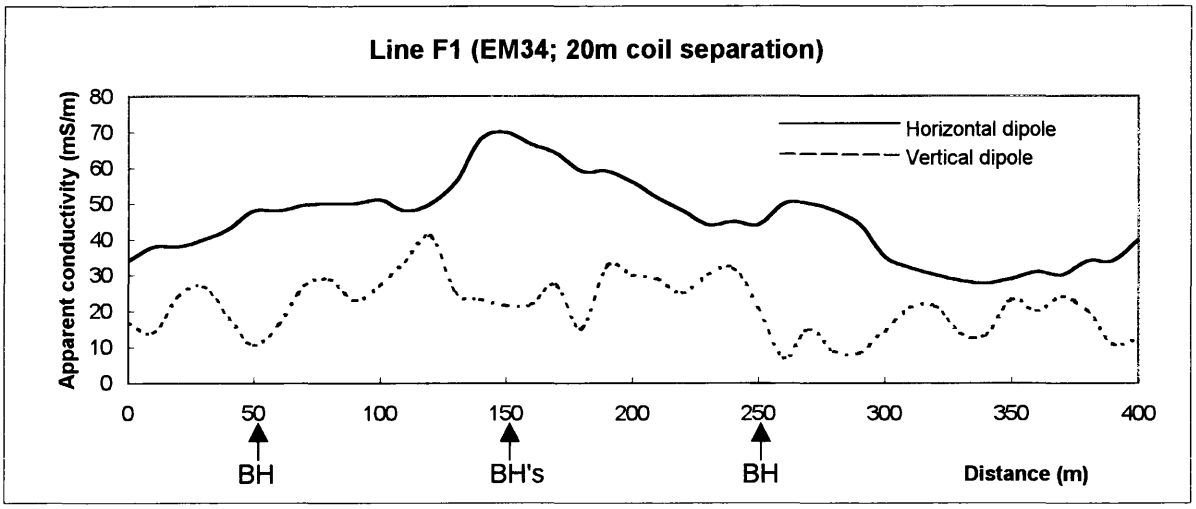

Figure 45a: Profiles for line F1.

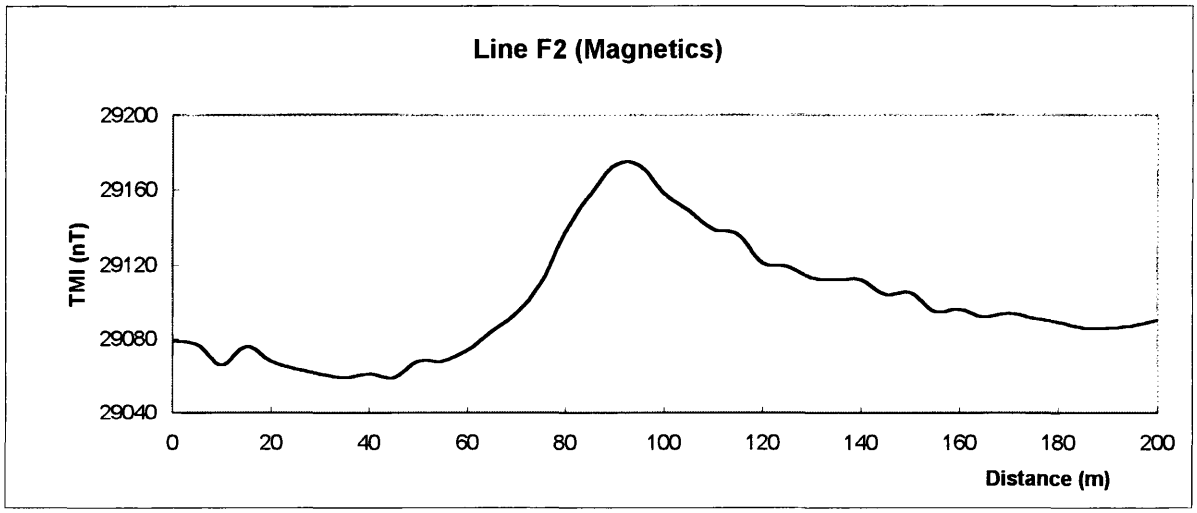

Figure 45b: Profile for line F2.

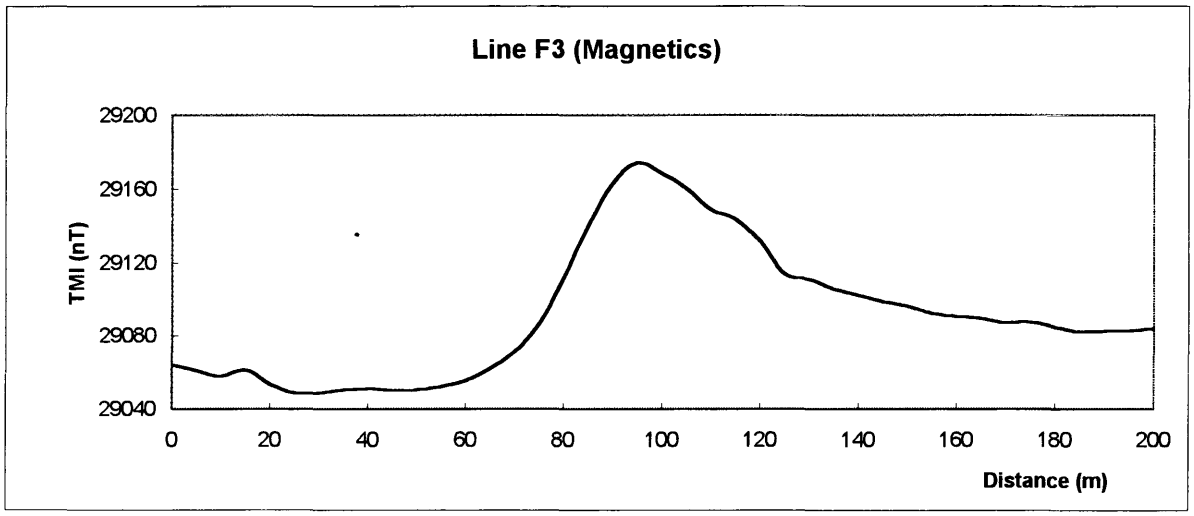

Figure 45c: Profile for line F3.

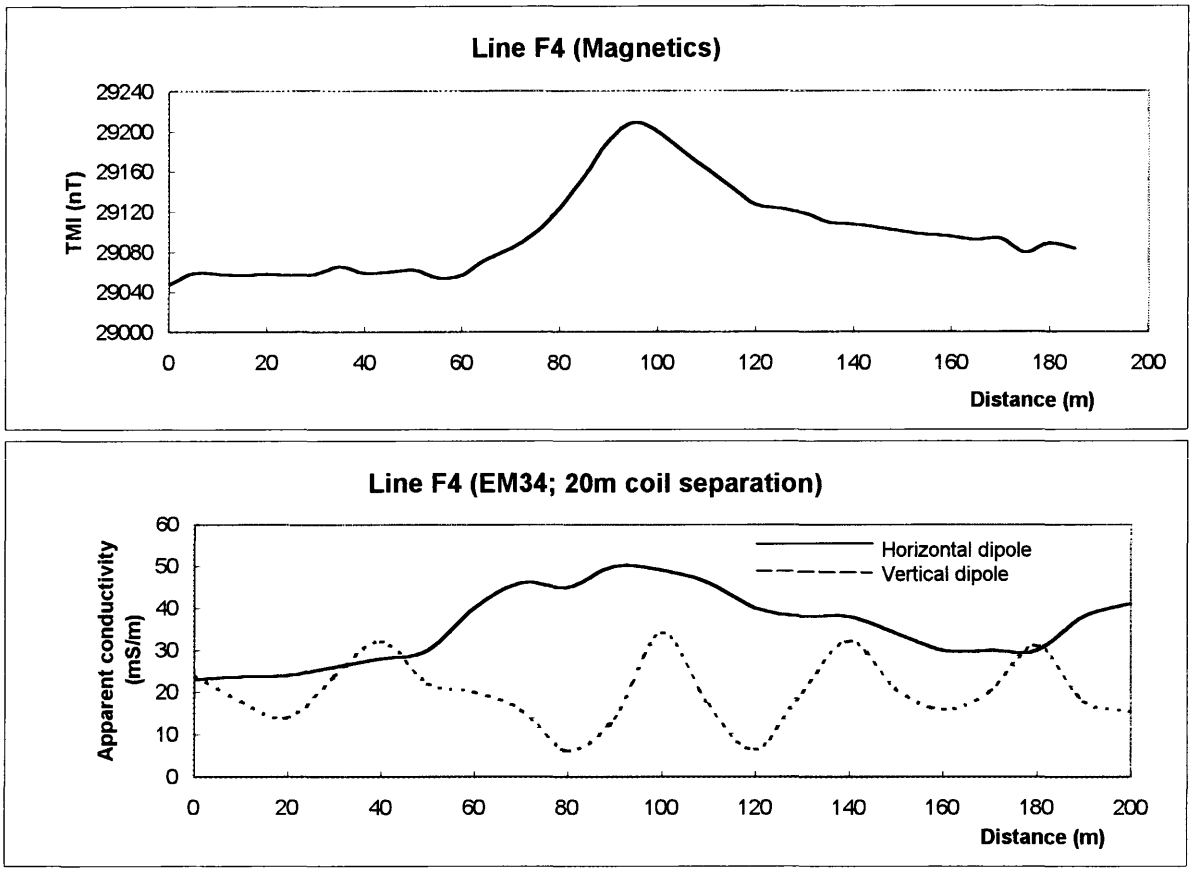

Figure 45d: Profiles for line F4.

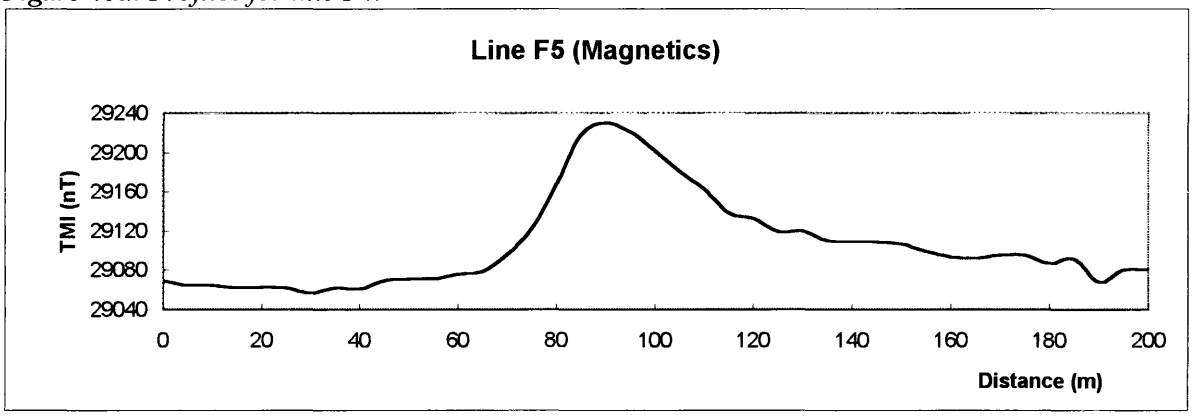

Figure 45e: Profile for line F5.

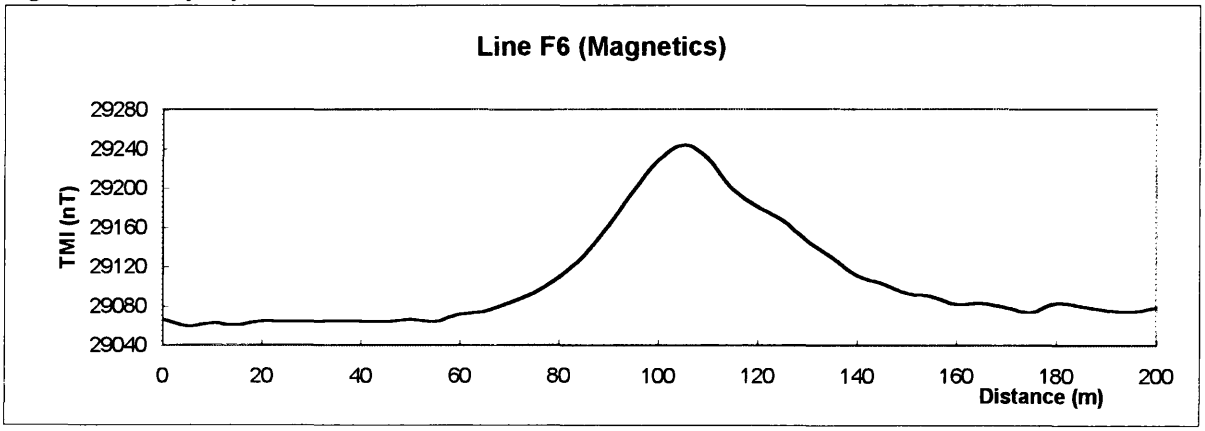

Figure 45f: Profiles for line F6.

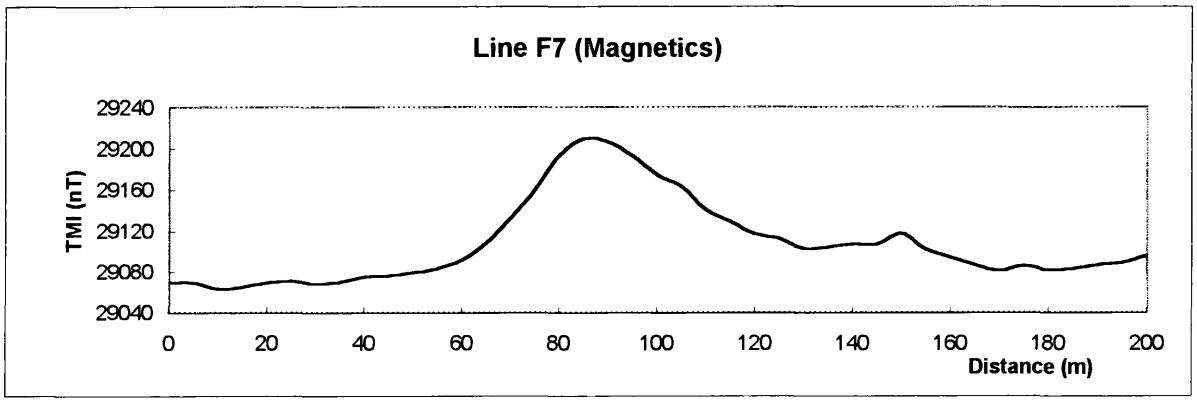

Figure 45g: Profile for line F7.

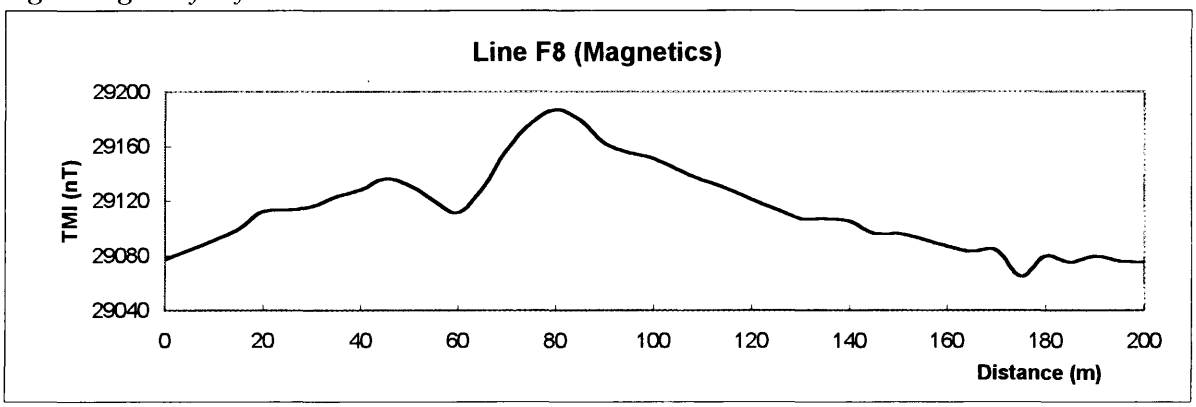

Figure 45h: Profile for line F8.

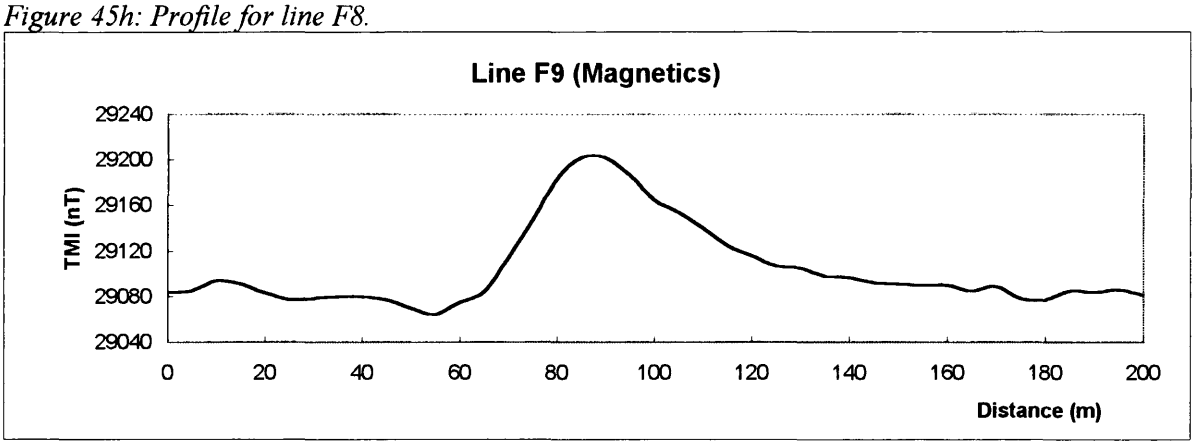

Figure 45i: Profile for line F9.

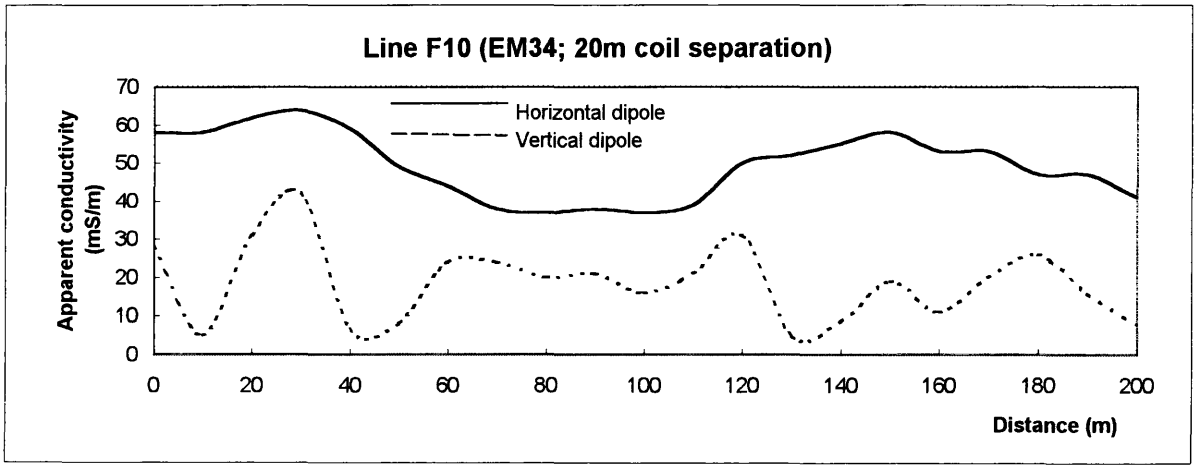

Figure 45j: Profile for line F10.

Site GH&K:

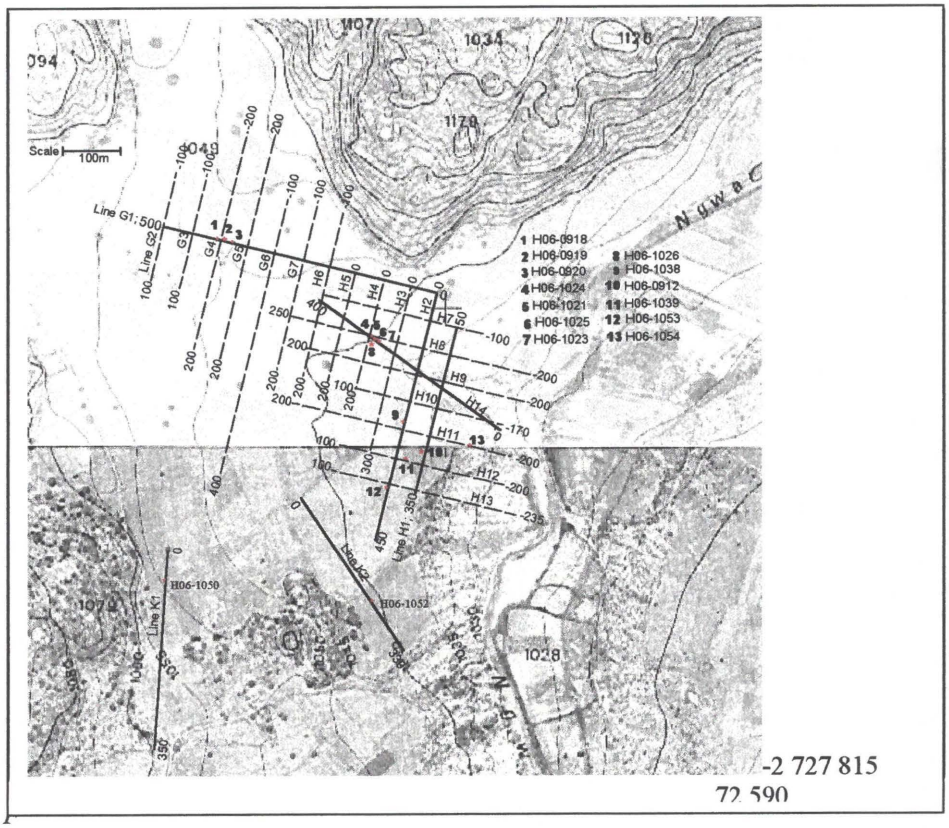

Figure 46a: Location map with field profiles and borehole positions (Orthphoto series, 1983).

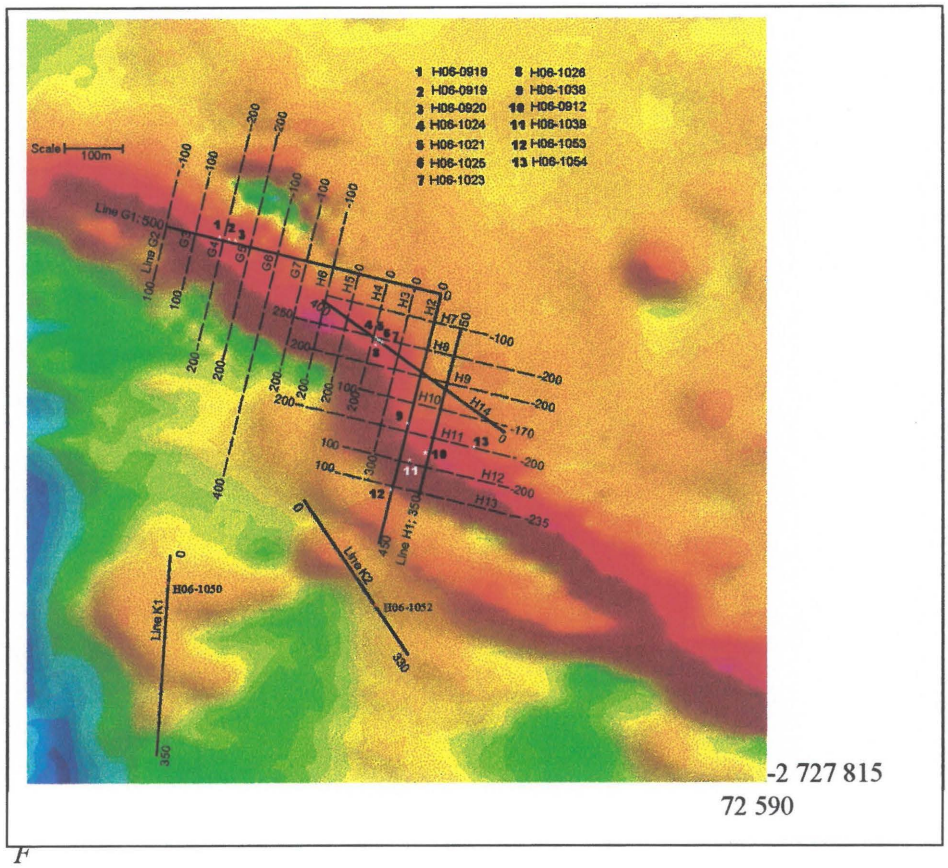

Figure 46b: Airborne magnetic data for the same area as shown above.

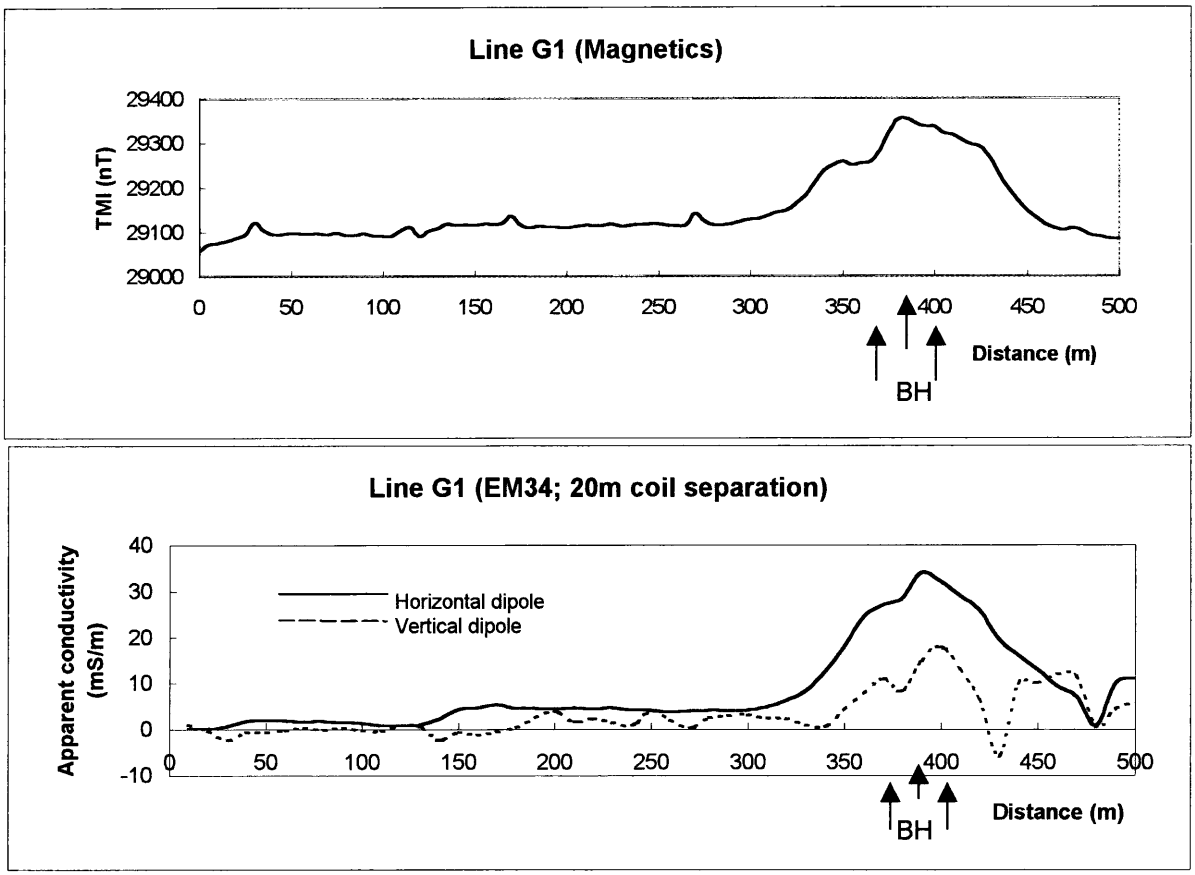

Figure 47a: Profiles for line G1.

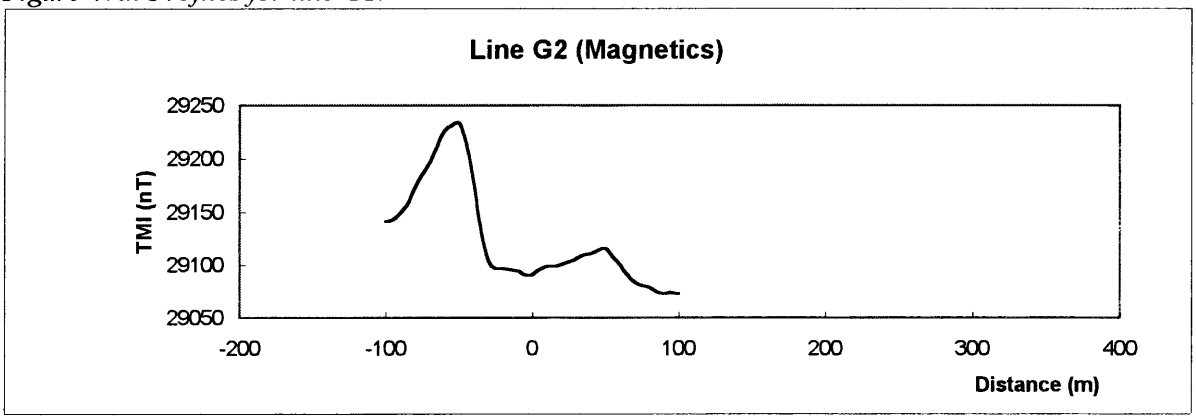

Figure 47b: Profile for line G2.

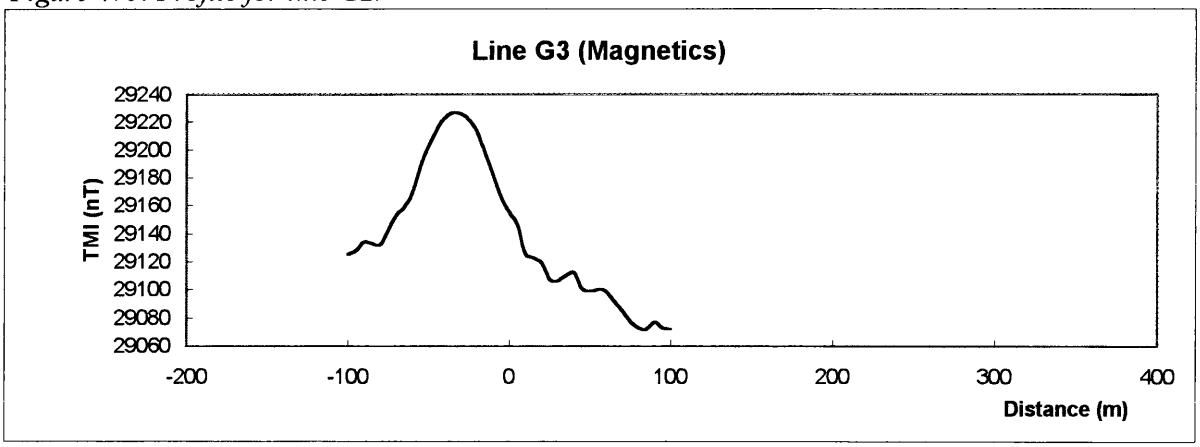

Figure 47c: Profile for line G3.

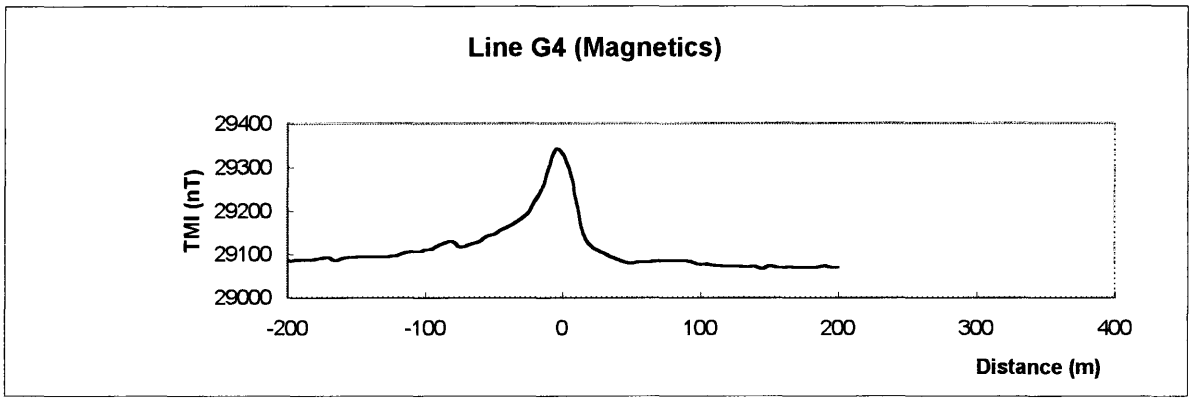

Figure 47d: Profiles for line G4.

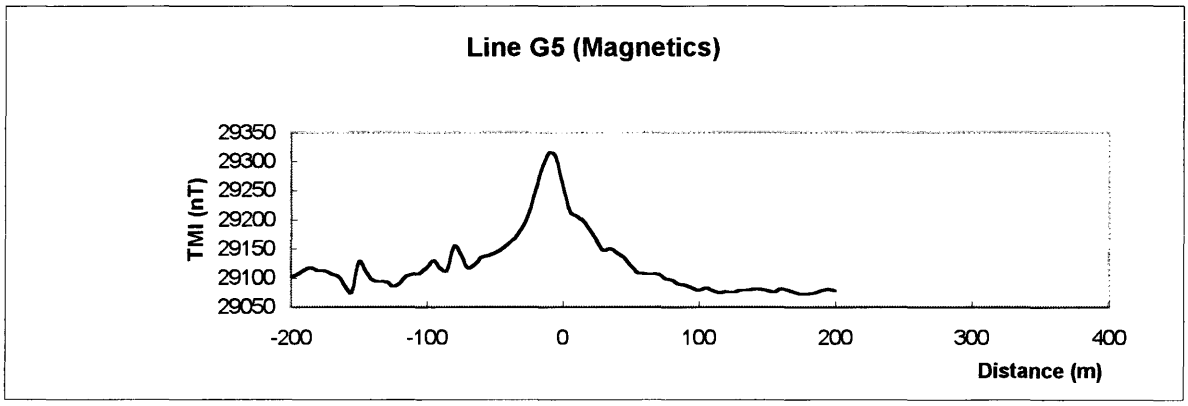

Figure 47e: Profiles for line G5.

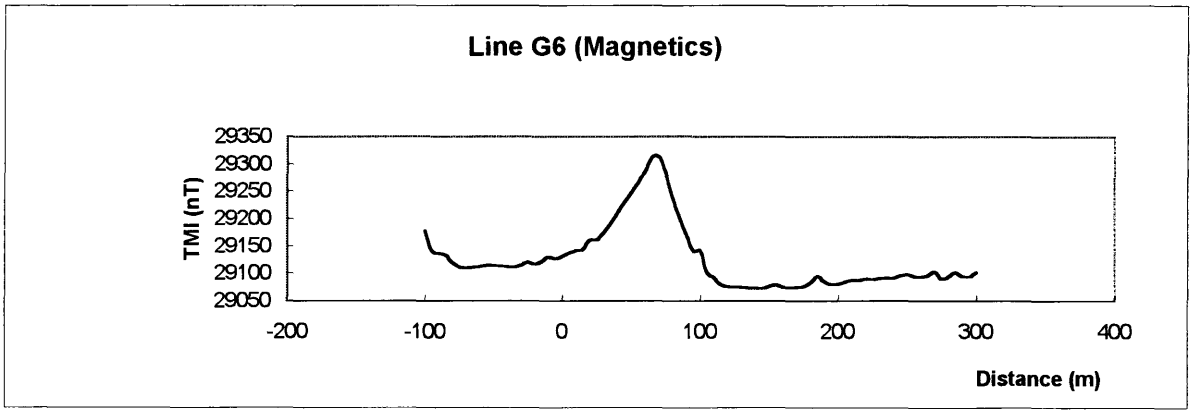

Figure 47f: Profiles for line G6.

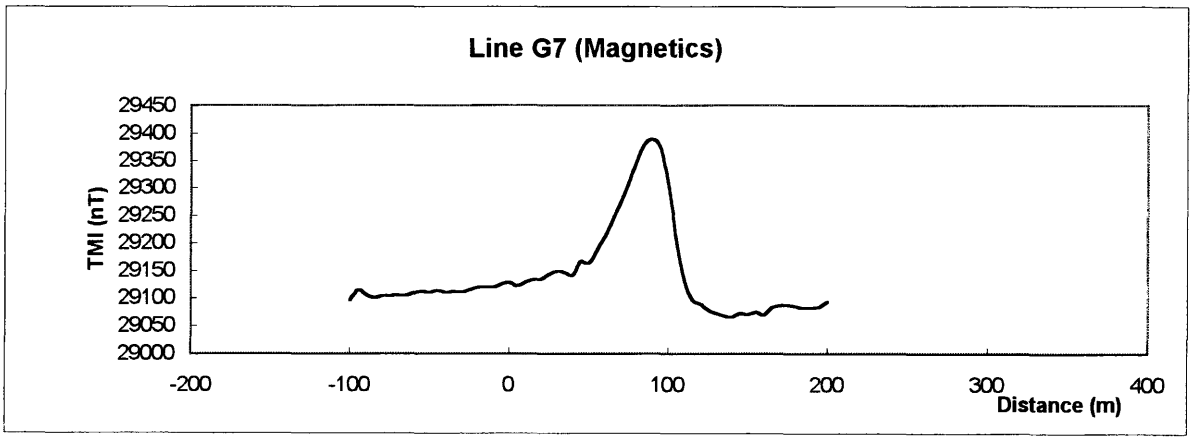

Figure 47g: Profiles for line G7.

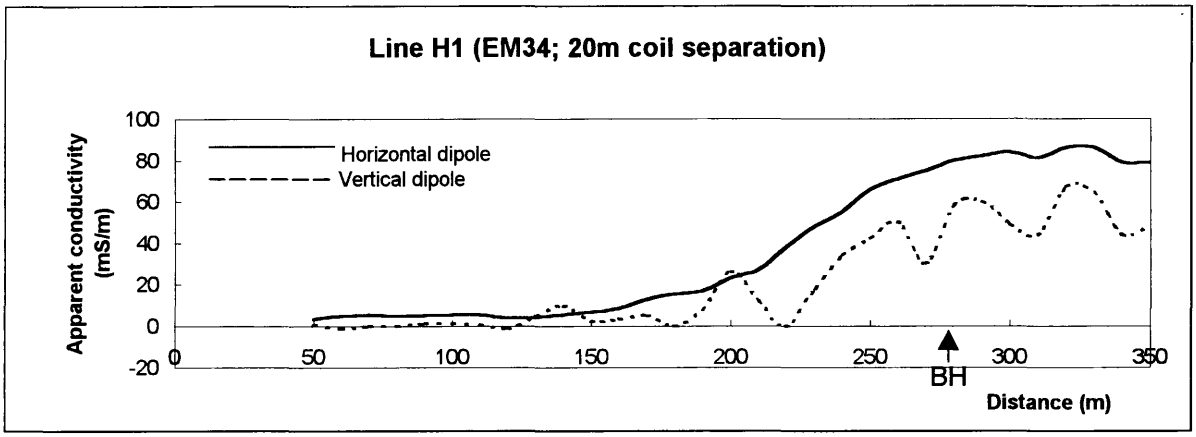

Figure 48a: Profile for line H1.

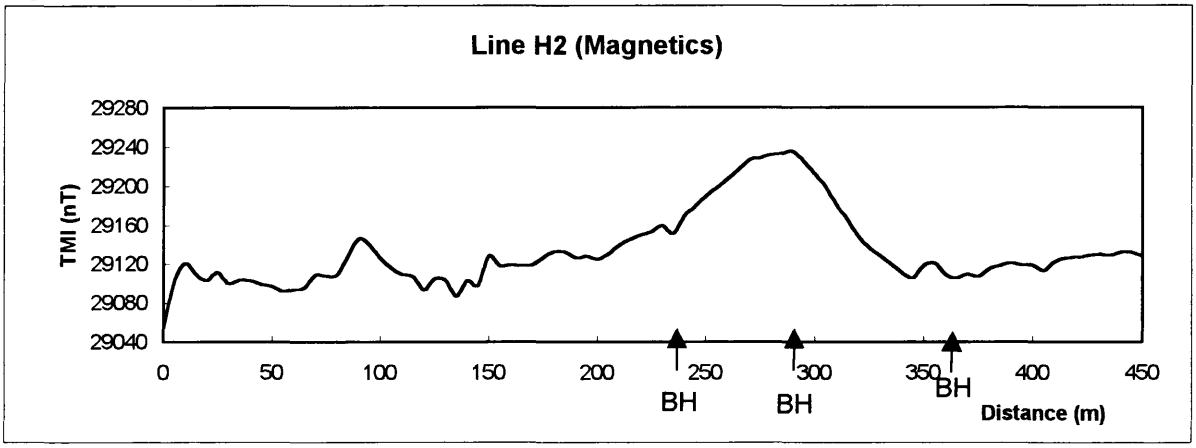

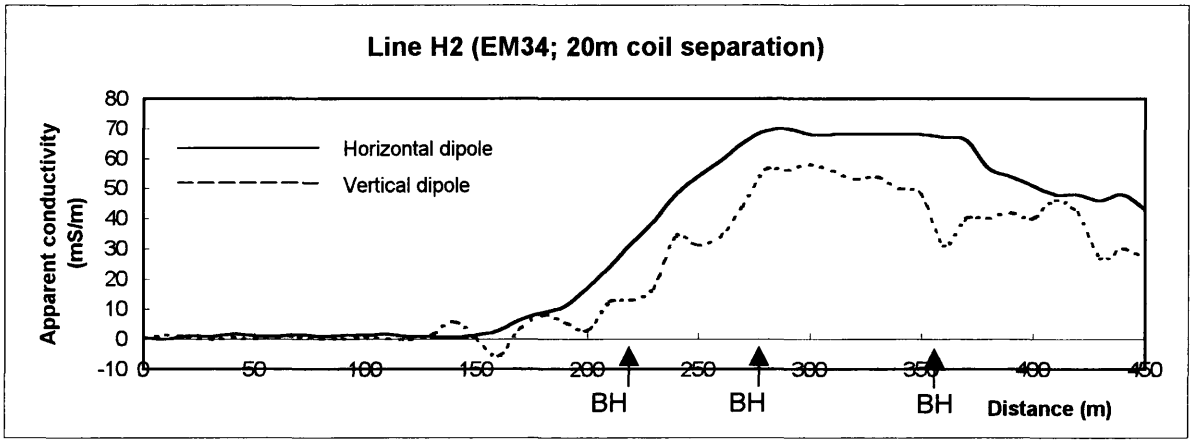

Figure 48b: Profiles for line H2.

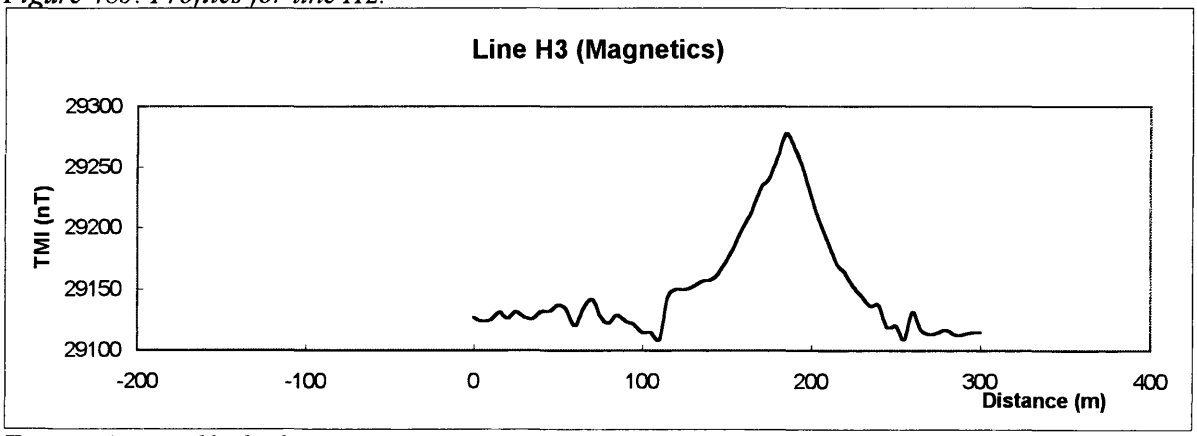

Figure 48c: Profile for line H3.

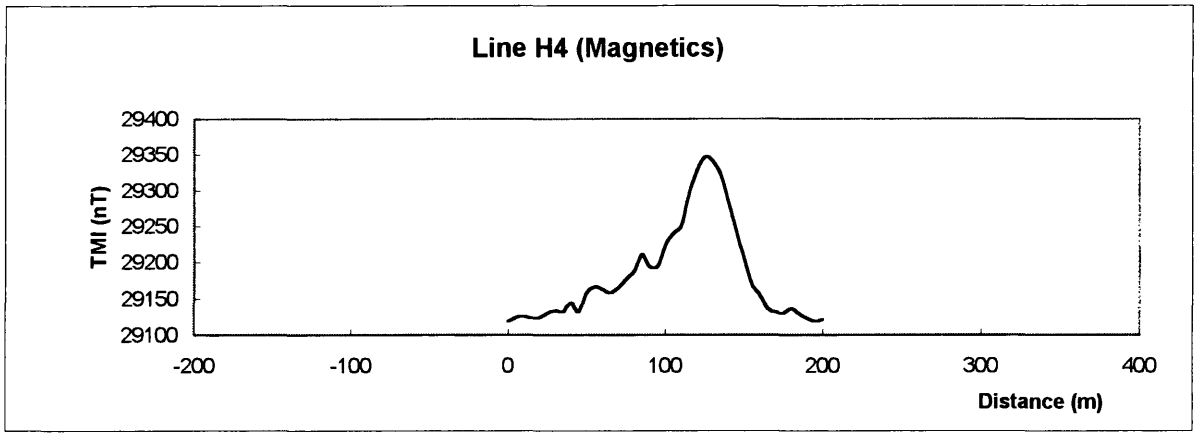

Figure 48d: Profile for line H4.

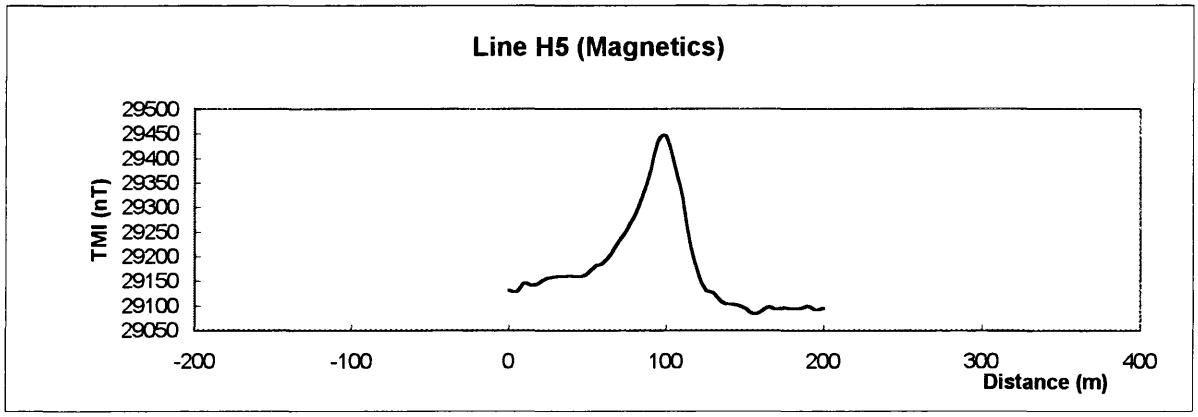

Figure 48e: Profile for line H5.

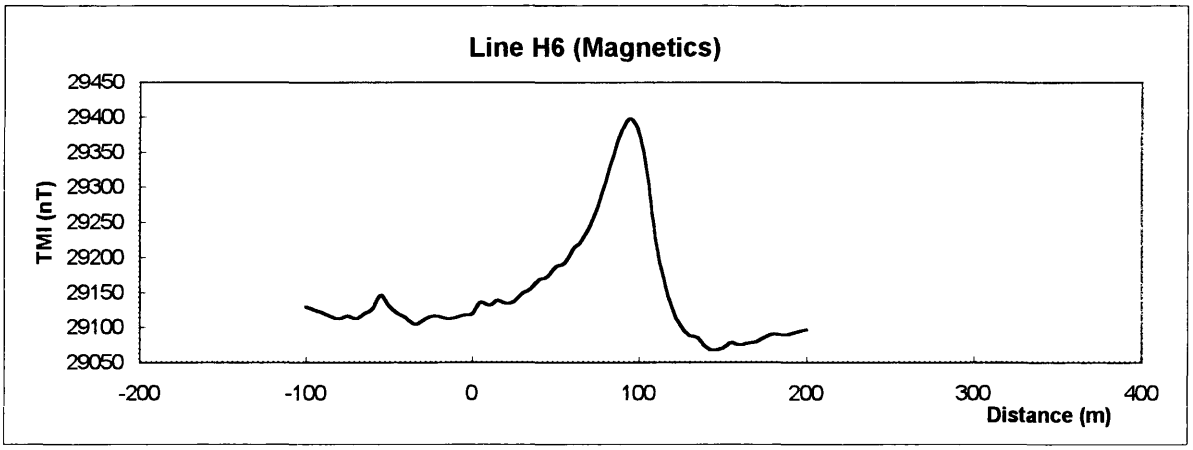

Figure 48f: Profile for line H6.

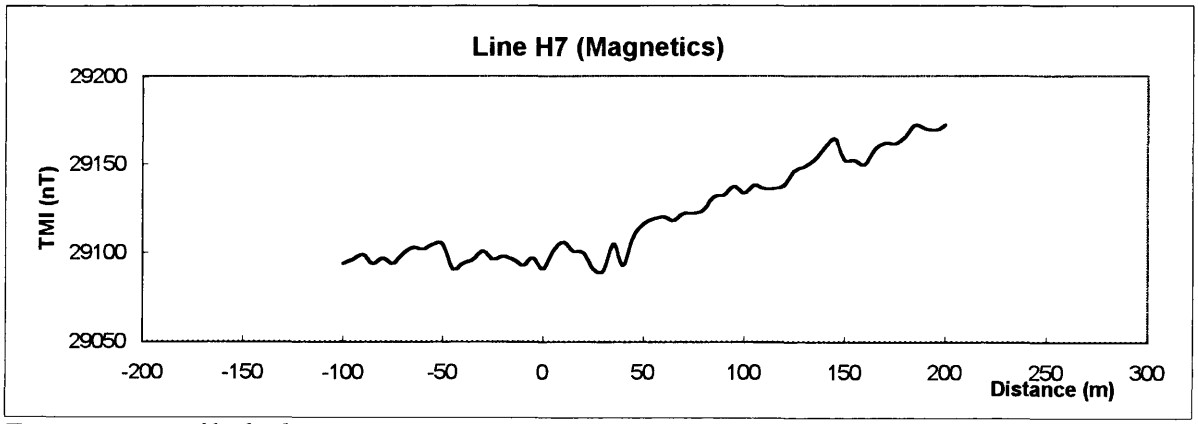

Figure 48g: Profile for line H7.

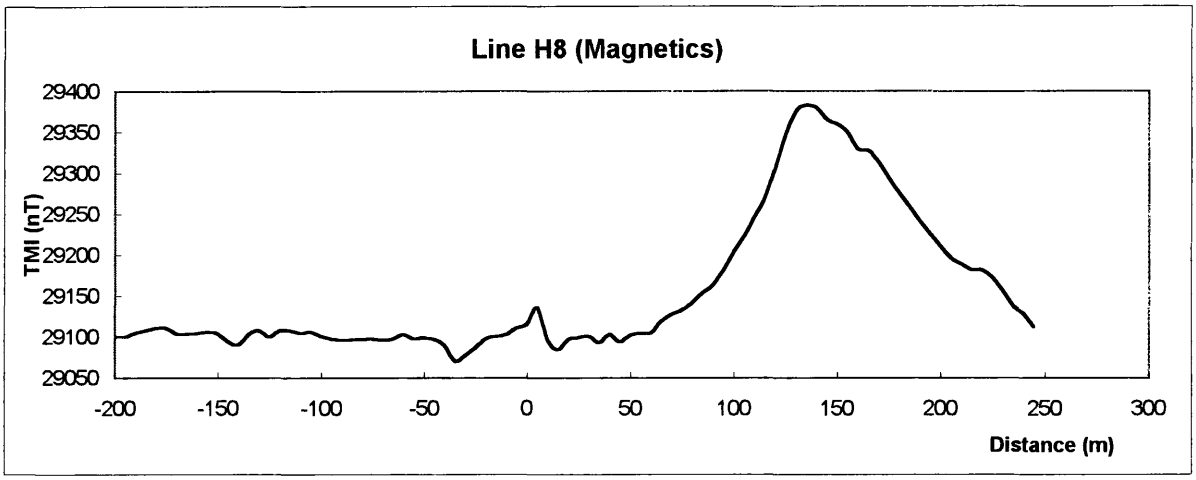

Figure 48h: Profile for line H8.

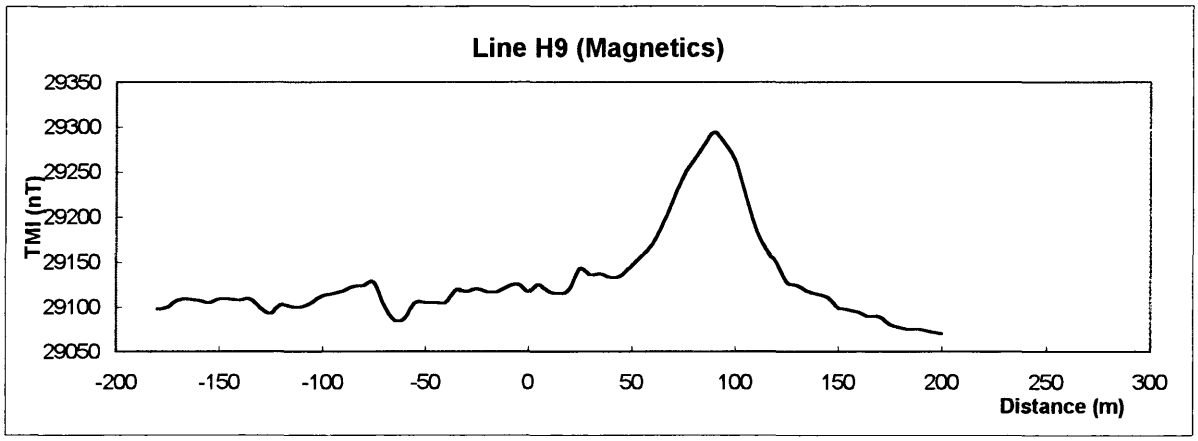

Figure 48i: Profile for line H9.

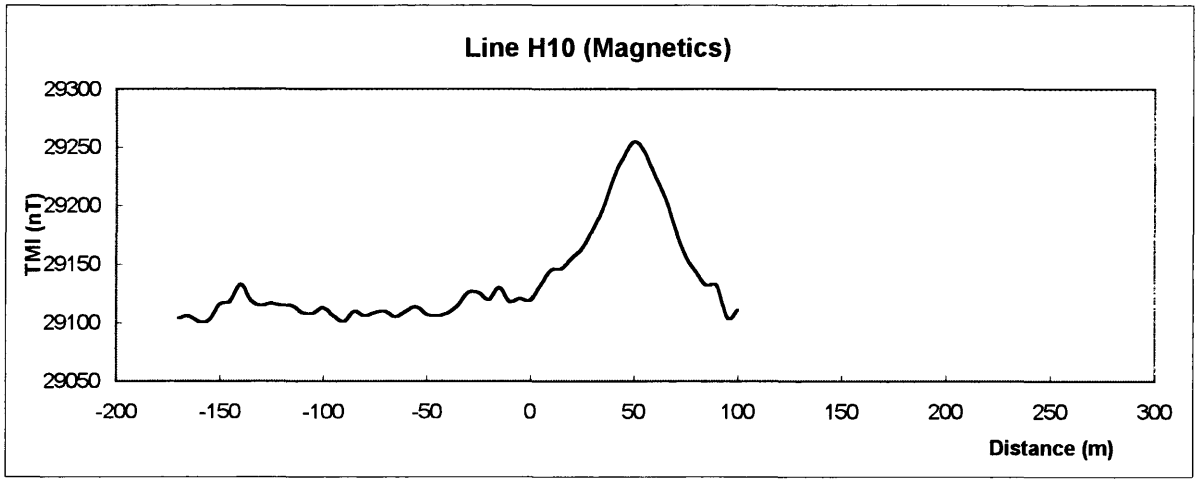

Figure 48j: Profile for line H10.

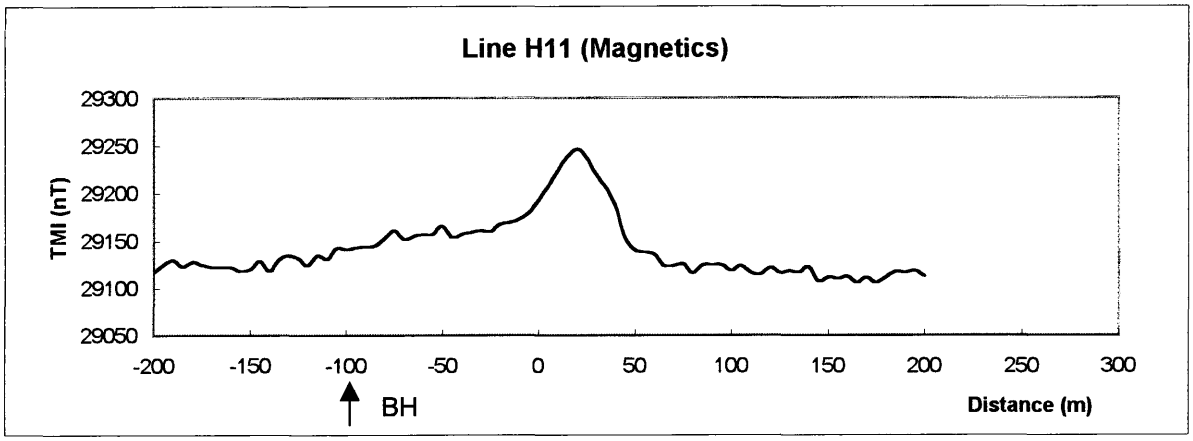

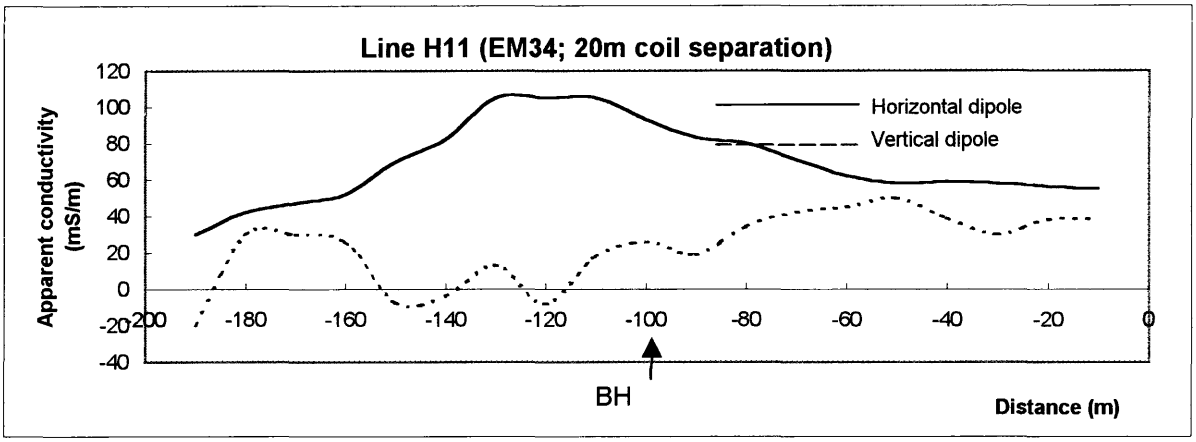

Figure 48k: Profiles for line H11.

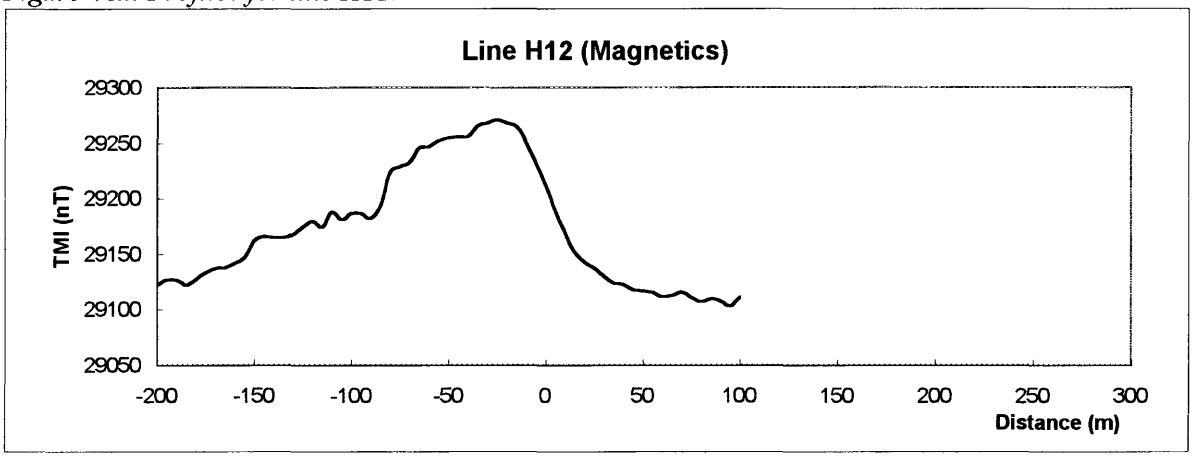

Figure 48l: Profile for line H12.

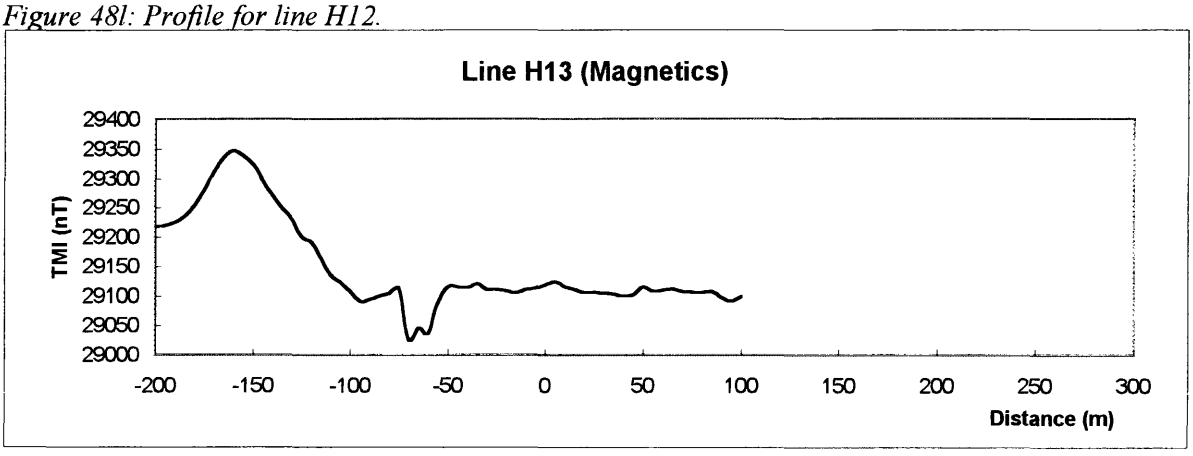

Figure 48m: Profile for line H13.

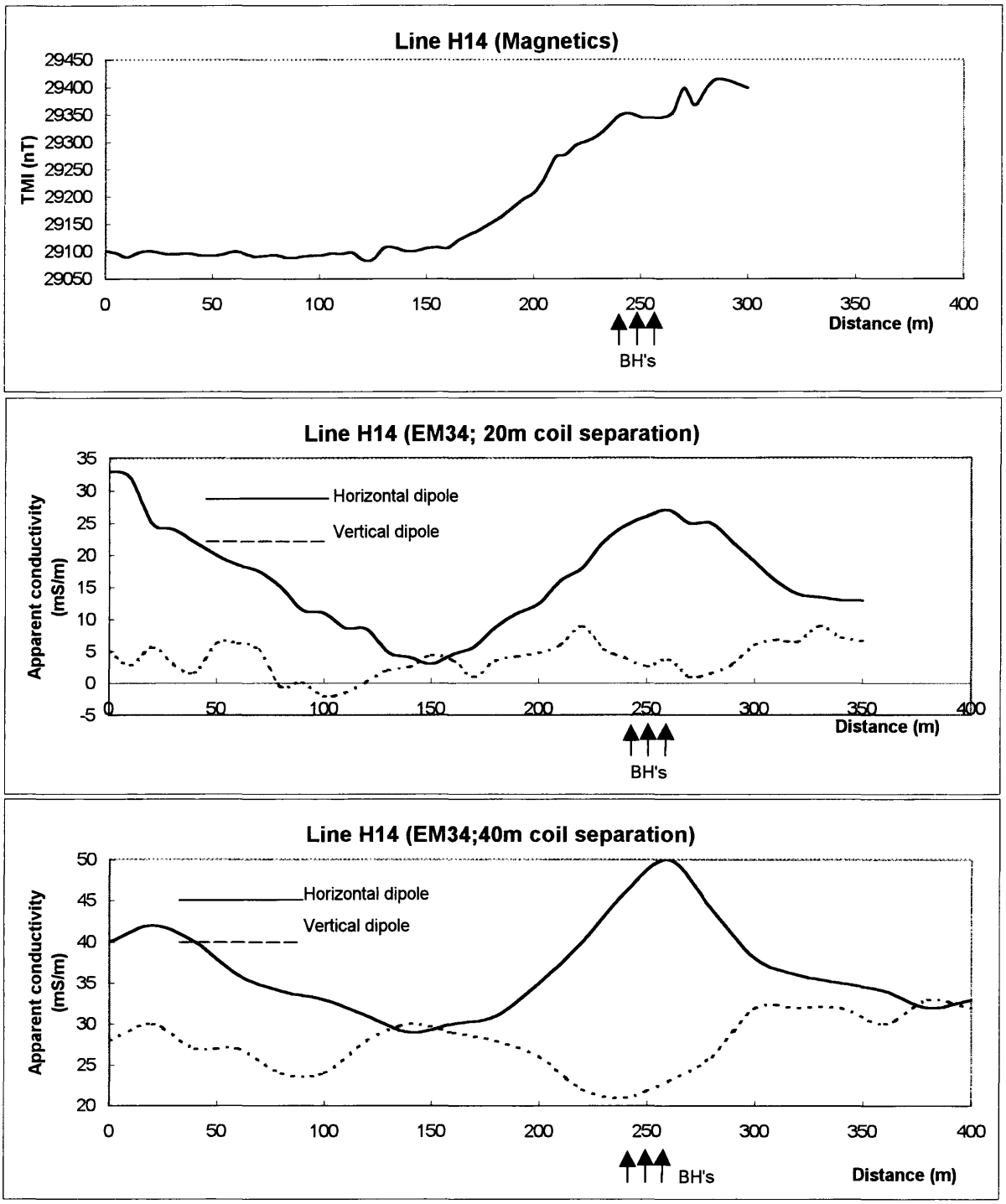

Figure 48n: Profiles for line H14.

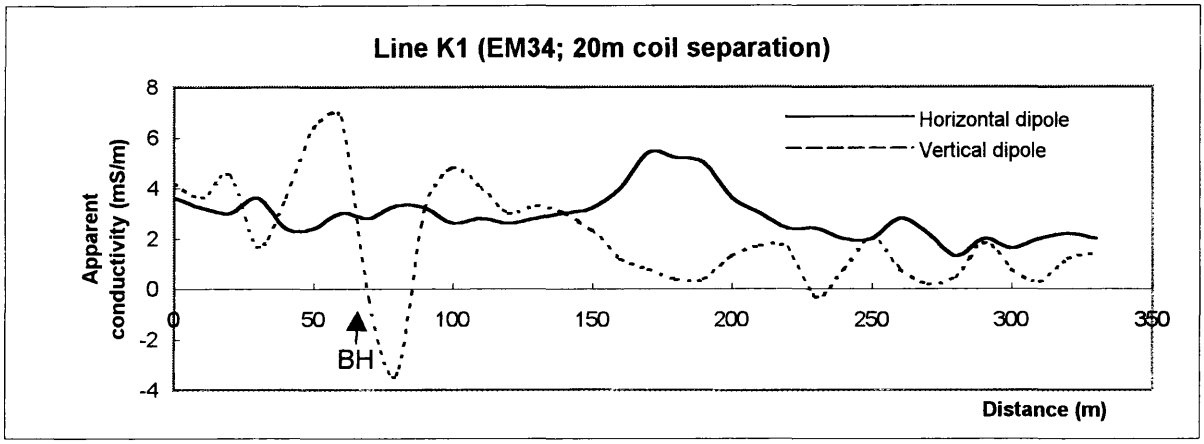

Figure 49a: Profile for line K1.

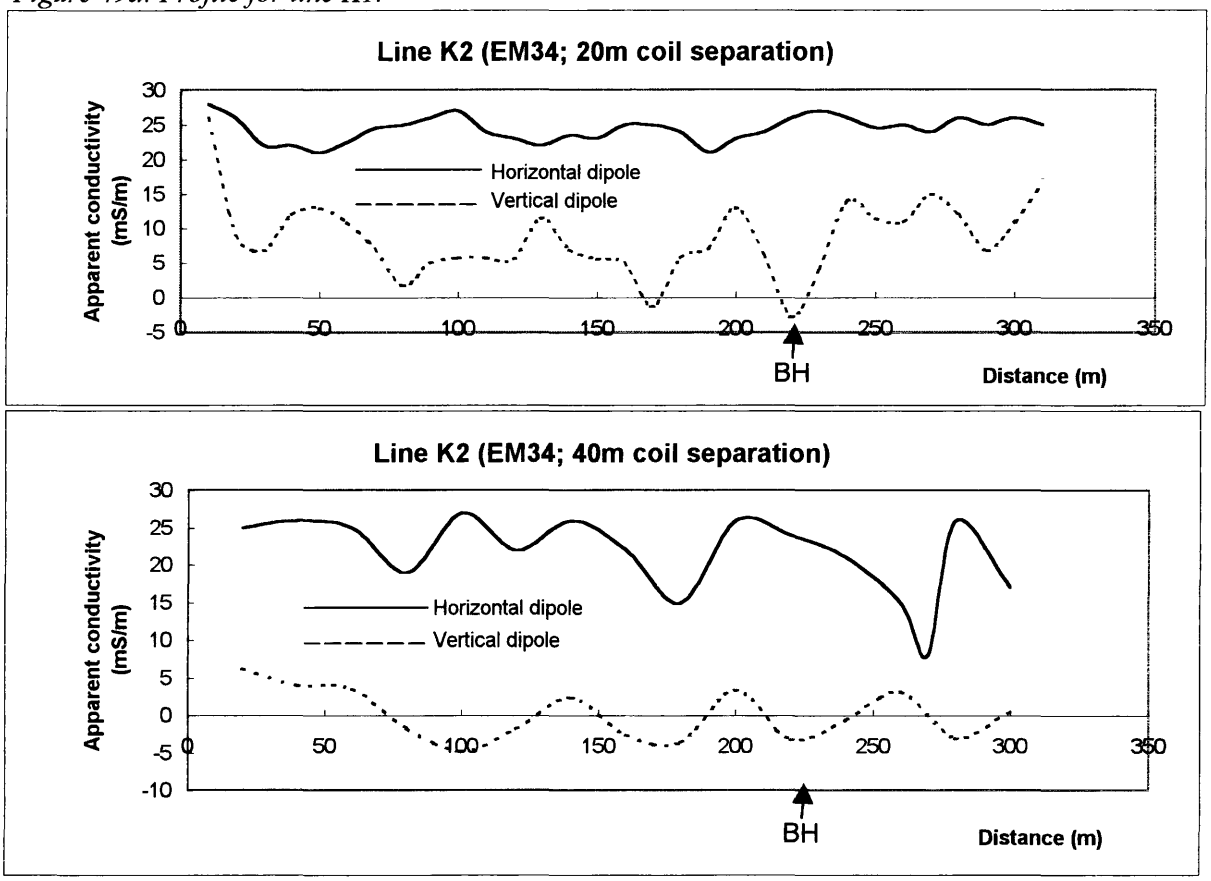

Figure 49b: Profiles for line K2.

Site I

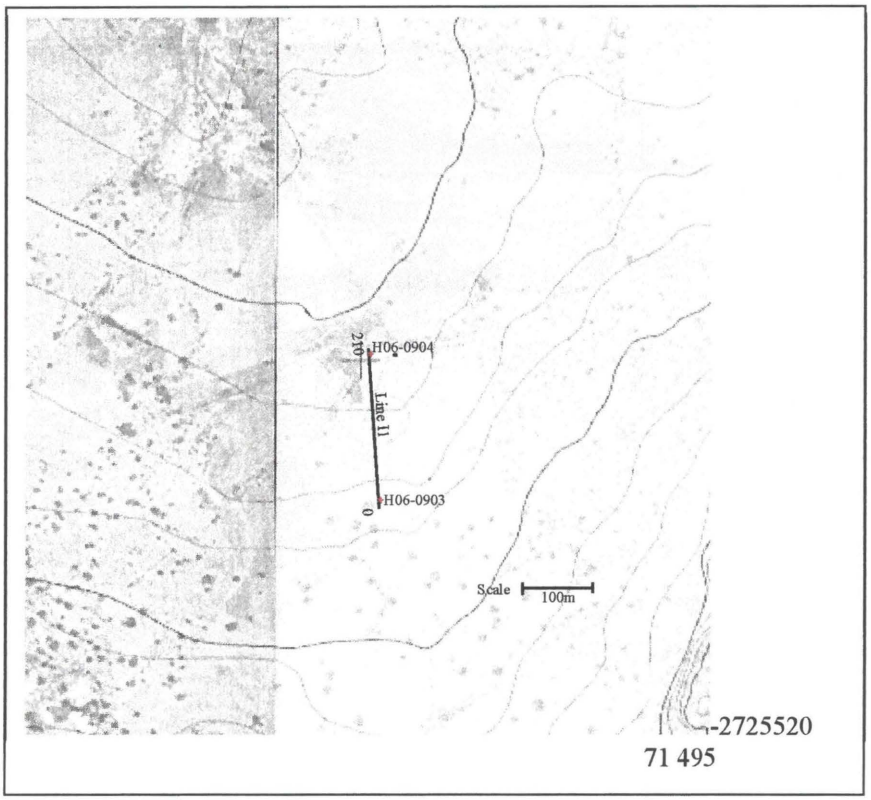

Figure 50a: Location map with field profiles and borehole positions (Orthophoto series, 1983).

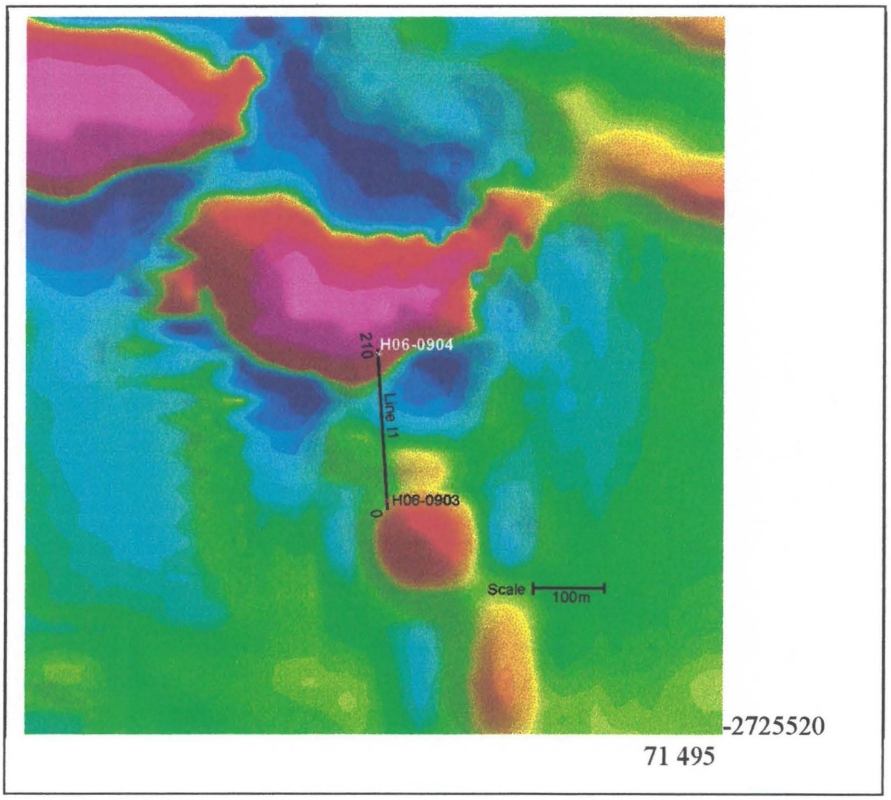

Figure 50b: Airborne magnetic data for the same area as shown above.

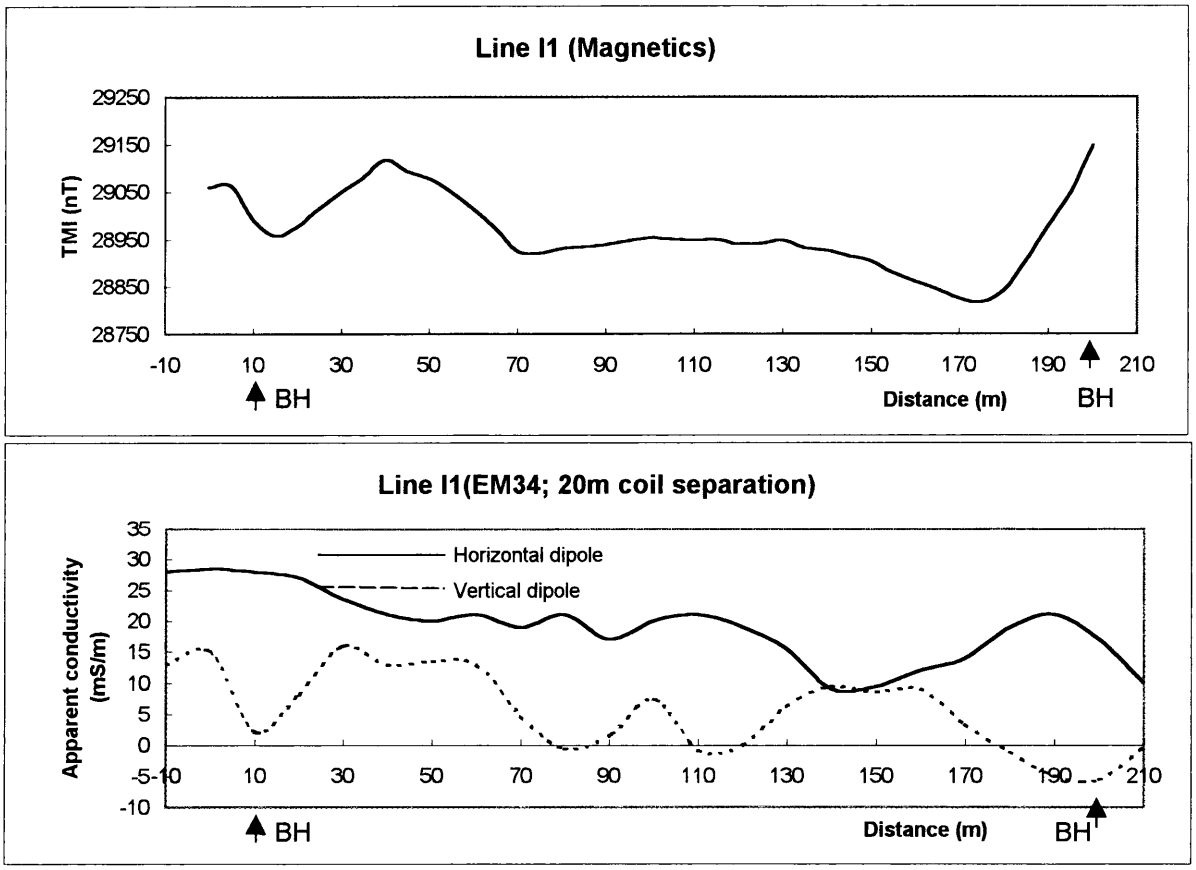

Figure 51: Profiles for line I1.

Site J:

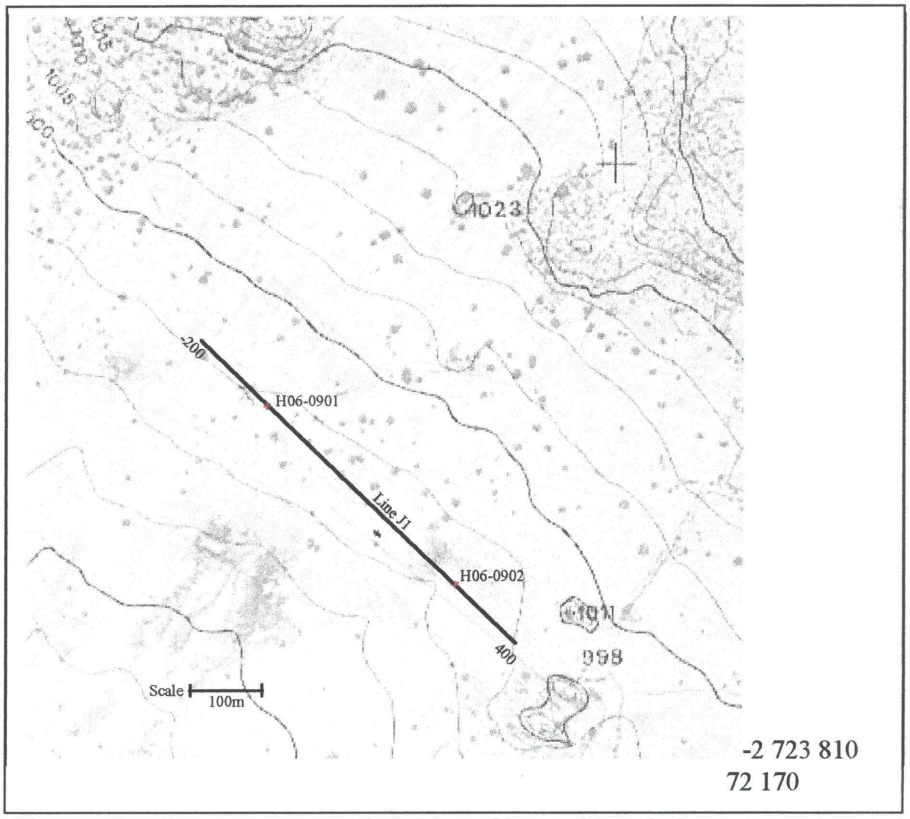

Figure 52a: Location map with field profiles and borehole positions (Orthophoto series, 1983).

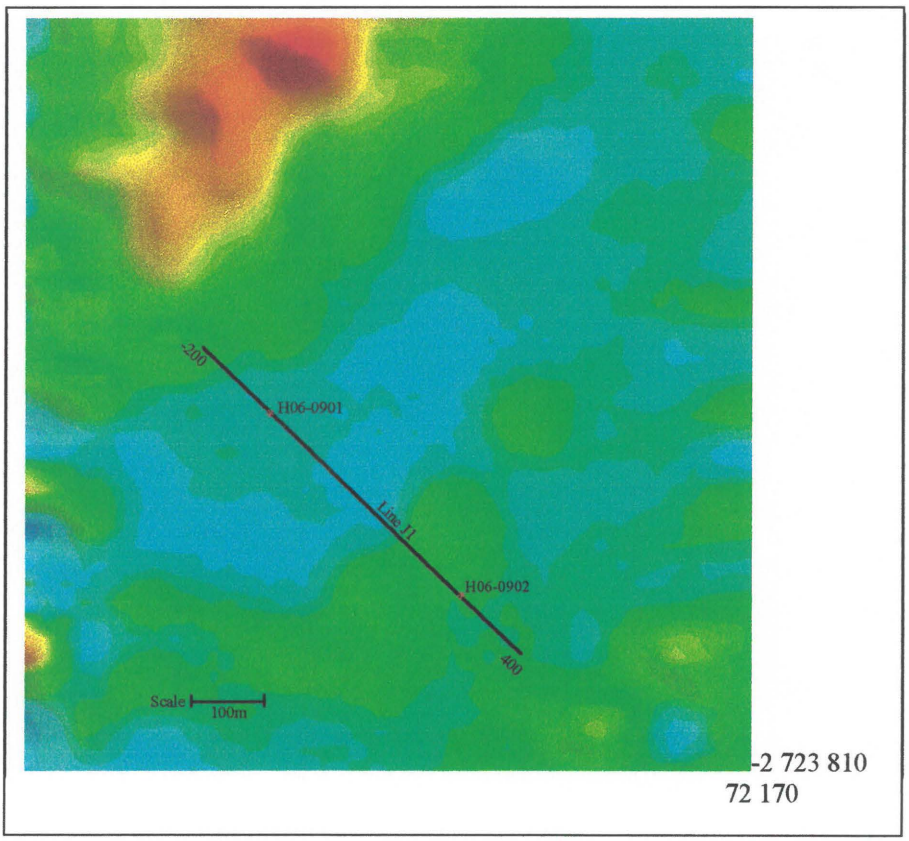

Figure 52b: Airborne magnetic data for the same area as shown above.

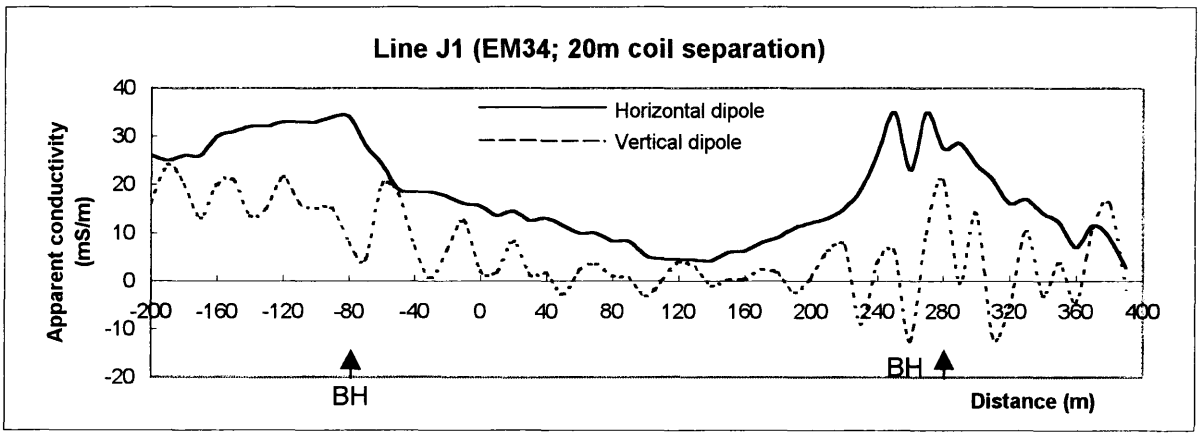

Figure 53: Profile for line J1.

Site L:

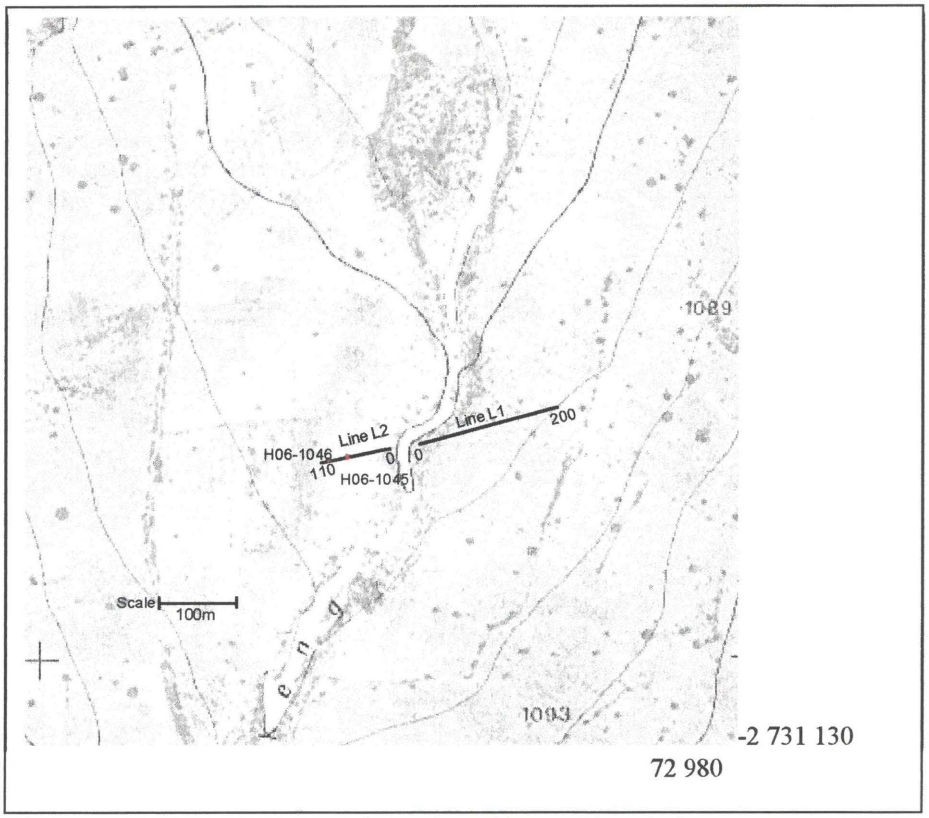

Figure 54a: Location map with field profiles and borehole positions (Orthophoto series 1983).

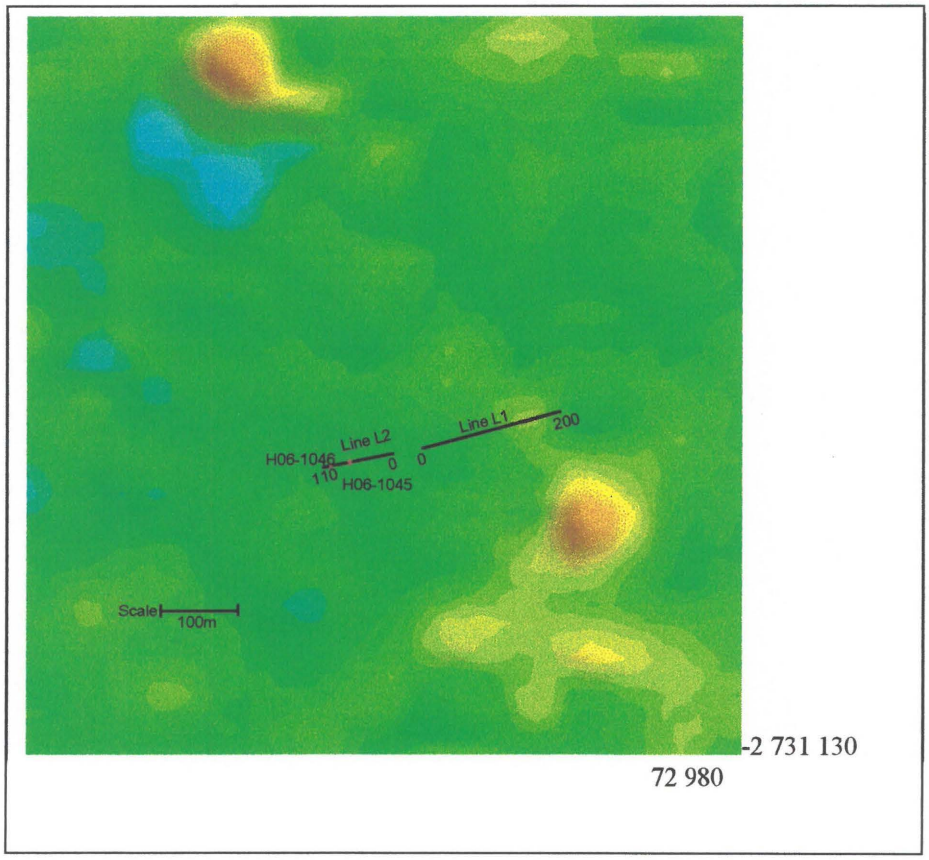

Figure 54b: Airborne magnetic data for the same area as shown above.

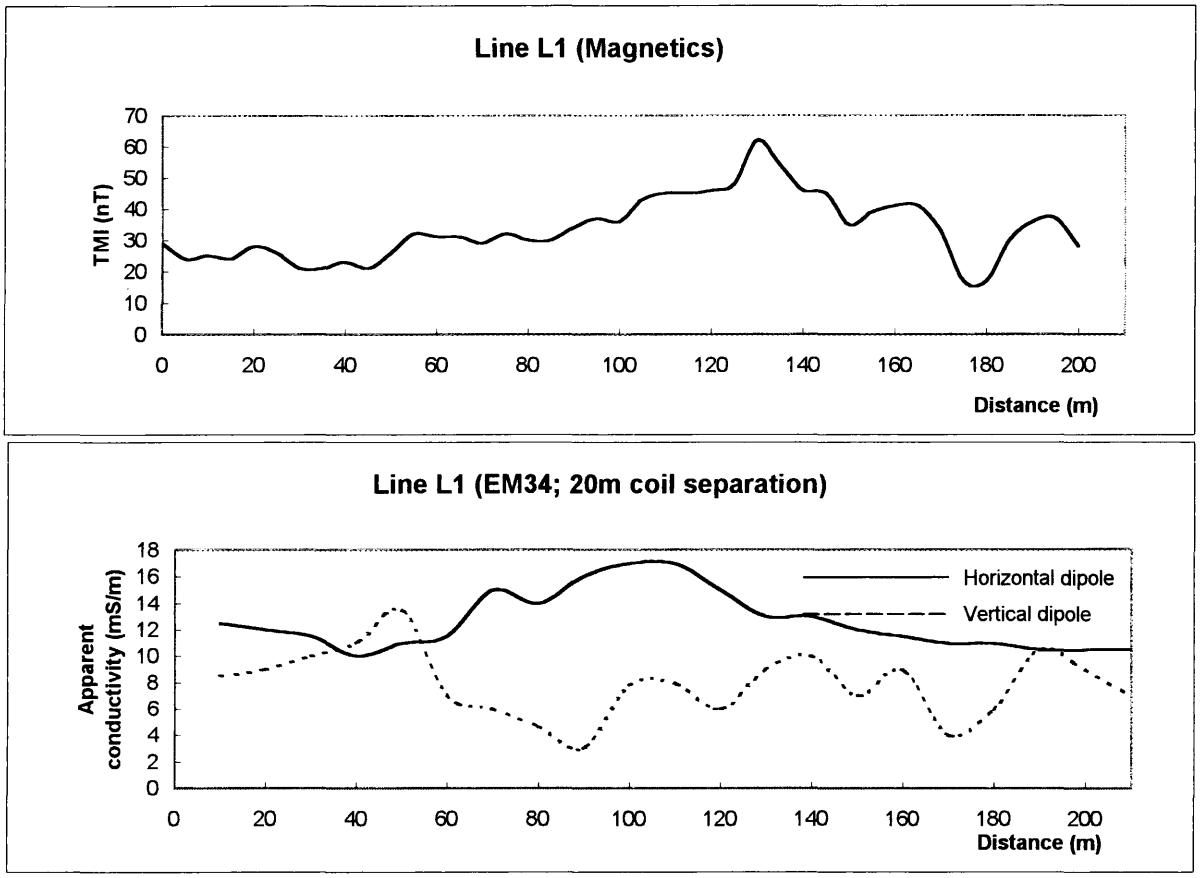

Figure 55a: Profiles for line L1.

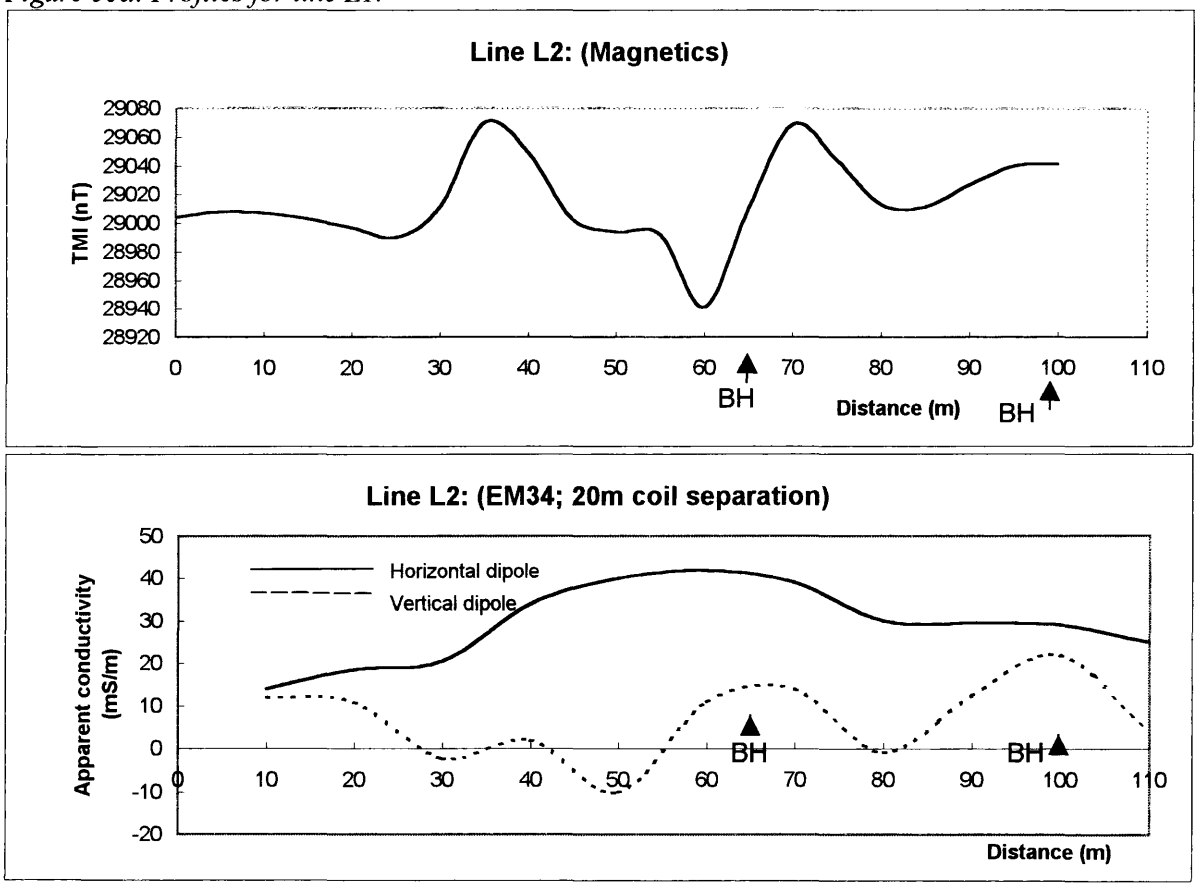

Figure 55b: Profiles for line L2.

Site M:

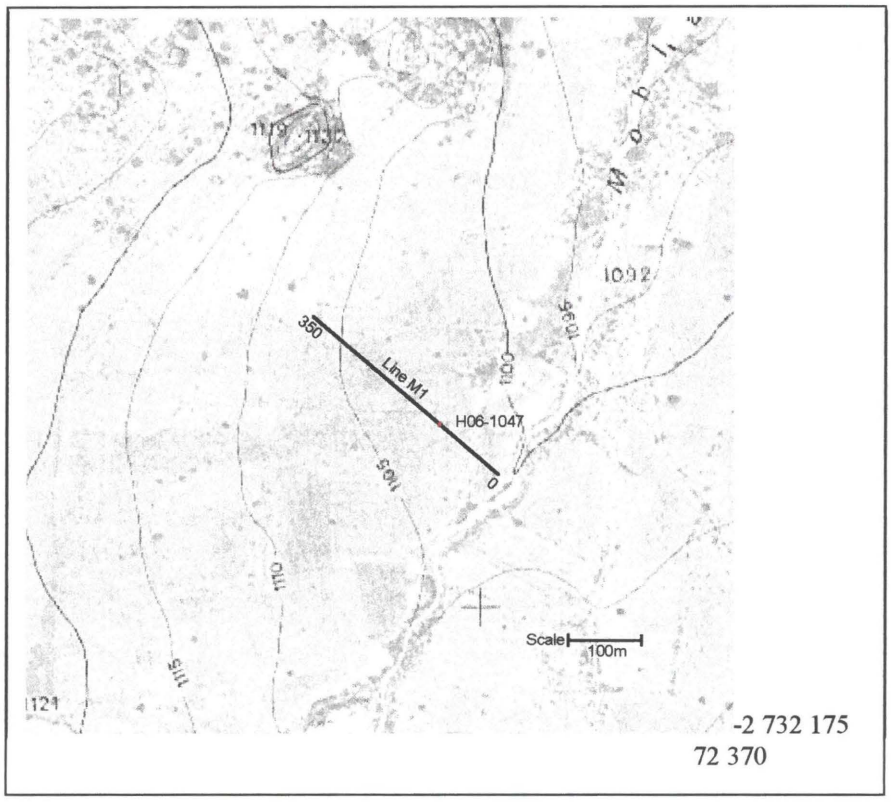

Figure 56a: Location map with field profile and borehole position (Orthophoto series, 1983).

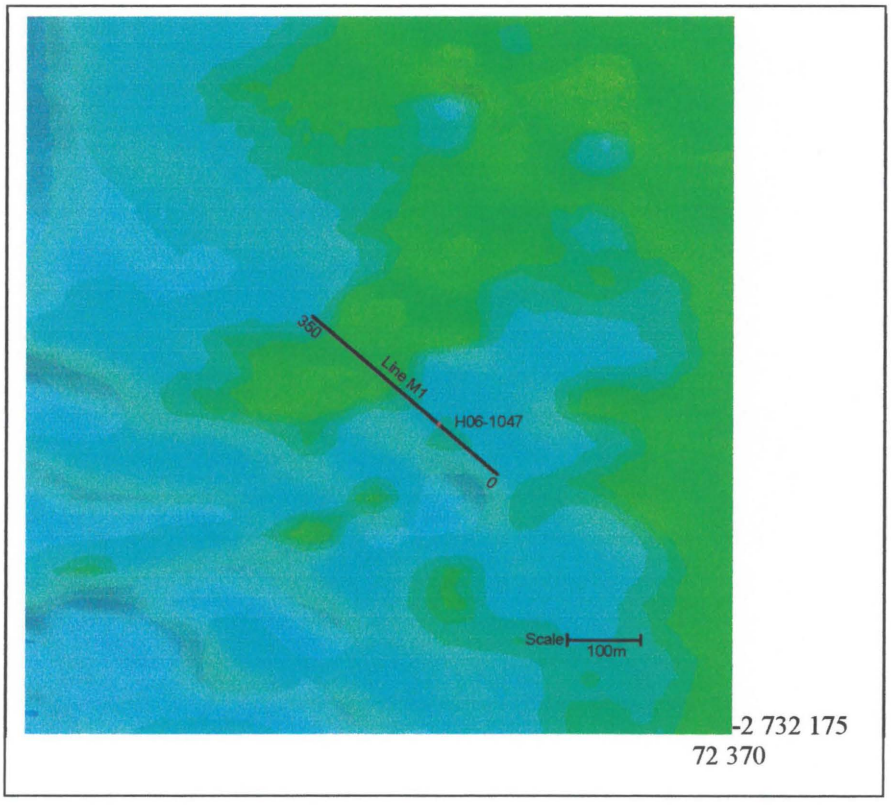

Figure 56b: Airborne magnetic data for the same area as shown above.

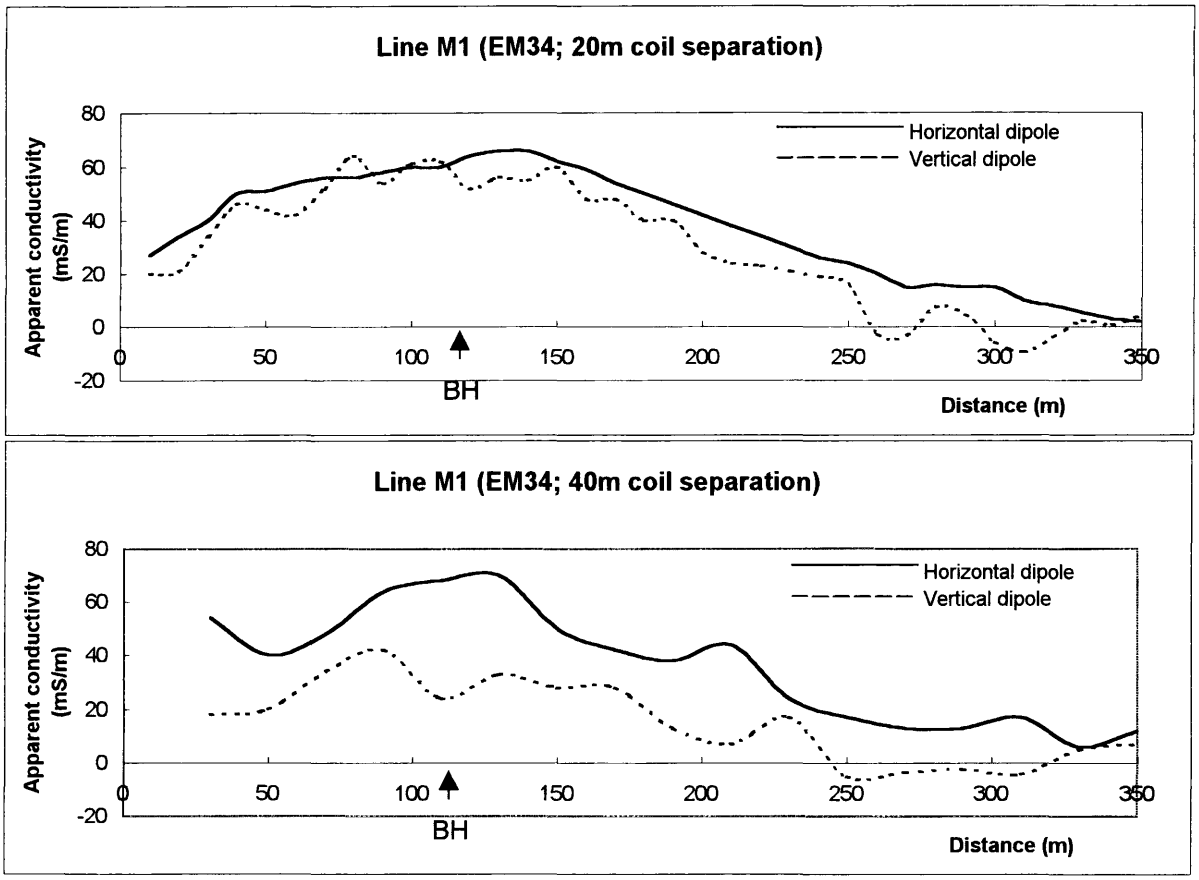

Figure 57: Profiles for line M1.

Site N:

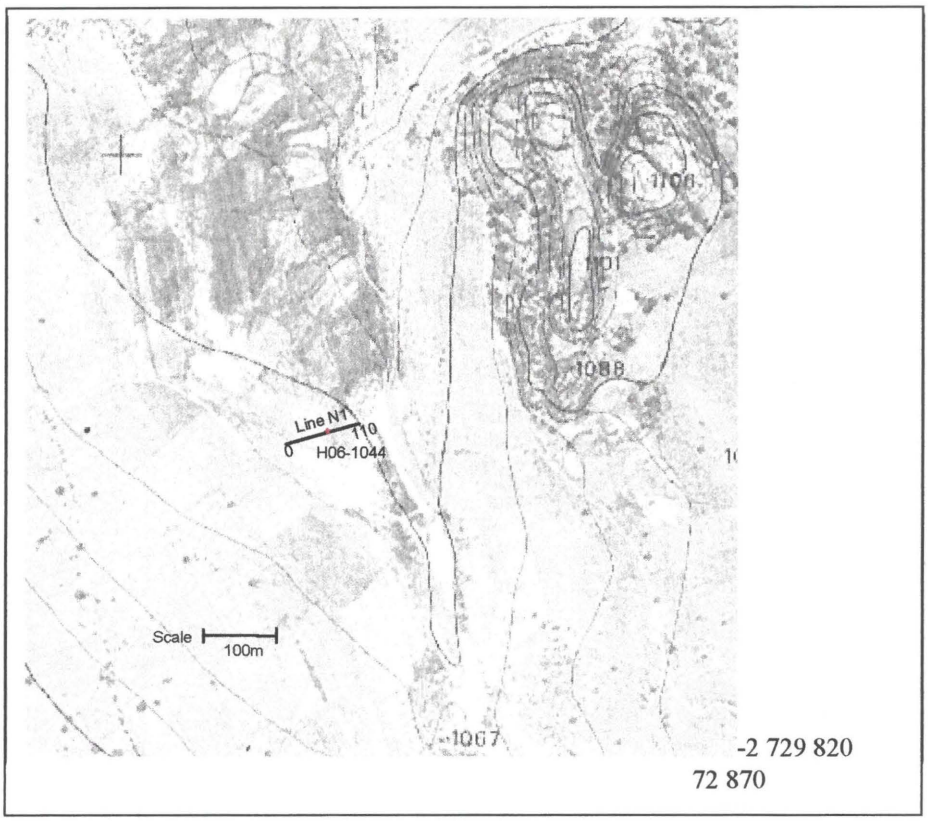

Figure 58a: Location map with field profile and borehole position (Orthophoto series, 1983).

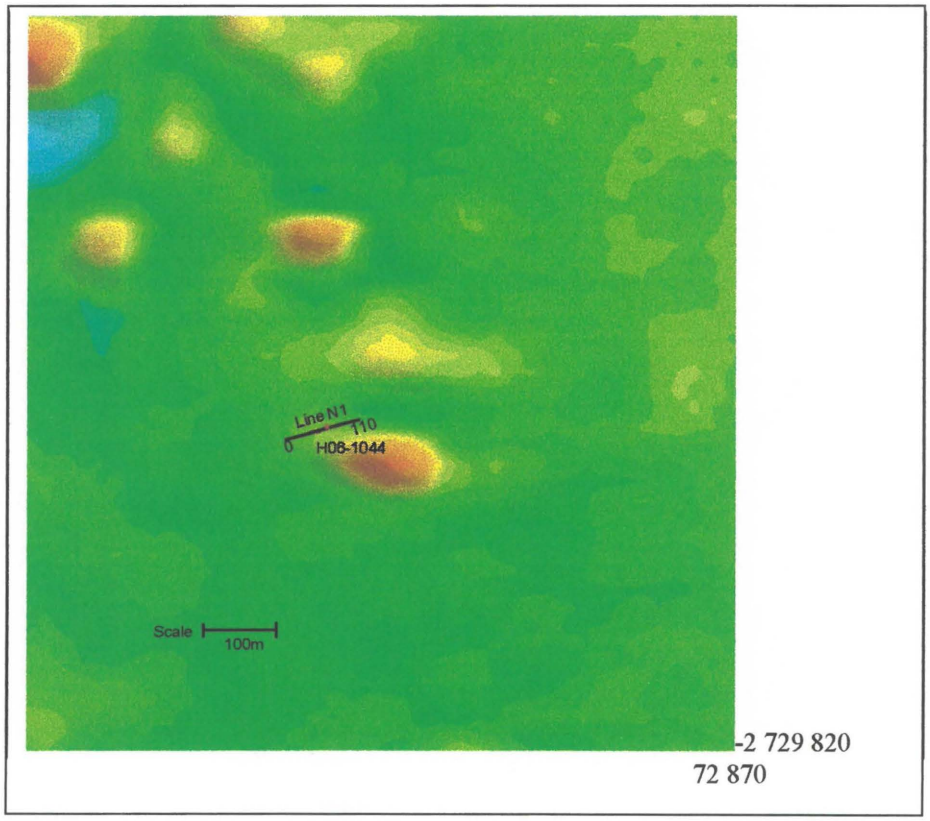

Figure 58b: Airborne magnetic data for the same area as shown above.

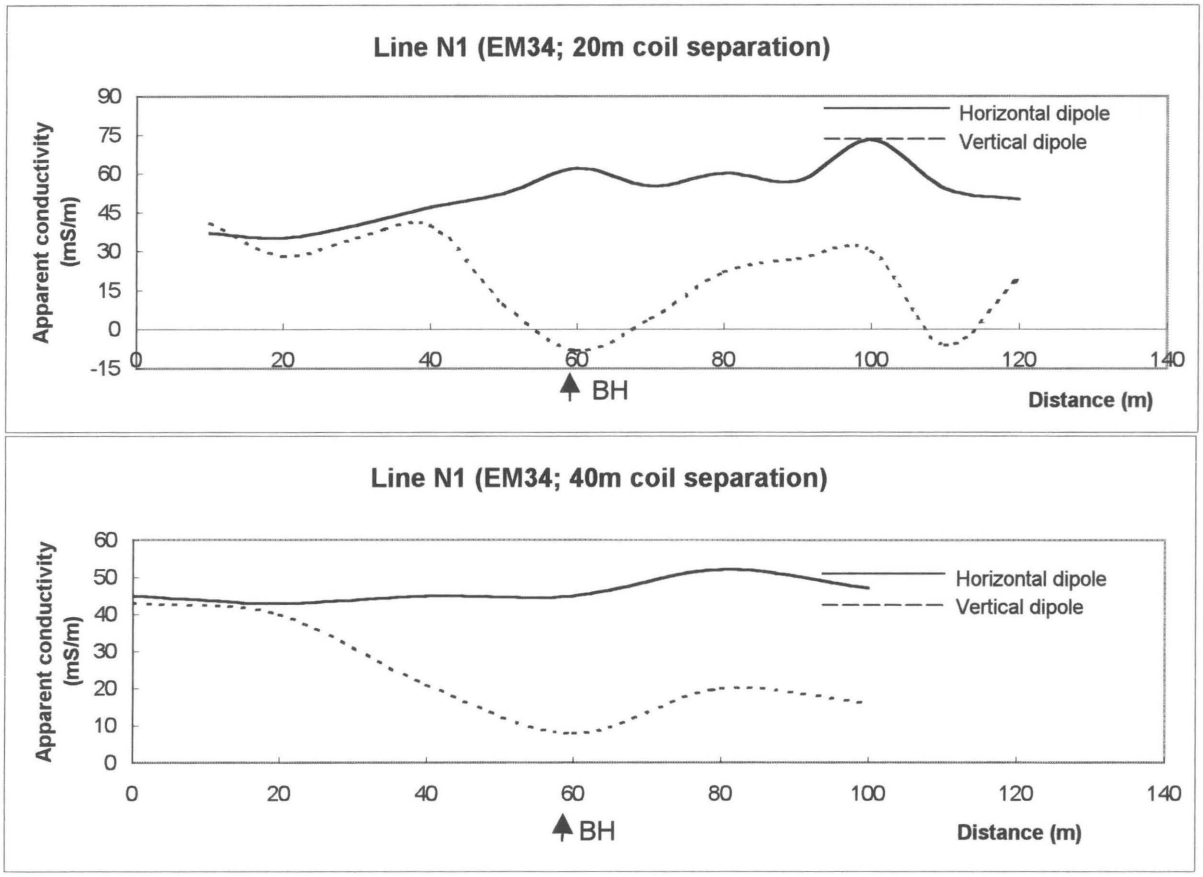

Figure 59: Profiles for line N1.

6.3 DRILLING RESULTS

There existed 40 holes in the study area before this project commenced. The highest yield that could be determined from the existing information on the boreholes was 1l/s and the total yield was 5.4 l/s. Although this information is not available on all the boreholes, these are the data that have been used in the past to classify the groundwater potential of the Ga-Masemola region. Based on these facts the area has been declared unsuitable for groundwater development.

In order to evaluate the application of the airborne geophysical techniques, the holes that were sited based on the ground follow–up work, were drilled by the Department of Water Affairs and Forestry. The borehole numbers, coordinates, depths, air lift and depth of the deepest water strike are presented in Table 3. Holes that yielded an air lift of more than 0.1 l/s are rated as successful because they can be fitted with handpumps.

The holes are grouped together as sites. Each site represents a certain structure or combination of structures. At sites F,H and G a number of holes were drilled close to one another on the same feature to serve as observation holes for pump testing and to compare the nature of fractured zones in granite to fractured zones in dolerite. The granite was more fractured than the dolerite dykes on the same fault with maximum weathering occuring at the contact. (Compare the yields of H06-1021 (dlrt), H06-1026 (grnt) and H06-1038 (contact)).

At site I, H06-0904 was drilled to investigate the weathering associated with the dolerite/granite contact in the absence of a fault. Although the EM34 data show a small anomaly at this contact (Fig. 51), there are very limited signs of weathering and no water. This observation was confirmed at other sites where fault zones were drilled at a dolerite-granite contact – the fault zones yielding water but not the contacts.

A total of 33 boreholes were drilled based on the airborne geophysical targets. The highest air lift yield was 36 l/s and the total yield of the holes is 74 l/s. This is enough water to supply 319680 people with 20 l/capita/day, depending on the water quality and sustainability which is being investigated in an FRD sponsored project.

Site	Borehole nr.	LOx	LOy	Depth(m)	Air Lift (l/s)	Deepest water strike(m)
A	H06-0881	-2722535	68516	50	**1**	7
B	H06-0882	-2723302	67714	30	**2**	1.8
C	H06-0916	-2731093	68136	72	0.1	15
	H06-0917	-2731100	68143	72	0	*
					0.1	
E	W6128	-2731749	72925	138	**3**	
F	H06-1027	-2725669	74096	84	0.03	
	H06-1028	-2725630	74009	72	3.41	49
	H06-1029	-2725631	74010	88	1.9	35
	H06-1030	-2725621	74013	72	0.14	18
	H06-1031	-2725587	73920	72	1.8	54
					7.28	
G	H06-0918	-2726876	71595	90	2	26
	H06-0919	-2726877	71605	60	0.002	28
	H06-0920	-2726880	71625	72	0.001	28
					2.003	
H	H06-1054	-2727244	72041			
	H06-1053	-2727319	71895	150	3	
	H06-1021	-2727051	71870	72	0.3	23
	H06-1023	-2727059	71880	72	0.3	
	H06-1024	-2727048	71867	72	0.04	
	H06-1025	-2727057	71879	72	0.6	
	H06-1026	-2727062	71866	72	5	
	H06-1038	-2727201	71926	102	36	98
	H06-1039	-2727265	71928	114	5	80
	H06-0912	-2727255	71958	72	5	36
					55.24	
I	H06-0903	-2725179	71045	43	0.9	28
	H06-0904	-2724991	71055	43	0	*
					0.9	
J	H06-0901	-2726625	71524	49	0	*
	H06-0902	-2726568	71780	43	0.6	16
					0.6	
K	H06-1052	-2727521	71867	150	0	*
	H06-1050	-2727479	71499	150	0.2	
					0.2	
L	H06-1045	-2730734	72435	150	0	*
	H06-1046	-2730740	72412	150	3	20
					3	
M	H06-1047	-2731751	71960	150	**0.9**	
N	H06-1044	-2729380	72284	150	**0.3**	

Table 4: Summary of drilling results.

An analysis of the drilling results based on the number of holes and the number of sites are given in table 5.

Dry holes	15%	Dry sites	7.6%
Successful holes	85%	Successful sites	92.3%
Holes yielding > 0.5 l/s	51%	Sites yielding > 0.5 l/s	77%
Holes yielding > 2 l/s	27%	Sites yielding > 2 l/s	46%
Average yield/hole	2.18l/s	Average yield/site	5.8 l/s (1.5 l/s excl. site H)

Table 5: Analysis of drilling results.

6.4 CONCLUSIONS

From the borehole results, the following can be concluded:

- A regional approach to groundwater exploration is essential.
- A previously conceived pearl of wisdom applied to the Ga-Masemola area, that drilling deeper than 30m is a waste of effort due to the closure of fractures and faults, has been disproved. It is recommended that boreholes can be drilled to a depth of 130m.
- There is an adequate amount of groundwater available in the Nebo granites to supply the population to RDP standards, at least on a temporary basis, provided the water is used judiciously.

Re-processing and evaluation of the airborne data led to the conclusion that:

- As is evident from the depicted examples the airomagnetic data adds tremendous value to the mapped geology and in areas where only granite was mapped, strong linear features were present in the airborne magnetic data. In the Ga-Masemola area many of the structures visible on the EM data were also shown out by the magnetic data set and it is therefore possible to generate the same exploration targets using only airborne magnetic data. This has a very significant impact on the exploration cost for the moment, until cheaper EM systems are available.
- The recommended line spacing for future aeromagnetic surveying is 50m. A line spacing of 100m is permissible but small important structures may be missed.

References:

Botha, F. S., 1998. FRD progress report – A strategic groundwater information and management system for sites on the Nebo Granites: Bushveld Igneous Complex: Northern Province.

Debeglia N., and Corpel. J., 1997. Automatic interpretation of potential field data using analytical signal derivatives. Geophysics, **62**, 87-96.

Environmental Potential Atlas Version 1 (ENPAT), 1994. Developed by GisLAB at the University of Pretoria for the Department of Environmental Affairs.

Fraser, 1978. Resistivity mapping with an airborne multicoil electromagnetic system: Geophysics, **43**, 144-172.

Geosoft Inc., 1995. Euler 3D Deconvolution (Euler 3D), Processing, Analysis and Visualization System for 3D Inversion of Potential Field Data, User Guide. 9-27 pp.

Geosoft Inc., 1996. MAGMAPTM (FFT-2D), 2-D Frequency Domain Processing of Potential Field Data, User Guide, 38-50 pp.

Hoffman, C., 1997. Geological and Structural Geological Study on the Nebo Granites (Hons project, unpublished), Department of Geology, U. P.

Keller, G. V. and Frischknecht, F. C., 1966. Electrical methods in Geophysical Prospecting. Pergamon Press Ltd., Oxford. 90-196 pp.

McNeil, J.D., 1980, Electromagnetic terrain conductivity measurement at low induction numbers: Geonics Ltd., Toronto, TN7

McNeil, J.D., 1983, EM34-3 survey interpretation techniques: Geonics Ltd., Toronto, TN8.

Nabighian, M. N., 1972. The Analytic signal of two-dimensional magnetic bodies with polygonal cross-section: its properties and use for automated anomaly interpretation. Geophysics, **37**, 507-517.

Nabighian, M. N., 1984. Toward a three-dimensional automatic interpretation of potential field data via generalized Hilbert transforms: Fundamental relations: Geophysics, **49**, 780-786.

National Groundwater Information System (NGIS), Department of Water Affairs and Forestry

Pritchard, R.A., 1997. DIGHEMV SURVEY FOR THE COUNCIL FOR GEOSCIENCE, GA-MASEMOLA AREA , RSA; Report #769, Dighem, A division of CGG Canada Ltd., Mississauga, Ontario.

Project Panel, 1981. (Chairman: Ingemar Larsson). Groundwater in hard rocks, Project 8.6 of the International Hydrogeological Program, UNESCO, 71-83 pp.

Reid, A. B. et al., 1990. Magnetic interpretation in three dimensions using Euler deconvolution. Geophysics, **55**, 80-91.

Sengpiel, K.P., 1983. Resistivity/depth mapping with airborne electromagnetic survey data. Geophysics, **48**, 181-196.

South African Commitee for the Stratigraphy, 1980. In: L. E. Kent (Editor) Lithostratigraphy of the Republic of South Africa, South West Africa/Namibia, and the Republics of Bophuthatswana, Transkei and Venda. South African Geol. Survey, Handbook 8, 633 pp.

Tankard, A. J., 1982. Crustal Evolution of Southern Africa. Springer-Verlag Inc.,New York.

Telford, W.M. et al, 1990. Applied Geophysics, Second Edition. Cambridge University Press, Cambridge, New York, 62-134,343-577 pp.

Thompson, D. T., 1982, EULDPH-A new technique for making computer-assisted depth estimates from magnetic data: Geophysics, **47**, 31-37

Van Zijl, J. S. V., 1985. A practical manual on the resistivity method. WNNR report K79, Geophysics Division, 3-12 pp.

Vegter, J. R., 1995. An Explanation of a set of National Groundwater Maps (Including Maps: Groundwater Resources of the Republic of South Africa). Water Research Commission, Department of Water Affairs and Forestry, South Africa.